Targeting IKKε/TBK1 for the treatment of diffuse large B-cell lymphoma

Thesis submitted for the degree of
Doctor of Philosophy
at the University of Leicester

by
Matthew D. Carr (MRes)
Department of Cancer Studies
University of Leicester

September 2018

Abstract

Targeting IKKε/TBK1 for the treatment of diffuse large B-cell lymphoma

Matthew Carr

Diffuse large B-cell lymphoma (DLBCL) is the most common of the non-Hodgkin lymphomas. Current treatment with conventional chemotherapy results in an overall 5-year survival rate of between 50-60%, and it is recognised that there are two major subtypes; germinal centre (GC) and activated B-cell (ABC). ABC DLBCL has a poor prognosis, highlighting a need for new treatments.

IKKε and TBK1 are homologous kinases which function in innate immunity by regulating both the anti-viral response and the NF-κB pathway. IKKε and TBK1 may therefore represent attractive targets to repress NF-κB signalling in DLBCL.

There was an association between *TBK1* mRNA level and overall survival in DLBCL, and staining of primary DLBCL revealed that ~66% of cases expressed either TBK1 or IKKε at the protein level with association towards the non-GC DLBCL subtype.

IKKε/TBK1 inhibitors were used to screen a panel of DLBCL cell lines. Sensitive DLBCL cell lines represented the ABC DLBCL subtype and showed expression of phosphorylated STAT3. ABC DLBCL are thought to rely on constitutive activation of the NF-κB pathway. Treatment of an ABC DLBCL cell line with DMX3433- a dual IKKε/TBK1 inhibitor abrogated phosphorylation of P65 and STAT3. Additionally, DMX3433 treatment significantly reduced secreted levels of IL-10, CLL3 and CCL4. Addition of IL-10 to the culture medium restored STAT3 phosphorylation. This suggests a model in which IKKε/TBK1 inhibition represses NF-κB driven IL-10 transcription to suppress JAK2/STAT3 signalling.

Finally, two of four patient derived xenograft (PDX) DLBCL models were sensitive to IKKε/TBK1 inhibition. Treated PDX models show a reduction in levels of phosphorylated STAT3 and NF-κB and immune related signalling at the transcriptional level.

It is proposed that targeting IKKε/TBK1 can disrupt NF-κB and STAT3 signalling, and therefore these kinases may be a novel therapeutic avenue in DLBCL especially the ABC subtype with high expression of phosphorylated STAT3.

Acknowledgements

First and foremost I would like to sincerely thank my supervisor Simon Wagner. He has provided me with the most excellent guidance and advice throughout the entirety of my project, and for that I will always be grateful.

Secondly, I would like to thank my supervisors Trevor Perrior and Katie Chapman from Domainex for their input and support throughout this project.

Thirdly, my thanks to my PhD committee, Drs Ildiko Gryory and Patricia Muller for their guidance throughout this project.

I wish to thank members of the Wagner laboratory both past and present. In no particular order, Dr Daniel Beck, Amy Wilson, Dr Katie Wickenden, Dr Eleni Ladikou, Dr Elliot Byford, Afaf Al-Harthi, Dr Rebecca Allchin, Nadia Nawaz and Dr Sami Mamand have all helped me in numerous ways throughout this PhD, and their help and support cannot be forgotten. Particular thanks to Dr Larissa Lezina who has provided continuous support, both technically and emotionally.

Throughout this project I have been fortunate enough to benefit from the facilities provided by the MRC Toxicology unit and the University of Leicester. Special thanks must be given to Paul Alexander for assistance with all aspects of cell culture. I would like to thank Jenny Edwards, Madhu Das and Leah Officer for their assistance with tissue staining. My sincere thanks go to the many technical staff who have provided an excellent working condition throughout the entirety of this project.

My family and friends have been a constant source of support, without which I would unlikely be in a situation to undertake this PhD. I can never forget the help they have given me.

Finally, my deepest thanks go to Trisha. Her unwavering love and support has helped me immeasurably and I cannot thank her enough.

Table of contents

List of tables

List of figures

List of abbreviations

ABC - Activated B-cell

AID - Activation induced deaminase

BCA - Bicinchoninic acid assay

BCR - B-cell receptor

BSA - Bovine serum albumin

BTK - Bruton's tyrosine kinase

cGAMP - Cyclic guanosine monophosphate-adenosine monophosphate

cGAS - Cyclic guanosine monophosphate-adenosine monophosphate synthase

CHOP - Cyclophosphamide, adriamycin, vincristine and prednisolone

CIA - Collagen 2 induced rheumatoid arthritis

COO - Cell of origin

cRNA - complementary RNA

CTG - CellTiter-Glo®

DAB- 3, 3'Diaminobenzidine

DLBCL - Diffuse large B-cell lymphoma

DMX - Domainex

DPX - Di-N-Butyle Phthalate in Xylene

ECL - Electrochemiluminescene

EF - Embryonic fibroblast

ELISA - Enzyme-linked immunosorbent assay

FCS – Foetal calf serum

GCB – Germinal centre B- cell

GSEA - Gene set enrichment analysis

IHC - Immunohistochemistry

IKBKE, IKK-I, IKKε - Inhibitor of nuclear factor kappa-B kinase subunit epsilon

IKK - IκB kinase

IKK - Inhibitor of nuclear factor kappa-B kinase

IL - Interleukin

Interferon - IFN

IRF – Interferon regulatory factor

ISG – Interferon stimulated gene

ISRE - Interferon stimulated response element

IκB - Inhibitor of NF-κB

JAK - Janus kinase

MAVS - Mitochondrial antiviral signalling protein

MeV - Multiple experiment viewer

MSigDB - Molecular signature database

NF-κB - Nuclear factor kappa-light-chain-enhancer of activated B cells

NGS - Next generation sequencing

NHL - Non Hodgkin's lymphoma

NIK – NF-κB inducing kinase

NSCLC - Non-small cell lung cancer

PAMP- Pathogen associated molecular pattern

PARP – Poly ADP ribose polymerase

PBS - Phosphate buffered saline

PDAC - Pancreatic ductal adenocarcinoma

PDK1 - 3-phosphoinositide-dependent kinase 1

PDX - Patient derived xenograft

R-CHOP - Rituximab, cyclophosphamide, adriamycin, vincristine and prednisolone

RHD - Rel homology domain

RIG-1 - Retinoic acid inducible gene-1

RIPA - radioimmunoprecipitation

RSEM - Mean RNA-Seq by expectation maximum

RT -Reverse transcription

SAM - Statistical analysis for microarrays

SLE - Systemic lupus erythematosus

STAT – Signal transducer and activator of transcription

STING - Stimulator of interferon genes

TBK1 – TANK binding kinase 1

TCGA - The cancer genome atlas

TLR - Toll like receptor

TRIF - TIR domain-containing-adapter inducing IFN

Chapter 1 - Introduction

1.1 Lymphoma

Lymphoma is a malignancy of mature lymphocytes – specialised cells of the immune system normally involved in the adaptive immune response (Young and Staudt, 2013). Lymphocytes are of either T-cell or B-cell lineage and despite the approximately equal numbers of B and T lymphocytes in the body, roughly 95% of all lymphomas are of B-cell origin (Kuppers, 2005).

Lymphocytes are characterised by surface markers detectable by staining with diagnostic antibodies, which allow separation of lineages i.e. T- and B-cells and the distinction of different stages of development (Foon et al., 1982).

Patients generally present with painless lymphadenopathy accompanied by features suggesting malignancy such as weight loss, fevers and night sweats. Diagnosis requires lymph node biopsy and immunohistochemistry with panels of antibodies designed to aid in the identification of the many subtypes (Swerdlow et al., 2016).

1.1.1 B-cell lymphoma

Normal germinal centres are recognised histologically as areas of intense B-cell proliferation with a dark zone containing proliferating cells (centroblasts) and a light zone that contains T-cells as well as B-cells (centrocytes). In the light zone, B-cells compete for survival signals by binding antigen on follicular dendritic cells or T-follicular helper cells (Gatto and Brink, 2010).

As well as being a site of B-cell proliferation, other processes requiring the enzyme activation induced deaminase (AID) are essential for normal immunity i.e. somatic hypermutation, and class switching also take place in the germinal centre (Gatto and Brink, 2010). This process selects for B-cells that have successfully gained mutations that lead to a higher affinity towards the antigen in question. In order to raise antibody affinity AID introduces point mutations into the DNA sequence of immunoglobulin genes and the generation of DNA single and double stranded breaks occur as part of its mechanism of action. The production of these breaks together with intense proliferation rates are believed to predispose the germinal centre to be a site of lymphoma formation (Figure 1.1) (Shaffer et al., 2002, Noia and Neuberger, 2007). Normal B-cells that are positively selected in the light zone can then

undergo differentiation into plasma cells, which exit the germinal centre to traffic to the bone marrow, or memory B-cells, which enter the circulation (Gatto and Brink, 2010).

1.1.1.1 B-cell Non-Hodgkin lymphoma

B-cell lymphomas are divided into two distinct categories, Hodgkin's or non-Hodgkin's. Hodgkin's lymphomas can either be classified as classical or nodular lymphocyte predominant, and are characterized by the presence of Reed-Sternberg or lymphocytic/histiocytic cells, respectively (Re et al., 2005). The majority of lymphoma diagnoses (~85%) are classified as non-Hodgkin lymphoma (NHL) (Smith et al., 2015).

Of all the cases of NHL diagnoses, the vast majority (85-90%) are derived from B-cells, with the remaining portion split between T or NK cells (Armitage et al., 2017). B-cell lymphomas are broadly divided into high-grade diseases with high rates of proliferation such as Burkitt lymphoma and diffuse large B-cell lymphoma (DLBCL) and low-grade disease such as follicular lymphoma, mantle cell lymphoma and small cell lymphocytic lymphoma. The most common subtypes are follicular lymphoma and DLBCL.

Although considered incurable, follicular lymphoma is, in most cases, an indolent disease characterised by long survival (Swenson et al., 2005). A subset of indolent follicular lymphoma can undergo transformation to DLBCL (Montoto and Fitzgibbon, 2011).

1.2 Diffuse large B-cell lymphoma

DLBCL is a highly heterogeneous disease at the clinical, genetic and morphological levels (De Paepe and De Wolf-Peeters, 2006). Standard treatment is with the combination chemotherapy regimen R-CHOP (rituximab, cyclophosphamide, adriamycin, vincristine and prednisolone) (described in more detail in Section 3 below). Some patients respond well to treatment while for others the disease resists chemotherapy (Coiffier et al., 2010). The molecular basis for the clinical heterogeneity has been investigated over the last twenty years by gene expression profiling and more recently by next generation sequencing.

1.2.1 Molecular classification of DLBCL

Technological advances at the turn of the millennium allowed gene expression analysis to be carried out by microarray (Duggan et al., 1999), and provided a platform for the molecular classification of DLBCL. These advancements led to DLBCL classification based on the proposed cell of origin of the disease (Alizadeh et al., 2000).

1.2.1.1 Classification by cell of origin (COO)

The cell of origin (COO) classification of DLBCL identifies subtypes based on similarities between the gene expression profile of normal B-cells and malignant B-cells.

The first comprehensive genome-wide gene expression analysis of DLBCL involved the characterization of ~100 primary DLBCL cases by their gene expression (Alizadeh et al., 2000). Unsurprisingly, this study revealed a large degree of heterogeneity in gene expression amongst DLBCL samples, which is reflective of the variation seen in disease phenotype. However, a striking result from this study was the discovery of two distinct sub-types of DLBCL whose gene expression profiles were each similar to separate stages of B-cell differentiation. One group had a gene expression profile characteristic of B-cells found within the germinal centre - germinal centre B (GCB) like DLBCL, whereas the other group had gene expression characteristic of activated peripheral blood B cells that had exited the germinal centre reaction – activated B cell-like (ABC) DLBCL (Alizadeh et al., 2000).

The distinction between GCB and ABC like DLBCL represented a major step forward in the classification of DLBCL and has been a cornerstone of subsequent DLBCL research. This finding was validated in a later study, again, utilising DNA microarray technology, which successfully identified the previously defined GCB and ABC like subtypes of DLBCL in 240 patients (Alizadeh et al., 2000, Rosenwald et al., 2002). Additionally, a third sub-group based on gene expression was identified which contained tumours which did not highly express GC or ABC associated gene sets, and was termed ‘type 3 DLBCL’.

Further refinement of gene expression analysis resulted in the production of a 27-gene panel whose expression related to the probability of a DLBCL falling into GCB, ABC or type 3 DLBCL. (Wright et al., 2003). Collectively, these studies formed the basis of the cell of origin (COO) classification of DLBCL (Abramson and Shipp, 2005).

An overview of the germinal centre reaction and the stages at which GCB and ABC DLBCL are thought to be derived is presented in Figure 1:1.

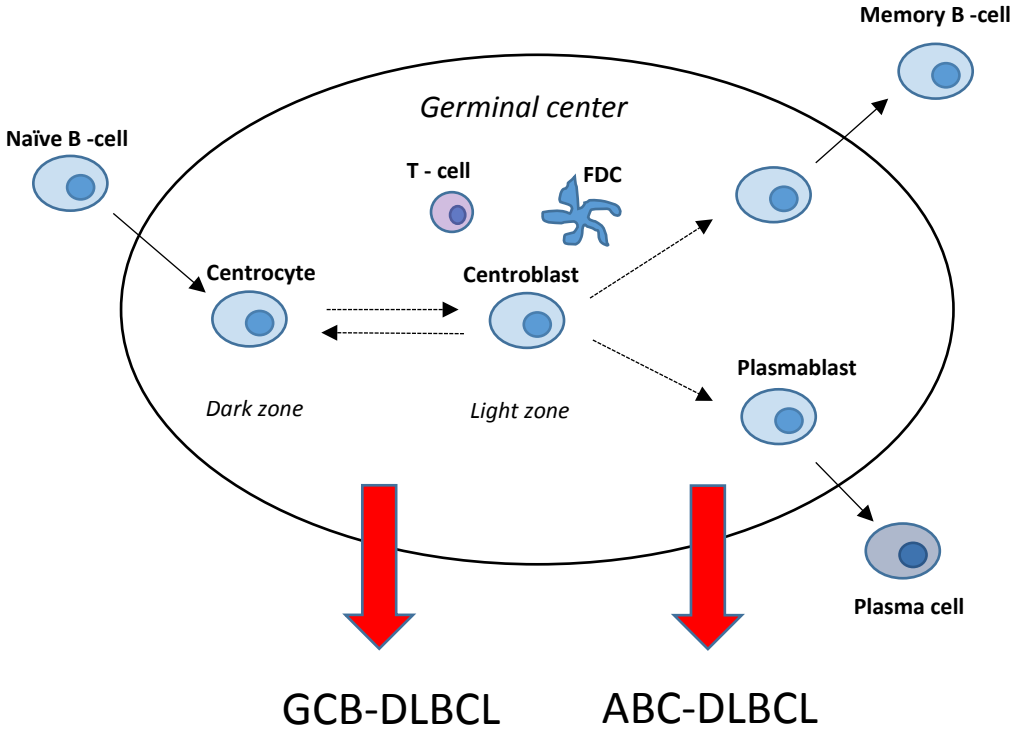

Figure 1:1. An overview of the germinal centre reaction and the stages at which the GCB and ABC subtypes of DLBCL are thought to be derived. Adapted from (Camicia et al., 2015).

1.2.1.2 COO classification as a predictor of prognosis

GC and ABC DLBCL subtypes also showed a stark contrast in overall patient survival with GCB like DLBCL being associated with a more favourable prognosis (Alizadeh et al., 2000).

Echoing previous associations between GC DLBCL status and favourable prognosis (Alizadeh et al., 2000), Rosenwald et al, (2002) presented 5-year survival rates as 60%, 35% and 39% for GC DLBCL, ABC DLBCL and type 3 DLBCL, respectively. Importantly, this study demonstrated that gene expression levels of a panel of genes taken from biopsy was an

accurate predictor of survival, and that this prediction may prove more effective than the international prognostic index in stratifying DLBCL patients (Rosenwald et al., 2002).

It was subsequently demonstrated that gene expression profiling could be carried out on formalin-fixed, paraffin-embedded tissue, and that association between ABC DLBCL gene expression and poorer prognosis remained true (Hans et al., 2004, Rimsza et al., 2008).

1.2.1.3 Other gene expression classifications

A slightly later gene expression study identified three discrete subsets of DLBCL termed "OxPhos", "B- cell receptor (BCR)/proliferation" and "Host response (HR)"(Shipp et al., 2002). The OxPhos cluster of was enriched for genes involved in oxidative phosphorylation and the function of mitochondria. BCR/proliferation DLBCLs were characterized by enrichment for the expression of genes involved in the BCR pathway and cell cycle regulation. The third cluster, the HR group, had abundant expression of genes associated with the host response such as the T/NK cell activation, complement activation, and antigen processing (Monti et al., 2005).

Others have shown that a classification based on stromal cell signatures can predict clinical outcome (Lenz et al., 2008b).

Despite this work, the COO system remains the most widely used form of DLBCL classification and it has been used to inform the design of clinical trials (e.g. REMoDL-B tested the addition of bortezomib to R-CHOP for patients classified as ABC DLBCL (Davies et al., 2015)) and interpret the results of clinical trials.

1.2.1.4 Implementing COO in the clinic

On account of the difficulty and expense of implementing gene expression analysis in clinical practice, several attempts have been made to accurately reproduce the proposed cell of origin classifications using widely available diagnostic techniques such as immunohistochemistry. Perhaps the most widely used method for the discrimination of DLBCL cases into GCB or non-GCB status is a three-protein immunohistochemistry based algorithm which tests for protein expression of CD10, BCL6 and MUM1 (Hans et al., 2004). An overview of this algorithm is shown in Figure 1:2.

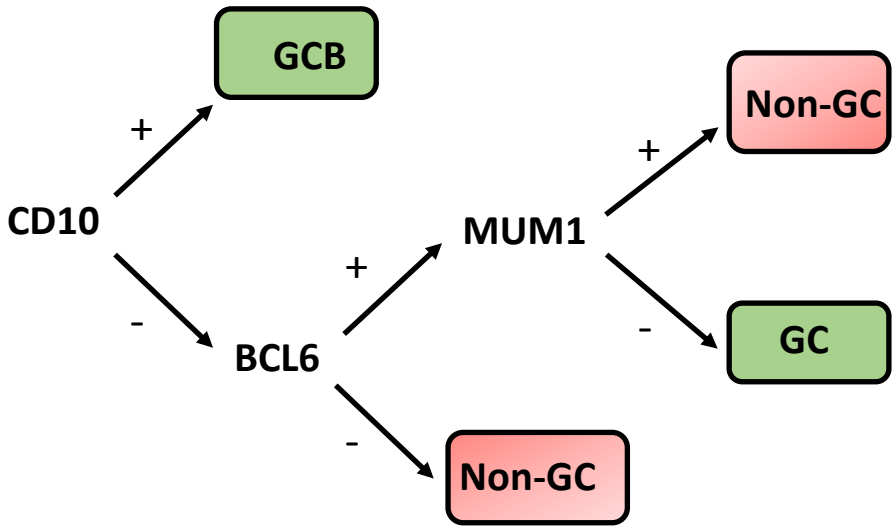

Figure 1:2. An overview of the immunohistochemistry staining algorithm developed by Hans et al., (2004) for the classification of DLBCL into GCB or non-GCB status.

However, there have been doubts about how reliably such immunohistochemistry based techniques reflect the gene expression profiling classification (Ott et al., 2010) and this is one reason why they have not yet found a place in routine patient management.

1.2.2 Molecular pathogenesis of DLBCL

As previously discussed, DLBCL is a clinically heterogeneous group of diseases, and it therefore comes as no surprise that a diverse range of oncogenes have been implicated in DLBCL pathophysiology.

There are a number of genetic lesions that are shared between both the GCB and ABC like DLBCLs.

1.2.2.1 P53

Due to its integral role as a tumour suppressor, mutations in *TP53*, the gene encoding P53 are detected in ~50% of all human malignancies (Levine and Oren, 2009). DLBCL is no exception to this, and ~22% of DLBCL patients harbour *TP53* mutations. These mutations occur in roughly equal proportions in GCB and ABC like DLBCL and their presence is associated with poor survival (Xu-Monette et al., 2012).

1.2.2.2 BCL6

BCL6 is a zinc finger transcription factor (Ye et al., 1993) transcriptional repressor (Chang et al., 1996), which is necessary for the formation of germinal centres, and is the most frequently involved oncogene in DLBCL (Ye, 2000). BCL6 translocations were associated with relatively good clinical outcomes in the earliest studies (Offit et al., 1994) an association that has been sustained in the era of gene expression as demonstrated by BCL6 being a key component of the GCB DLBCL signature (Alizadeh et al., 2000). There are several other routes to constitutive BCL6 expression in DLBCL including promoter mutations (Wang et al., 2002), deubiquitinase mutations (Duan et al., 2011) and acetyl transferase mutations (Pasqualucci et al., 2011a). Inactivating mutations in the acetyltransferase genes *CREBBP* and/or *EP300* occur in ~30% of DLBCL cases with a slight preference to GCB DLBCL. It is thought that these mutations contribute to lymphomagenesis through impaired acetylation of BCL6 and P53 (Pasqualucci et al., 2011a, Pasqualucci and Dalla-Favera, 2015).

As discussed, the germinal centres are areas in which B-cells undergo rapid proliferation and hypermutation of their immunoglobulin and BCL6 is thought to foster these interactions by repressing the DNA damage response (Phan and Dalla-Favera, 2004), promoting proliferation and preventing differentiation (Reljic et al., 2000, Fearon et al., 2001, Tunyaplin et al., 2004).

1.2.2.3 Histone modification

Mutations in the histone methyltransferase *EZH2* are relatively common (~22% of cases) in GCB like DLBCL, but are not present in ABC like DLBCL (Morin et al., 2010). These mutations are thought to alter the catalytic activity of EZH2 leading to a shift in increased histone methylation and subsequent gene repression of regulatory genes which may lead to lymphomagenesis (Sehn and Gascoyne, 2015). Mutations in *MLL2*, another methyltransferase occur in 1/3 of DLBCL, and the majority of which are thought to be inactivating mutations. These, like *EZH2* mutations, are thought to contribute to lymphomagenesis by remodelling of the epigenome.

1.2.2.4 Next generation sequencing

Recent studies involving next generation sequencing (NGS) have allowed a more in depth analysis of the genetic drivers of DLBCL. NGS analysis of ~600 DLBCL samples led to the description of four distinct groups of DLBCL characterised by their genetic lesions (Schmitz et al., 2018). These groups included the 'MCD' group which showed co-occurrence of *MYD88* and *CD79b* mutations – the functional consequence of which will be discussed in section 2.3.2.1. Other groups included the 'BN2 group' which presented with *BCL6* fusions and *NOTCH2* mutations. The 'N1' group showed *NOTCH*1 mutations, while the 'EZB' group showed the presence of *EZH2* mutations with *BCL2* translocations (Schmitz et al., 2018). At a similar time, Chapuy et al., (2018) identified 5 distinct groups of DLBCL patients through NGS technologies. Several of these mirrored those seen by Schmitz et al., (2018), but some were unique including 'C2' DLBCLs which were characterised by frequent inactivating mutations in *TP53*. This study also identified a group of largely GCB DLBCL tumours which harboured mutations in NF-κB modifiers and RAS/JAK/STAT pathway members – termed 'C4' DLBCLs (Chapuy et al., 2018).

Reddy et al., (2017) tied NGS technology with functional CRISPR screens to identify driver mutations in DLBCL. This study revealed 150 driver mutations in DLBCL, with many belonging to genes who contribute to signalling pathways (Reddy et al., 2017).

1.2.3 Signalling pathways in DLBCL

Several distinct cell signalling pathways have been shown to be essential for the survival of subsets of DLBCL's and include PI3K-AKT (Ennishi et al., 2016), NF-κB (Davis et al., 2001), and JAK/STAT (Ding et al., 2008) signalling pathways.

Of particular relevance to this project are survival pathways often associated with the ABC subtype of DLBCL which include, NF-κB signalling, JAK/STAT signalling. These pathways and their relevance to DLBCL will be discussed in more detail.

1.2.3.1 NF-κB signalling

The transcription factor nuclear factor-κB (NF-κB) is essential for immune and inflammatory responses (Baeuerle and Baltimore, 1996). There are five members of the NF-κB family of transcription factors: p105/50, p100/52, p65 (RelA), c-Rel and RelB. All family members contain a N-terminal Rel homology domain (RHD) which allows them to bind as dimers to kB sites found within the promoter regions of target genes and promote transcription (Hayden and Ghosh, 2008).

NF-κB dimers are regulated by a family of proteins called the inhibitors of NF-κB (IkBs) which contain IkBα, IkBβ, IkBε and BCL3. The IkBs all contain ankyrin repeats which are able to interact with the RHD domains of NF-κB sub units. This interaction results in the sequestration of the NF-κB in the cytoplasm and thus prevents entry to the nucleus and transcriptional activation. IkBα, IkBβ and IkBε each contain two conserved serine residues which are targets of the IkB kinase (IKK) family. The IKKs are able to phosphorylate the conserved serine residues on the IkB proteins which leads to their proteasome-dependent degradation. The degradation of IkB proteins releases NF-κB subunits to translocate to the nucleus where they can subsequently enhance the transcription of NF-κB target genes (Dolcet et al., 2005).

NF-κB signalling has traditionally been split into canonical or non-canonical signalling. Canonical NF-κB signalling is characterised by NF-κB dimers containing either RelA or c-Rel coupled with P50 held in an inactive state in the cytoplasm by IkBs. Upon activation by ligands such as TNFα or IL-1β, the IKK complex (consisting of IKKα, IKKβ, and the regulatory subunit NEMO) phosphorylates (largely through IKKβ) the IkB proteins leading to ubiquitin-dependent proteasomal degradation (Dolcet et al., 2005, Chen, 2005).

Alternatively, the non-canonical pathway is typically activated by a subset of tumour TNF receptor family members such as LTβR and BAFFR (Sun, 2010). NF-κB dimers involved in non-canonical signalling consist of RelB and p100 subunits. The p100 subunit is processed by IKKα and the NF-κB inducing kinase (NIK). This results in the proteolysis of p100 forming the p52 subunit. This allows a RelB/p52 dimer to translocate to the nucleus (Dolcet et al., 2005, Sun, 2010).

An overview of both canonical and non-canonical NF-κB signalling is presented in Figure 1:3.

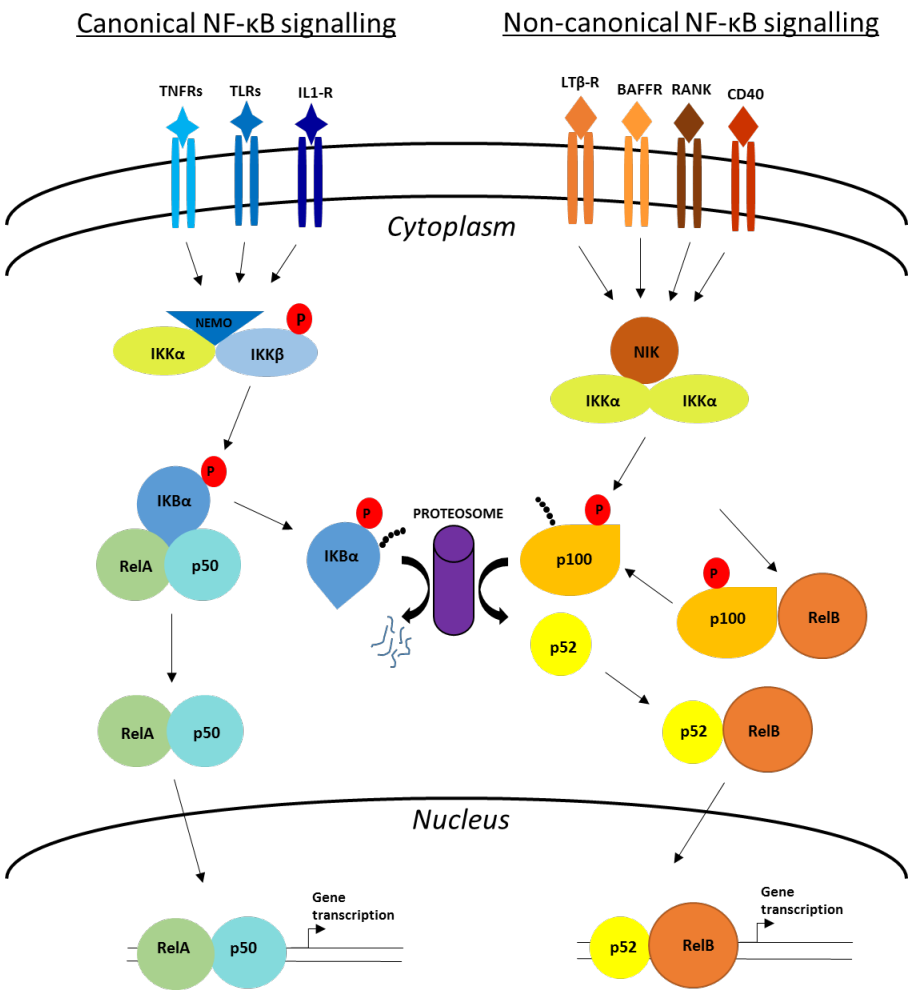

Figure 1:3. A simplified overview of canonical and non-canonical NF-κB signalling. Adapted from (Williams et al., 2014) and (Sun, 2010).

1.2.3.2 NF-κB in DLBCL

An early study examining the differences in survival pathway signalling between GC and non-GC DLBCL cell lines identified NF-κB signalling as a hallmark of ABC DLBCL (Davis et al., 2001).

1.2.3.2.1 Mechanisms of activation of NF-κB in DLBCL

Several key genetic mutations in genes such as *CARD11*, *MYD88*, *TNFAIP3* and *CD79b* have been identified which are thought to lead to the constitutive NF-κB signalling so often seen in non-GC DLBCL (Pasqualucci et al., 2011b).

TNFAIP3, also known as A20 is a protein with a known function as a suppressor of NF-κB signalling (Lee et al., 2000, Zhang et al., 2000). Chromosomal deletion has been observed in NHLs, including DLBCL, where it is unsurprisingly more associated with the ABC like subtype of the disease (Honma et al., 2009). Re-introduction of A20 into A20 deficient cells was sufficient to trigger apoptosis, and knockdown of A20 was shown to induce constitutive NF-κB activation. The loss of A20 can be attributed to chromosomal deletion, mutation or epigenetic modification (Honma et al., 2009), and 30% of DLBCL have a bi-allelic loss of *A20* (Compagno et al., 2009).

CARD11, also known as CARMA1 forms a signalling scaffold with MALT1 and BCL10 (the CBM complex) and induces NF-κB activity via activation of IκB kinase β in antigen stimulated lymphocytes (Rawlings et al., 2006). Through a shRNA screen, CARD11 was identified as having an essential role in NF-κB signalling in non-GC DLBCL cell lines (Ngo et al., 2006). Examination of coding exons of *CARD11* in DLBCL biopsies revealed somatic mutations which affected the coiled-coil (activating) domain of *CARD11* in ~ 10% and 4% of non-GC and GC DLBCL biopsies, respectively. Introduction of these coiled-coil mutants into lymphoma cell lines was sufficient to constitutively activate NF-κB activity (Lenz et al., 2008a). However, as *CARD11* mutations occur only in a small percentage of non-GC DLBCL, yet it's activity is essential for NF-κB signalling in these lymphomas, there must be an alternative mechanism of CARD11 activation in ABC like DLBCL (Davis et al., 2010).

The mechanism by which wild type *CARD11* becomes activated in ABC like DLBCL was identified as chronic signalling through the BCR (Davis et al., 2010). In resting B-cells, the BCR is responsible for maintaining homeostasis, and upon antigen binding, directs cells into

the cell cycle and differentiation (Rickert, 2013) .Signalling is mediated through the CD79a/CD79b heterodimer which becomes phosphorylated by Src family kinases upon antigen stimulation. Binding of the tyrosine kinase SYK to phosphorylated CD79a/b triggers a signalling cascade involving Bruton's tyrosine kinase (BTK), among others, ultimately leading to the phosphorylation of CARD11 and the subsequent formation of the CBM complex and NF-κB activation (Dal Porto et al., 2004). By means of a RNA interference screen, Davis et al., (2010) identified a kinase component of the BCR pathway – BTK, is essential for the survival of wild type *CARD11* ABC-DLBCL cell lines. Several proximal BCR subunits including CD79a and CD79b were also shown to be essential for the survival of these cells. Mutations in *CD79b* were found in 21% of ABC DLBCL compared to only 3% of GC DLBCL. Analysis of these mutations showed that they prevent negative autoregulation of BCR signalling and therefore lead to chronic active BCR signalling (Davis et al., 2010).

MYD88 functions as an adaptor protein between Toll-like receptors (TLRs) and NF-κB signalling. In brief, upon TLR activation, MYD88 forms protein complexes involving IRAK proteins and TRAF6. The activation of TRAF6 allows further complex formation and activation of TAK1 which is able to phosphorylate the traditional IKK complex and lead to subsequent NF-κB activation (Akira and Takeda, 2004).

Ngo et al., 2010 reported that shRNA targeting MYD88 was toxic to non-GC but not GC cell lines (Ngo et al., 2010). From sequencing of the *MYD88* coding region in lymphoma biopsy samples, a recurring mutation (L265P) was detected in 29% of all non-GC DLBCL biopsies. Non-GC cell lines were shown to be dependent on this mutation for survival. The mutant was demonstrated to be responsible for the assembly of a complex containing IRAK1 and IRAK4, and knockdown of MYD88 L265P in a non-GC cell line reduced NF-κB and STAT3 gene signalling along with interleukin (IL) 6, IL-10 and IFN-B secretion (Ngo et al., 2010).

By introducing a form of IKβ that cannot be phosphorylated by IKKβ, and therefore repressing NF-κB activity, Lam et al. 2008, identified that the cytokine genes, *IL10* and *IL6* were NF-κB target genes in the non-GC representing cell lines Ly10 and Ly03, respectively (Lam et al., 2008). This is of particular interest as both IL-6 (Hirano et al., 2000) and IL-10 (Riley et al., 1999) are known drivers of Janus kinase (JAK)/ signal transducer and activator of transcription (STAT) signalling- a known survival pathway in DLBCL.

1.2.3.3 JAK/STAT/IL-10 signalling

As with NF-κB signalling, JAK-STAT signalling is an essential component of the immune response (Shuai and Liu, 2003).

There are seven known members of the STAT family found in humans – STATs 1, 2, 3, 4, 5a, 5b, and 6 (Schindler et al., 2007).

Upon activation of cell surface receptors by ligand binding, JAK family members (JAK1, JAK2, JAK3 and Tyk2) become recruited. Auto phosphorylation of JAKs leads to activation and subsequent phosphorylation of cytoplasmic receptor tails. These phospho-tyrosines recruit cytoplasmic STAT monomers which subsequently become phosphorylated on their own tyrosine residues, inducing dimerization between two phosphorylated STAT monomers. These dimers are then able to translocate to the nucleus where they are able to bind to specific target regions in the promoters of genes and ultimately lead to enhancement of their transcription (Bowman et al., 2000). In addition to the canonical JAK mediated phosphorylation of Tyrosine residues, all STAT family members (except STAT2) may be phosphorylated at conserved serine residues found within their transcriptional activation domains. An array of protein kinases are able to phosphorylate these serine residues and serine phosphorylation is thought to regulate transcriptional activity (Schindler et al., 2007).

Upon their activation, the roles played by the STAT family members varies often with a high degree of pleiotropy. For example, STATs 1 and 2 respond to type 1 interferon signalling and their target genes influence both inflammatory responses and reduce proliferation (Schindler et al., 2007).

STAT3 is known to regulate expression of genes involved in cell cycle progression, anti-apoptosis and angiogenesis (Calo et al., 2003). It is therefore no surprise that persistent activation of STAT3 has been shown to increase proliferation and survival in several human cancers (Yu et al., 2009).

1.2.3.3.1 STAT3 signalling in DLBCL

Ding et al., (2008) show that STAT3 expression and phosphorylation at Y705 is detected primarily in non-GC but not GC cell lines. Phosphorylation of STAT3 at S727 was only detectable in non-GC cell lines. This association holds true in primary DLBCL cases where there was a significant association between non-GC status and STAT3 expression.

Additionally it was reported that inhibition of STAT3 by a JAK inhibitor induced cell cycle arrest and apoptosis in non-GC cell lines but not GC cell lines (Ding et al., 2008)

Immunohistochemistry (IHC) analysis of phospho-tyrosine STAT3 in 185 DLBCL patients showed detection in 37% of DLBCL cases, with a statistical enrichment for non-GC DLBCL. Additionally, this expression was significantly associated with a poor overall and event free survival (Huang et al., 2013). Furthermore, high nuclear expression of STAT3 was found to be significantly associated with poor survival in a DLBCL cohort (Wu et al., 2011).

Inhibition of STAT3 via short hairpin RNAs specific for STAT3 has proven lethal for ABC DLBCL mouse models *in vivo* through inhibition of proliferation and induction of apoptosis. Additionally, use of two small molecule inhibitors of STAT3 also showed anti-tumour effects *in vivo* (Scuto et al., 2011).

1.2.3.3.2 Mechanisms of action of STAT3 in DLBCL

Unlike NF-κB, mechanisms of STAT3 activation in DLBCL are not well characterized. The activation of STAT3 in ABC DLBCL appears to be dependent on MYD88 activity induced secretion of IL-6 and IL-10 through NF-κB signalling (Ngo et al., 2010). Further studies have supported this view and shown that activation of STAT3 in DLBCL is dependent on autocrine production of cytokines by lymphoma cells – most notably IL-10 (Lam et al., 2008, Gupta et al., 2012).

1.2.3.4 Interleukin 10

IL-10 was detected by enzyme-linked immunosorbent assay (ELISA) as a cytokine produced by malignant B lymphocytes in the early 1990's (O'Garra et al., 1990). Detectable levels of IL-10 in NHL patients was subsequently demonstrated to be a significant factor in poor prognosis and correlated with shorter survival and progression free survival (Blay et al., 1993).

In a later study, IL-10 was detectable by IHC techniques in ~ 50% of NHLs, and in the supernatants of purified B NHL cells from ~ 40% of patients. In addition, patients who exhibited secreted IL-10 in the supernatants of their cultured tumour cells also displayed increased IL-10 levels in their serum (Voorzanger et al., 1996).

IL-10 was shown to be a requisite factor for the progression of B-cell lymphoma in a knockout mouse model using NZB mice, a model which spontaneously develops B-cell malignancy in an age related manner (Czarneski et al., 2004).

Gupta et al., (2012) examined pre-treatment levels of JAK/STAT pathway associated cytokines IL-6, IL-10, IL-2 and EGF from the serum of 70 DLBCL patients. Of these secreted cytokines IL-10 and IL-6 were significantly higher in DLBCL patients compared to healthy controls, and of the two, only IL-10 could induce phosphorylation of JAK2 and STAT3 in SUDHL2 cells *in vitro*. When DLBCL patients were stratified into those with high and low IL-10 serum levels, those with high levels had a significantly shorter event free survival than the patients in the 'low' IL-10 group (Gupta et al., 2012).

IL-10RA and IL-10RB were found to be significantly overexpressed at the gene and protein level in primary DLBCL, a pattern reflected in DLBCL cell lines. High gene expression levels of IL-10 and IL-10R were found to be predictors of poor progression free-survival on a cohort of DLBCL patients. While ABC cell lines secreted more IL-10 than their GC counterparts, all DLBCL cell lines analysed secreted detectable levels of IL-10 into culture supernatant. Additionally, inhibiting IL-10 signalling by blocking the IL-10 receptor reduced the viability of most DLBCL cell lines treated. Cells treated with IL-10 receptor blocking antibodies were found to undergo cell cycle arrest and subsequent apoptosis due to inhibition of an IL-10 auto stimulatory loop mediated by JAK/STAT signalling (Beguelin et al., 2015).

1.2.3.5 Chemokines and growth factors in DLBCL

Lossos et al., (2004) took 36 genes previously reported for their ability to predict survival in DLBCL, assessed their expression by qPCR in a cohort of patients, and then ranked these genes on their ability to predict survival. They then produced a list of six genes which had high predictive power in DLBCL. The expression of *LMO2*, *BCL6* and *FN1* were predictive of longer survival, whereas the expression of *BCL2*, *CCND2* and *SCYA3* (also known as *MIP-1-alpha*/*CCL3*) were predictive of short survival (Lossos et al., 2004). CCL3 and CCL4 have been shown to be secreted by ABC like DLBCL cell lines, and that BCR signalling is required for this (Lossos et al., 2004). A separate study also demonstrated that high serum levels of CCL3 and CCL4 in patients with DLBCL corresponded with poor prognosis. The serum levels of CCL3 and CCL4 were, however, found to be independent of GCB/ABC classification (Takahashi et al., 2015).

In addition to CCL3 and CCL4, TNFα and IL-6 have also been shown to be associated with ABC DLBCL (Pedersen et al., 2005). A separate study identified significantly elevated levels of 14 different cytokines and growth factors in DLBCL patient sera (Charbonneau et al., 2012).

It is clear from the above studies that DLBCL cases can secret a host of cytokines. However, little work has been carried out to characterise a functional role for these secreted molecules.

1.3 Current and investigational treatments of DLBCL

The regimen of cyclophosphamide, adriamycin, vincristine and prednisolone (CHOP) was the standard treatment for those with DLBCL (Sehn and Gascoyne, 2015, Fisher et al., 1993). Treatment with this regimen was able to cure a subgroup of late stage NHL, with a reported 53% remission rate and a 30% survival after 12 years (Fisher et al., 1993). A major improvement in DLBCL came following the use of Rituximab, a monoclonal antibody specific against the B-cell antigen, CD20.The use of Rituximab was first reported in elderly DLBCL patients where addition of Rituximab to the CHOP regimen led to a 13% increase in complete response compared to those treated with CHOP alone (76% vs. 63%) (Coiffier et al., 2002). Several subsequent studies confirmed the benefit of adding Rituximab to CHOP (R-CHOP) (Habermann et al., 2006, Pfreundschuh et al., 2008, Sehn et al., 2005), and it is now the standard treatment regimen with those with DLBCL (Armitage et al., 2017).

1.3.1 The need for novel therapies in DLBCL

Despite the success of R-CHOP treatment for many patients, there still remains an unmet clinical need for patients who do not respond to R-CHOP therapy. Owing to this, there are numerous targeted therapies under investigation for their use in the treatment of DLBCL.

1.3.1.1 Targeting NF-κB in DLBCL

Targeting NF-κB was validated a therapeutic avenue in ABC-DLBCL by Lam et al., (2005) who demonstrated that drug based inhibition of the IKK complex is lethal for a ABC like DLBCL cell lines (Lam et al., 2005). Pre-clinical models of DLBCL have also shown that drug inhibition of IKKβ is lethal for lymphoma models *in vivo,* which is dependent on NF-κB

activity (Deng et al., 2014a). In the clinical setting, two drugs – ibrutinib and bortezomib, have been the focus of intense study in limiting NF-κB activity in DLBCL.

1.3.1.2 Ibrutinib

Building on the discovery that BTK was an essential part of BCR signalling in ABC-DLBCL cells, attempts have been made to use the BTK inhibitor – ibrutinib, in the DLBCL setting (Davis et al., 2010). Ibrutinib has been shown to be lethal for ABC DLBCL cell lines *in vitro* through inhibition of NF-κB activity (Davis et al., 2010, Yang et al., 2012). In a phase 1/2 clinical trial of relapsed/refractory DLBCL patients, ibrutinib therapy achieved partial or complete responses in ~40% of cases, the majority of which were ABC DLBCL cases (Wilson et al., 2015)

1.3.1.3 Bortezomib

Bortezomib is a proteasome inhibitor which is currently approved for the treatment of multiple myeloma in the US and Europe. The mechanism of action of bortezomib is thought to involve inhibition of the proteasome, thus preventing degradation of IkBα leading to subsequent retention of NF-κB subunits in the cytoplasm (Murray et al., 2014).

There have been several clinical trials, including REMoDL-B (mentioned in Section 1.2.1.3, (Davies et al., 2015)) assessing the potential of bortezomib in the DLBCL setting. Early clinical data showed that addition of bortezomib to R-CHOP in untreated DLBCL patients was beneficial and suggested improved survival in the ABC DLBCL patients (Ruan et al., 2011). However, subsequent clinical trials have failed to show a benefit of the addition of bortezomib to R-CHOP therapy (Leonard et al., 2015). The use of bortezomib therefore remains contentious and has yet to enter widespread clinical use.

1.3.1.2 Targeting STAT3 in DLBCL

Compared to targeting the NF-κB pathway in, inhibition of JAK/STAT signalling has been less explored in DLBCL.

Treatment with a JAK inhibitor *in vitro* was shown to be lethal for ABC DLBCL cell lines (Lam et al., 2008). A later study confirmed this by showing treatment with the JAK1/2 inhibitors AZD1480 or ruxolitininb resulted in apoptosis in ABC DLBCL cell lines (Rui et al., 2016). Despite promising potential for the use of JAK inhibitors as a means of inhibiting STAT3 signalling, little progress has been made clinically.

1.4 Identification of IKKε/TBK1 inhibitors as potential novel therapeutics in DLBCL

To attempt to discover novel candidate agents for the treatment of DLBCL, Beck *et al*., (2016), performed a small molecule screen against a conditionally BCL6-deficient Burkitt lymphoma cell line. The purpose of this screen was to highlight inhibitors which were active in BCL6 deficient cells, while remaining relatively inactive in BCL6 positive cells, and thus identify inhibitors which may be preferentially active against non-GC DLBCL (Beck et al., 2016). This study focussed on JAK2 inhibitors, however, several novel dual inhibitors of the kinases IKKε and TBK1 were identified as showing activity predominantly against BCL6 non-expressing cells (Wagner Laboratory, unpublished data).

Neither IKKε nor TBK1 have previously been identified as potential therapeutic targets in DLBCL, and a role for either kinase in B-cell lymphoma has not been described. That said, both kinases have been shown to be important in the pathogenesis of several human malignancies, and their functions in health and disease overlap with many of the survival pathways seen in DLBCL.

1.4.1 IKKε and TBK1

Inhibitor of nuclear factor kappa-B kinase subunit epsilon (IKKε) and TANK binding kinase 1 (TBK1) are structurally related pair of kinases which belong to the IKK family - the family of kinases conventionally linked to regulation of the NF-κB pathway. Both IKKε and TBK1 however have characterized roles in the interferon response in addition to being NF-κB effectors (Shen and Hahn, 2011).

1.4.1.1 Discovery and structure

Shimada et al. (1999) observed that upon stimulation with LPS, the expression of the *KIAA0151* gene product was induced in macrophage cells. This gene product was subsequently identified as a protein kinase whose catalytic domain shared a 30% identity with the catalytic domain of IKKβ and was referred to as IKK-i (Shimada et al., 1999).

Independent of this study but at a similar time, Peters et al. (2000) also identified the product of the gene *KIAA0151* as a homolog of IKKα and IKKβ. The group identified an amino acid identity of 33% and 31% with the kinase domain of IKKα and IKKβ, respectively, and named the kinase IKKε (Peters et al., 2000)

At a similar time, TBK1, was first identified from a two-hybrid screen using TANK as bait. TBK1 was characterised as a protein kinase, with a 27% identical and 45% similar homology to IKKα and IKKβ. TBK1 was shown to be able to activate the NF-κB pathway and form a complex with TANK and TRAF2 (Pomerantz and Baltimore, 1999).

In addition to their structural homology to the canonical IKKs, IKKε and TBK1 have been shown to exhibit a high degree of homology to each other. There has been a described homology of 49% amino acid identity between IKKε and TBK1 (Pham and TenOever, 2010). The homology between members of the IKK family is summarised in Figure 1:4.

Figure 1:4. The structural homology between the IKK family members. Adapted from (Pham and TenOever, 2010).

1.4.1.2 Expression of IKKε and TBK1

Despite their structural similarity, IKKε and TBK1 have differing expression patterns. IKKε expression has been found to be predominantly limited to the tissue of the immune system (thymus, spleen, placenta and pancreas), with T-cells constitutively expressing IKKε, whereas B cell populations expressed IKKε in an inducible fashion as a response to LPS (Shimada et al., 1999). TBK1 on the other hand has been shown by northern blot analysis of human tissue to be ubiquitously expressed (Tojima et al., 2000).

1.4.2 The functions of IKKε and TBK1

A diverse range of functions for both IKKε and TBK1 have been described in health and disease. Perhaps the most intensely studied area is their role in regulating NF-κB and the type 1 interferon response.

1.4.2.1 IKKε/TBK1 as regulators of the type 1 interferon response

Initiation of the interferon response begins by detection of pathogen-associated molecular patterns (PAMPs) by cell receptors. This can include detection of viral RNA by retinoic acid

inducible gene-1 (RIG-1) like receptors (Mitsutoshi and Takashi, 2009), cytosolic DNA by cyclic guanosine monophosphate–adenosine monophosphate (cGAMP) synthase (cGAS) (Sun et al., 2013), or more broad ligand detection by TLRs (Akira et al., 2006). These receptors then utilise adaptor proteins such as mitochondrial antiviral signalling protein (MAVS) and stimulator of interferon genes (STING) in the case of RIG-1 and cGAMP activation, respectively (Vazquez and Horner, 2015, Sun et al., 2013). In the case of TLR activation by viral detection, the adaptor protein TRIF is required for downstream activation of the interferon response (Akira et al., 2006).

The subsequent interferon response is characterised by activation of several transcription factor families, including, but not limited to NF-κB, interferon regulatory factors (IRFs) and STATs. Activation of these transcription factors leads to enhanced transcription of a set of immune-regulatory genes, including the type 1 interferons- largely interferon (IFN) β and α (Grandvaux et al., 2002). IFN γ may also be secreted in the antiviral response, and is classed as a type 2 interferon (Platanias, 2005) . Secretion of interferons then leads to a secondary process where interferon binding at cell surface receptors results downstream activation of IFN stimulated genes (ISGs) via JAK/STAT signalling (de Veer Michael et al., 2001). Type 1 interferon binding at the type 1 interferon receptor causes activation of the JAKs JAK1 or TYK2. This activation leads to the phosphorylation of STAT1 and STAT2. This in turn results in the formation of either STAT1 homodimers or STAT1-STAT2-IRF9 complexes, referred to as IFN-stimulated gene factor 3 (ISGF3) complexes. ISGF3 complexes are able to translocate to the nucleus and bind interferon-stimulated response elements (ISREs), and enhance the transcription of ISGs. Type 2 interferon receptor activation activates JAK1 and JAK2 which leads to the formation of STAT1 homodimers exclusively. These STAT1 homodimers are able to bind IFN-γ-activated sites (GAS) elements of a subset of ISGs (Platanias, 2005). Gene expression analysis from cells treated with IFN α, β, or γ revealed that there are both shared and unique subsets of ISGs which are stimulated by type 1 or type 2 interferon signalling, respectively (Der et al., 1998).

Despite being members of the IKK family, the family canonically thought to activate NF-κB signalling, the best characterized role for both IKKε and TBK1 in antiviral immunity is their function as kinases necessary for IRF activation (Clément et al., 2008).

Both kinases have were shown to be essential for the TIR domain-containing-adapter-inducing IFN (TRIF) mediated activation of IRF3 - a transcription factor, which, as a response to viral infection is required for the expression of interferon beta (IFN-β) and

RANTES (CCL5) (Fitzgerald et al., 2003). The activation of IRFs is dependent upon phosphorylation at their C-terminal domain. Expression of IKKε, but not IKKα/β in HEK293 cells was sufficient to induce phosphorylation of IRF3 and IRF7 in an *in vitro* kinase assay. Expression of both IKKε and TBK1 was shown to be sufficient to induce phosphorylation and enhance both nuclear translocation and DNA binding of IRF3 and 7 (Sharma et al., 2003). Recent dissection of IRF3 signalling revealed that the RIG-1 activated adaptor protein MAVS was phosphorylated by IKKε and TBK1, whereas the STING adaptor protein (activated by cGAS), could only be phosphorylated by TBK1. Phosphorylated MAVS and STING then recruit and bind IRF3 which itself then becomes phosphorylated by TBK1. A similar TBK1 dependent mechanism was identified for TRIF, the adaptor protein activated by TLR3/4 (Liu et al., 2015).

Further advancements in the understanding of IKKε and TBK1 function came from the generation of *Ikbke* $^{-/-}$ and *Tbk1*$^{-/-}$ knockout mice. Work in embryonic fibroblasts (EFs) from knockout mice demonstrated that it is largely TBK1 that is crucial for the induction of IFN-β and ISGs upon TLR stimulation as well as virus infection (Hemmi et al., 2004). A separate study showed that the impaired IFN response of *Tbk1* $^{-/-}$ EFs can be restored by reconstitution with wild type IKKε – demonstrating redundancy between the kinases in the process (Perry et al., 2004). In a later study, compared to their wildtype counterparts, *Ikbke*$^{-/-}$ mice displayed hypersensitivity to viral infection. While no clear reduction in virally induced cytokines such as IFNα/β/γ was observed, there was a marked reduction in the expression of a subset of ISGs including *IFIT3*, *IFI203* and *ADAR1* upon viral infection. This places IKKε as being necessary not for the initial activation of the interferon response, but for the signalling resulting in full ISG transcription. Additionally, STAT1 was shown to be directly phosphorylated by IKKε (tenOever et al., 2007). Subsequent work demonstrated that this phosphorylation of STAT1 by IKKε disrupts the formation of STAT1 homodimers, but not STAT1:STAT2 heterodimers. This results in promotion of type 1, and diminishment of type 2 interferon signalling (Ng et al., 2011).

1.4.2.2 IKKε/TBK1 as regulators of NF-κB signalling

Despite their structural similarity with the canonical IKK's, neither TBK1 nor IKKε are thought to associate within the classical IKK complex (Peters et al., 2000, Tojima et al., 2000). Despite this, both kinases have been implicated as regulators of NF-κB signalling.

The phenotype of Tbk1 deficient mice is similar to that of IKKγ or RelA deficient mice, with embryonic lethality occurring due to apoptosis in the liver, suggesting TBK1 may be an important NF-κB regulator (Beg et al., 1995, Bonnard et al., 2000, Li et al., 1999, Makris et al., 2000).

In early studies, recombinant IKKε was shown to directly phosphorylate S36 of IκBα, but an observed high-molecular weight complex containing IKKε was reported to phosphorylate both S32 and S36 of IkBα (Peters et al., 2000). At a similar time, wildtype IKK-i was overexpressed in HEK293 cells and was demonstrated to phosphorylate S32, but preferentially S36 of IκBα, resulting in stimulation of the NF-κB pathway (Shimada et al., 1999).

Adli and Baldwin (2006) found that both IKKε and TBK1 can activate a NF-κB reporter construct in HEK293T cells, and that IKKε and TBK1 expression was sufficient to induce P65 phosphorylation at the serine 536 residue. Mouse EF's deficient for IKKε/TBK1 had unaffected P65 phosphorylation following LPS/TNFα stimulation, suggesting that IKKε/TBK1 play a role in basal P65 signalling rather than stimulation dependent P65 signalling. This suspicion was confirmed in HeLa cells with constitutive P65 phosphorylation where IKKε knockdown diminished P65 S536 phosphorylation and basal NF-κB activity (Adli and Baldwin, 2006).

IKKε also has a described role in the regulation of the NF-κB subunit c-Rel. Expression of IKKε resulted in a significant increase in 32P incorporation into c-Rel, whereas a mutant inactive kinase did not. Kinase assays using Flag-tagged proteins revealed that wildtype IKKε could directly phosphorylate c-Rel (Harris et al., 2006).

Finally, IKKε has been shown to directly phosphorylate CYLD which supresses it's de-ubiquitinase activity which is associated with an increase in NF-κB activity (Hutti et al., 2009).

1.4.2.3 Cytokine production and JAK/STAT signalling

In a non-small cell lung cancer (NSCLC) model, STAT3 was shown to bind directly to two putative STAT3 binding sites within the *IKBKE* promoter region and subsequently upregulate *IKBKE* at both the mRNA and protein level (Guo et al., 2013). More recently, evidence has emerged which suggests that IKKε and TBK1 kinases can regulate STAT3 phosphorylation. Overexpression of both IKKε and TBK1 led to indirect phosphorylation on Y705 of STAT3, in addition to direct phosphorylation at S754 by TBK1 (Hsia et al., 2017). Additionally,

silencing of IKKε and/or TBK1 by means of short hairpin RNA was sufficient to reduce Y705 phosphorylation levels of STAT3 in HTLV-1 transformed T lymphocytes (Zhang et al., 2016).

In an inducible cell line model, IKKε expression resulted in the secretion of the inflammatory cytokines IL-8 and RANTES (CCL5) into the supernatant of HEK293T cells. Additionally, induction of IKKε resulted in an increase in phosphorylation of several STAT family members – STAT1 (Y701), STAT3 (Y705), and STAT5 (Y694). The increase in phosphorylation of these STAT family members occurred 4 hours post IKKε detection, suggesting there is not a direct interaction (Sankar et al., 2006).

These studies highlight the need for cytokine secretion in the mechanism of IKKε and TBK1 promoting Y705 phosphorylation on STAT3, as neither IKKε nor TBK1 is able to directly phosphorylate tyrosine residues as they are both serine/threonine kinases.

1.4.3 IKKε/TBK1 in human disease

1.4.3.1 Autoimmunity

In a collagen II induced rheumatoid arthritis (CIA) mouse model, IKKε$^{-/-}$ mice with CIA, showed decreased NF-κB expression, nociception, and secreted IL-1β, IL-6 and TNF-α when compared to wild type mice. Treatment of wild type mice with Amlexanox (a dual IKKε/TBK1 inhibitor) produced a similar phenotype to that of IKKε deficient mice (Zhou et al., 2018).

Hasan et al., 2015 identified systemic lupus erythematosus (SLE) patient leukocytes had elevated TBK1 expression. Drug inhibition of TBK1 reduced immune activation and the autoimmune phenotype in autoimmune susceptible mice. Additionally, *TREX* (a gene whose mutation is associated with various autoimmune diseases) mutant patient lymphoblasts treated with a TBK1 inhibitor showed a dampened IFN gene expression signal (Hasan et al., 2015).

1.4.3.2 Breast cancer

IKBKE was first linked to malignancy in a study examining the pathogenesis of breast cancer (Eddy et al., 2005). The study noted IKKε expression in primary breast cancer samples and

several breast cancer cell lines, but not in untransformed breast epithelial cells. The group demonstrated that expression of a kinase inactive form of IKKε reduced NF-κB reporter activity, providing evidence that IKKε drives NF-κB signalling in breast cancer cells. Additionally, evidence was provided that suggests that, in this model at least, IKKε expression at both the protein and transcript level is regulated by the activity of the serine/threonine protein kinase CK2 (Eddy et al., 2005).

A major study linking *IKBKE* to malignancy in breast cancer identified IKKε from a pool of activated kinases as being sufficient to replace PI3K signalling in its co-operation with ERK to transform HEK293 cells. (Boehm et al., 2007). This discovery prompted the authors to examine *IKBKE* expression and functionality in breast cancer. The group found amplifications of the loci encoding *IKBKE* (1q32) in ~ 16% of breast cancer cell lines, and demonstrated 1q32 amplification in 30% of primary human breast cancer samples. This amplification was shown to correspond with *IKBKE* mRNA and IKKε protein levels, and, interestingly, *IKBKE* overexpression was demonstrated in a further ~50% of breast cancer specimens even in the absence of 1q32 amplification. To explore function of IKKε in breast cancer, the group went on supress *IKBKE* expression by shRNA technology, resulting in decreased viability and proliferation in breast cancer cell lines harbouring *IKBKE* amplification. The introduction of *IKBKE* into human mammary epithelial cells was sufficient to promote transformation, enforcing the role of *IKBKE* as a transforming oncogene in breast cancer. Consistent with the known physiological roles of *IKBKE*, cells expressing *IKBKE* were shown to have increased IRF3-responsive interferon-stimulated regulatory element activity in addition to increased transcription of *CCL5* and *IFNB1*. With regards to the NF-κB pathway, in primary breast cancer tissue, IKKε expression correlated with nuclear c-Rel expression. Additionally, overexpression of *IKBKE* led to a decrease in cytoplasmic IkBα, and a cytoplasmic-nuclear shift in P50 sub-cellular localization and an increase in NF-κB reporter activity, all features indicative of activation of the NF-κB pathway. When examining the effect of silencing the interferon response, IRF3 specific shRNAs failed to suppress growth in transformed cells expressing myristoylated *IKBKE*. However, when the *IKBKE* induced NF-κB response was nullified by expression of a mutant form IkBα, *IKBKE* expression failed to induce transformation of HEK293 cells, suggesting that the capacity of *IKBKE* to transform cells is attributable to its activation of the NF-κB pathway and not the interferon response (Boehm et al., 2007).

TBK1 was identified from a shRNA kinome screen as being vital for the survival HER2 positive breast cancer cells. Drug inhibition of TBK1 and IKKε by a dual inhibitor (TBK1-II) induced senescence in part by inhibiting the phosphorylation of P65 (S536) (Deng et al., 2014b).

1.4.3.3 Lung cancer

In the lung cancer setting, there have been several studies implicating TBK1 specifically in *KRAS* mediated oncogenesis. Mutations which activate *KRAS* are often seen as driver mutations in oncogenesis (Hobbs et al., 2016). TBK1 was shown to be engaged by Ras through recruitment to the Ras effector complex RalB/sec5, and necessary for *KRAS* mediated oncogenic transformation (Chien et al., 2006). A subsequent study showed that TBK1 was essential for *KRAS* mutant lung cancer cells by exerting NF-κB mediated anti-apoptotic ability on the cells through c-Rel and BCL-XL (Barbie et al., 2009). Other studies have attributed the dependence of *KRAS* mutant lung cancer cell lines on TBK1 to TBK1s ability to support the AKT/mTOR pathway (Cooper et al., 2017). Indeed, TBK1 had previously been shown to be able to directly phosphorylate AKT during oncogenic transformation (Ou et al., 2011).

1.4.3.4 Ovarian cancer

Overexpression and activation of IKKε was observed in ovarian cancer cell lines, and ~ 66% of ovarian cancer specimens, with an association towards late stage, high grade tumours and poor survival (Guo et al., 2009).

1.4.3.5 Glioma

In glioma, cell lines and primary tissue samples had elevated IKKε expression in comparison to their non-malignant counterparts. *IKBKE* expression was shown to have anti-apoptotic effects through increased BCL2 expression, and a strong positive influence on NF-κB signalling associated with P65 and P50 (Guan et al., 2011) .

A further study showed that *IKBKE* knockdown resulted in reduced proliferation and migration in a glioblastoma cell line. *IKBKE* knockdown led to a reduction in NF-κB and

STAT5b activity as measured by luciferase reporter assay. Additionally, high IKKε protein expression correlated with nuclear P65 in primary glioblastoma tumours (Dubois et al., 2018).

1.4.3.6 Prostate cancer

Inducible downregulation of IKKε in a prostate cancer cell line demonstrated that IKKε knockdown was accompanied by a 50% reduction in IL-6 secretion. Over expression of IKKε resulted in strong *IL6* promoter activity, and through inhibition of NF-κB, the IKKε dependent regulation of IL-6 was independent of NF-κB. Instead, this regulation was shown to be dependent on C/EBPβ. IKKε was shown to directly bind the transcription factor C/EBPβ, induce its phosphorylation and cause its nuclear translocation (Péant et al., 2017). In a cohort of mice xenograft models, IKKε depletion resulted in a significant growth delay in tumour cells, and a decrease in IL-6 secretion which correlated with growth inhibition (Péant et al., 2017).

1.4.3.7 Pancreatic cancer

Overexpression of IKKε has been identified in the malignant pancreas (Zubair et al., 2016). Pancreatic ductal adenocarcinoma cell proliferation was reduced upon knockdown of IKKε. Silencing of IKKε was further shown to alter glucose-metabolism related genes along with glucose uptake. The diminishment of IKKε led to a reduction in nuclear c-MYC, shown to be associated with a reduction in AKT phosphorylation (Zubair et al., 2016).

1.4.4 Current knowledge of IKKε and TBK1 in DLBCL

While a collection of studies have identified functional roles for IKKε and TBK1 in promoting and maintaining the pathogenesis of an assorted array of human malignancies, there has been no direct evidence of an implication for either of the kinases in lymphoid malignancy.

Despite this, there is substantial literature linking both kinases to signalling pathways of known importance to survival of DLBCL cells. For example, positive up-regulation of NF-κB signalling is a hallmark of non-GC DLBCL (Davis et al., 2001), and both IKKε and

TBK1 have been shown to directly modulate the activity of several key proteins involved in NF-κB signalling (Adli and Baldwin, 2006, Harris et al., 2006, Hutti et al., 2009).

Additionally, there is association between IKKε/TBK1 activity and the upregulation of STAT signalling, most notably, STAT3 (Zhang et al., 2016, Hsia et al., 2017). Active STAT3 signalling has been demonstrated to be functionally important in the pathogenesis of DLBCL, with preference toward the non-GC subtype (Ding et al., 2008, Gupta et al., 2012, Huang et al., 2013).

This project aims to identify whether inhibition of IKKε/TBK1 by novel dual inhibitors may serve as potential therapeutic agents in DLBCL.

1.5. Project aims

This project aims to complete the following:

1. Assess the expression of IKKε and TBK1 in DLBCL and to determine if this expression has any prognostic value.

2. Determine the efficacy of a dual IKKε/TBK1 inhibitors in DLBCL cell lines.

3. Determine the cellular consequences of IKKε/TBK1 inhibition in DLBCL.

4. Assess the potency and consequences on gene expression of IKKε/TBK1 inhibition in patient derived xenograft models of DLBCL.

Chapter 2 - Materials and Methods

2.1 Cell culture

2.1.1 Cell culture conditions

Ly03, Ly19, SUDHL4, SUDHL6, Toledo and Pfeiffer cell lines were grown in RPMI 1640 medium containing L-glutamine (Invitrogen, ThermoFisher Scientific, Waltham, MA, USA), and supplemented with 10% foetal calf serum (FCS) (Lonza, Basel, Switzerland) . Ly10 cells were grown in IMDM containing L-glutamine and 25mM HEPES (Invitrogen), and supplemented with 10% FCS (Lonza). All cell lines were incubated at 37 ˚C in a humidified environment with 5% CO_2.

Ly03 and Ly10 are representative of ABC DLBCL while SUDHL4 and SUDHL6 are representative of GC DLBCL.

2.1.2 Cell counting

Cells were counted by adding 10µL of cells growing in culture medium to 10µL of 0.4% Trypan blue and mixing well. Following this, 10µL of cells in Trypan blue solution was added to a chamber of a TC20tm cell counter dual-chamber slide (BioRad, Hercules, CA, USA). The slide was then inserted into a TC20tm automated cell counter (BioRad) to attain the concentration of cells per millilitre.

2.1.3 Freezing and resurrection conditions

All cell lines were frozen in 70% complete growth media, 20% FCS and 10% DMSO. Prior to freezing, the cell lines in question were grown to ~ 1 x 10^6 cells per mL, in a minimum of 10mLs of media. Cells were then pelleted by centrifugation at 200 x g for 5 minutes at room temperature. Pelleted cells were re-suspended in freezing media to a volume of 1mL per vial, with each vial containing ~ 1 x 10^7 cells. 1mL of re-suspended cells in freezing media was then added to a labelled cryovial and stored at -80 ˚C before transferring to liquid nitrogen storage.

To resurrect cells, frozen vials are transferred to tissue culture on dry ice. The vial(s) was then quickly defrosted by partial submersion into a 37 ˚C water bath until almost entirely

defrosted. The defrosted cells were then transferred into a 15mL Falcon tube to which 9mL of warm media was slowly added. This was then centrifuged at 200 X g for 5 minutes at room temperature to pellet the cells. Following removal of the supernatant, pelleted cells were re-suspended in 1mL of fresh media and added to a T-25 flask containing the following volume of warm fresh media dependent on the cell line being re-suspended:

Ly10 and Pfeiffer – 3mL
Ly19, Ly03, Toledo, SUDHL4 and SUDHL6 - 6mL

Cells were then incubated for 24h and split to keep cell density at < 1 x 10^6 cells per mL.

2.1.4 Cytokine treatment

The details of cytokines used in experiments are shown below:

Cytokine	Concentration
IL-10 (R&D systems, Minneapolis, MN, USA)	50ng/mL
CCL3 (R&D systems)	100ng/mL
CCL4 (R&D systems)	100ng/mL

Table 2:1. Details of cytokine used in experiments

Cells were counted while sub-confluent and the appropriate volume of cells in media centrifuged at 100 x g for eight minutes. Growth medium was then removed and the cells re-suspended in enough fresh media to result in in a concentration of 1 x 10^6 cells per mL. 1mL of cells were then seeded per well of a 24-well plate and incubated for the desired time with either CCL3/CCL4 (100ng) or IL-10 (50 ng) or a carrier control (Phosphate buffered saline (PBS)). Following cytokine incubation, cells were harvested and immediately placed on ice prior to lysate gathering.

2.1.5 Drug treatment

2.1.5.1 DMX compound screen

To a 96-well plate, 0.5µL of desired compound (in DMSO) was seeded to the bottom of a well in order to achieve the desired final concentration following addition of 100µL of media and cells (final DMSO concentration of 0.5%). Compounds were seeded in duplicate columns, testing a range of 8 concentrations per column. A control column containing 0.5µL of DMSO was seeded, in addition to a column containing no drug or DMSO (untreated control).

Ly10, Ly03, Ly19, SUDHL4 and Toledo cell lines were seeded at a density of 10,000 cells per well of a 96 well plate. SUDHL6 and Pfeiffer cell lines were seeded at 20,000 cells per well. 10/20 thousand cells were then added in 100µL in media to wells containing drug, DMSO or no treatment. A 96 well plate allows for the treatment of 3 cell lines with 8 concentrations of drug in duplicate and 2 control columns.

Following incubation, the plate(s) were removed from the incubator and allowed to cool to room temperature. To each well of the plate, 20µL of CellTiterGlo (CTG) lysis reagent (Promega, Madison, WI, USA) was added and the plate gently shaken for 5 minutes.

Luminescence (directly proportional to ATP levels) was then recorded using a Wallac VICTOR^2 multilabel counter (PerkinElmer, Waltham, MA, USA).

Raw luminescence values were then exported into Microsoft Excel where further analysis could be performed. Percentage viability was calculated by taking mean values for each condition and calculating as a percentage of the average value recorded for the DMSO controls. Values were then inputted into GraphPad Prism 7.0 and a sigmoidal, 4PL curve was fitted to generate EC50 values.

2.1.6 Cell cycle analysis

Post drug treatment, cells were harvested, span at 310 x g and the supernatant aspirated. Cell pellets were then washed in cold PBS, span again at 310 x g and re-suspended in 70µL of PBS. This mixture was vortexed continuously during the dropwise addition of 75% ethanol (930µL). This resulted in 1mL of cells in suspension in 70% ethanol. This suspension was

then cooled on ice and stored at -20 ˚C overnight. Following this, cells in solution were centrifuged at 400 x g and re-suspended in 1mL 0.5% bovine serum albumin (BSA) (Sigma-Alrdrich, St Louis, MO, USA) and centrifuged once more at 400 X g at 4 ˚C. Pelleted cells were then re-suspended in 200µL propidium iodide staining buffer (BD, Oxford, UK) plus RNAseA (0.1mg/mL) and incubated at 37 ˚C for 1 hour. Cells were then ran through a BD FACSCantoTM II (BD) machine and data was analysed using the BD FACSDiva (8.0) software (BD).

2.1.7 Analysis of apoptosis

FACS analysis of apoptotic cells was carried out using an Annexin V apoptosis detection kit (ThermoFisher).

Following incubation with drug, 1 X 10^6 Ly10 cells were harvested and centrifuged at 310 X g for 5 minutes to pellet. The cell pellet was then washed in cold PBS and centrifuged once more at 310 X g for 5 minutes. Cell pellets were then re-suspended in 100µL 1X Annexin V buffer with the addition of 3µL Annexin V FITC labelled antibody, and incubated in the dark at room temperature for 30 minutes. Following incubation, 400µL 1X Annexin V buffer was added, and the total 500µL transferred to a glass FACS tube, and kept on ice. Immediately prior to FACS analysis, 1µL of DRAQ7 dye (BioLegend, San Diego, CA, USA) and each tube was gently vortexed. FACS analysis was then carried out using BD FACSCantoTM II.

2.1.8 siRNA mediated Knockdown

All siRNAs were supplied by Thermo Fischer Scientific, and the following were used:
IKBKE (s18536)
TBK1 (s761)
Silencer negative control (AM4611)

2.1.8.1 Transfection

Sub-confluent Ly10 cells were counted and an appropriate volume of cells in media were centrifuged at 200 X g to pellet cells. The supernatant was aspirated off, and the cells re-suspended in supplemented SF Nucleofector 4D buffer (Lonza) at a volume to give 2 X 10^6

cells per 100µL of buffer, 100µL of which was added to a Nucleofector 4D system cuvette (Lonza) containing an appropriate amount siRNA in solution to yield a final concentration of 2µM. Cuvettes were then put into the Nucleofector 4D machine (Lonza) and transfected using programme CM150. The 100µL solution was removed from the cuvette by dropper pipette and added to 900µL of warm media, 500µL of which was added to 500µL of warm media in a well of a 24-well plate in duplicate. This results in 1 X 10^6 of post-transfected cells in 1mL of media in a well of a 24-well plate. Cells were kept in previously described tissue culture conditions for 48 hours and then harvested for downstream analysis.

Harvested cells were span at 310 X g. Supernatant was then removed and either stored at -80ºC or discarded. Pellets were then re-suspended in PBS and span again at 310 X g. PBS supernatant was removed and pellet was snap frozen on dry ice and stored at -80ºC.

2.2 Western blotting

2.2.1 Recipes used

Buffers used throughout the Western blotting procedure are shown in Table 2.2. All recipes were made up in de-ionized water (dH_2o) unless otherwise specified.

Solution	Recipe
5 x Running buffer	144g Glycine (1.92 M), 5g SDS (0.5%), 30g Tris Base (250 mM) for 1 Litre
10 x TBS	40g NaCl, 1g KCl, 15g Tris Base pH 7.4 for 500 mL
Wash buffer	90% H_2O, 10% 10 X TBS, 0.05% Tween
Blocking buffer	Either 5% non-fat Milk or 5% BSA (w/v) wash buffer
3 x loading buffer	2.4mL1M Tris, pH6.8, 3mL20% SDS, 3mLGlycerol,1.6mLβ-mercaptoethanol, 600µl Bromophenol blue
Radioimmunoprecipitation lysis buffer	50mM Tris-HCl pH 8.0, 150mM NaCl, 1 % sodium deoxycholate, 0.1 % SDS.

Table 2:2. Recipes of solutions used in the Western blotting procedure

2.2.2 Sample preparation

Harvested cells were centrifuged at 310 X g for 5 minutes at room temperature, the supernatant removed, and the pellet re-suspended with cold PBS and centrifuged once more at 310 X g at room temperature for 5 minutes. The PBS supernatant was removed and the resulting cell pellet was snap frozen on dry ice and stored at -80 ˚C until further analysis.

2.2.3 Lysate preparation

Cell pellets were re-suspended in radioimmunoprecipitation (RIPA) lysis buffer lysis buffer supplemented with 1 x protease inhibitor (Sigma-Alrdrich) and 1 X phosphatase inhibitor (Sigma-Aldrich). Following thorough mixture by pipetting, samples were vortexed and incubated on ice for 30 minutes.

Lysates were then centrifuged at 12,000 x g for 15 minutes at 4 ˚C, and the supernatant was removed to be used as whole cell lysate.

2.2.4 Bicinchoninic acid assay

In order to determine protein amounts in lysates a Bicinchoninic acid (BCA) assay was performed.

20μL of 0.1m copper (II) sulfate solution (Sigma-Aldrich) was added to a 1.5mL tube, to which 1mL of Bicinchoninic acid solution (Sigma-Aldrich) was added, and the tube inverted 5 times. To this solution, 5μL of cell lysate was added and briefly vortexed. Samples were then incubated at 37 ˚C for 30 minutes, and samples removed and allowed to cool to room temperature.

Absorbance at 562nm was then read, relative to water blank, on a photometer (Eppendorf, Hamburg, Germany), and the absorbance recorded for all samples. These absorbance values could then be cross-referenced to a standard curve consisting of known protein concentrations and their corresponding 562nm absorbance.

2.2.5 SDS-Gel electrophoresis

Prior to loading into a gel, samples were diluted with PBS to give ~ 50µg of protein per sample. To this, an adequate volume of 3 X loading buffer was added to achieve a final 1X concentration and mixed gently. Samples were then pulse span and heated at 98 ˚C for 5 minutes, allowed to cool and pulse span once more. Samples were then loaded into a Mini-PROTEAN TGX™ pre-cast polyacrylamide gel (BioRad, Hercules, CA, USA), alongside 5µL of Precision Plus Protein™ Dual Color Standard (BioRad). The gel was then ran at 120V in 1 X running buffer until the dye front reached the bottom.

2.2.6 Gel transfer

The polyacrylamide gel was then transferred onto a PVDF or nitrocellulose membrane (BioRad) by means of semi-dry transblot turbo apparatus (BioRad).

2.2.7 Blocking and primary antibody incubation

Membranes were then blocked in blocking buffer for a minimum of 1 hour at room temperature with gentle shaking. Post-blocking, membranes were incubated in primary antibody either overnight at 4 ˚C or at room temperature for 2 hours. All primary antibodies were used at a concentration of 1:1000 in blocking buffer unless stated otherwise. The following primary antibodies were obtained from Cell Signalling Technology (Danvers, MA, USA):

pAkt (S473) (#4060), Akt (#4691), pP65 (S536) (#3033), P65 (#8242), pSTAT3 (s727) (#9134), pSTAT3 (Y705) (#9145), STAT3 (#4904), pCYLD (#4500), CYLD (#8462), IKKε (#2904), TBK1 (#3013), β-actin (#8457), GAPDH (#2118).

Primary antibodies for GAPDH and β-actin were used at a concentration of 1:10,000.

2.2.8 Secondary antibody incubation

Post primary antibody incubation, membranes were washed a minimum of 3 times in wash buffer with gentle rocking.

Following this, membranes were incubated with HRP-coupled anti-rabbit/mouse secondary antibody (Cell Signalling Technology) for 1 hour at room temperature. Secondary antibody

was used at a concentration of 1:3300 with the exception of where GAPDH was used and the secondary concentration was 1:6600.

2.2.9 Membrane visualisation

Post-secondary antibody incubation, membranes were washed a minimum of 3 times in wash buffer with gentle rocking.

Membranes were then incubated with Electrochemiluminescene (ECL) substrate (BioRad) for 5 minutes at room temperature. Following this, excess ECL substrate was removed from membranes by gentle touching with a paper towel. Membranes were then wrapped in cling film and visualized with X-ray film (Fujifilm, Tokyo, Japan). X-ray films were then developed using an X-ray film developer (SRX-101A, Konica Minolta, Bloxham Mill, UK).

2.3 Immunohistochemistry

Paraffin slides were de-paraffinised by submersion into Xylene for 5 minutes, repeated twice. Sections were then submerged in IMS for 3 minutes, for a total of 3 times. Following this, sections were then submerged in 70% IMS for 3 minutes to partially re-hydrate samples.

Citrate antigen retrieval buffer: 10mM citrate acid monohydrate in dH_20, pH 6.0 plus 0.05% Tween20.

Following a 1 minute wash in running tap water, slides were submerged in Citrate antigen retrieval buffer and microwaved at 1000 watts for 20 minutes, and allowed to cool for 10 further minutes. Where BCL6 staining was to be carried out, instead of citrate buffer antigen retrieval, slides underwent EnVision™ FLEX, high pH (Link) (Agilent Technologies, Santa Clara, CA, USA) antigen retrieval.

Slides were then placed in de-ionized water for 5 minutes.

A ring was then drawn around each section with a wax pen to contain solution placed on the sections. Each section was then covered with an endogenous peroxidase blocking solution (Leica Microsystems, Milton Keynes, UK) for 5 minutes at room temperature.

Following this, slides were washed in PBS for 5 mins with gentle shaking. Non-specific binding blocking solution (Leica Microsystems) was then added to each section for 5 minutes

at room temperature, and slides washed twice more in PBS for 5 minutes each with slight rocking.

Primary antibody in PBS was applied to tissue microarray sections in the concentrations laid out in Table 2.3:

Antibody	Dilution in PBS	Incubation
IKKε (SAB1306435, Sigma-Aldrich)	1:50	Overnight at 4°C
TBK1(PA-5-34809, Thermo Fisher Scientific)	1:50	Overnight at 4°C
CD10 (M7308, DAKO, Glostrup, Denmark)	1:40	Overnight at 4°C
BCL6 (M7211, DAKO)	1:20	Overnight at 4°C
MUM1(M7259, DAKO)	1:40	Overnight at 4°C
Negative control mouse IgG1 (Isotype control) (X0931, DAKO)	Matched to the highest target antibody used	Overnight at 4°C
Rabbit IgG, monoclonal (Isotype control) (EPR25A, abcam, Cambridge, UK)	Matched to the highest target antibody used	Overnight at 4°C

Table 2:3. Details of antibodies used in the immunohistochemistry procedure

Following application of primary antibody, slides were washed twice in PBS with gentle shaking for 5 minutes each wash. Sections were then covered with secondary antibody solution (Leica Microsystems) for 30 minutes at room temperature, and subsequently washed twice more in PBS with shaking for 5 minutes. Sections were then covered with HRP solution (Leica Microsystems) for a further 30 minutes in the dark, and then washed twice in

PBS for 5 minutes with gentle shaking. Following this, sections were incubated with 3,3'Diaminobenzidine (DAB) staining solution (Leica Microsystems) for 3 minutes, or until visible browning of the tissue occurred. Slides were then placed in tap water for 2 minutes, prior to a 30 second submersion into haemotoxylin solution. Slides were then wahsed in warm running water for 1 minute, followed by a 1 minute wash in cool running tap water. Slides were then submerged in 70% IMS for 3 minutes, followed by 3 repeats of 2 minute submersions in 100% IMS. Finally, slides were submerged in xylene twice for 3 minutes prior to mounting.

Following submersion of cells in Xylene, excess solution was removed and a glass cover slip of sufficient size to cover the tissue section was mounted onto the slide using Di-N-Butyle Phthalate in Xylene (DPX) mountant and scanned using a Hamamatsu NanoZoomer (Hamamatsu Photonics, Hamamatsu, Japan)

2.4 Immunofluorescence Microscopy

Slides were deparaffinised in xylene, rehydrated in an ethanol gradient, and antigen retrieval performed by microwaving in citrate buffer (pH 6.0). Staining was carried out using the Opal 4-color automation IHC kit (PerkinElmer) and counterstained with DAPI (PerkinElmer).

Primary antibodies used and their respective fluorophores were as follows:

TBK1 (PA-5-34809, Thermo Fisher Scientific, Opal 520) used at 1:50 in PBS

IKKε (SAB1306435, Sigma-Aldrich, Opal 570) used at 1:50 in PBS

Antigen retrieval was carried out as described in section 2.3, and a ring drawn around each section with a wax pen to contain solution placed on the sections.

Slides were then incubated with non-specific binding blocking solution (Leica Microsystems) at room temperature for 10 minutes. Slides were then incubated in TBK1 primary antibody overnight at 4 ˚C. Following primary incubation, slides were washed three times in TBST for 15 minutes each wash. Slides were then incubated in anti-rabbit secondary (1:200 in PBS (Leica Microsystems) for 60 minutes at room temperature. Post-secondary incubation, slides were washed three times in TBST for 15 minutes each wash. Slides were then incubated in Opal 520 signal amplification fluorophore reagent (PerkinElmer) and incubated at room temperature for 10 minutes. Slides were protected from light from this point onwards. Slides were washed three times in TBST for 15 minutes each wash and then subjected to antigen

retrieval as previously described. The protocol was then repeated but with incubation with IKKε primary antibody and Opal 570 fluorophore reagent (PerkinElmer).

Slides were then mounted using ProLong™ Diamond Mountant (ThermoFisher Scientific) and scanned using a Hamamatsu NanoZoomer (Hamamatsu Photonics).

2.5 Luminex multiplex ELISA

2.5.1 Supernatant collection

Cell culture supernatants were obtained by harvesting of Ly10 cells, centrifugation at 310 X g for 5 minutes, followed by removal of the supernatant. Supernatants were stored at -80°C prior to analysis. Supernatants from treated PDX models were prepared by CrownBioscience (Beijing, China) by taking 50µL of cell supernatant from treated *ex vivo* 2D culture plates (prior to CellTiterGlo treatment) and storing samples at -20°C, prior to shipping on dry ice. Concentrations of TNF-alpha, Interferon beta, Interferon gamma, CXCL6, CXCL13, CCL3, CCL4, CCL17, CCL22, IL2, IL4, IL6, IL9, IL10, IL12, and IL13 were analysed by magnetic Luminex assay (R&D systems):

2.5.2 Luminex assay

To prepare standards, standard cocktails were reconstituted with sample diluent (volume was unique for each cocktail), and allowed to stand at room temperature for 10 minutes. 100µL of each cocktail provided was added to a polypropylene tube, and the total volume made up to 1mLwith sample diluent. From this, a threefold dilution was carried out by adding 100µL of standard 1 into 200µL of sample diluent. This threefold dilution series was continued until a total of 6 standards were produced.

Test sample supernatants were diluted by adding 40µL of sample to 60µL of 1 X sample diluent.

To each well containing 50µL of micro particle cocktail, 50µL of standard or 48µL of diluted sample was added (in duplicate for each sample). The plate was then sealed with a foil plate sealer and incubated for 2 hours at room temperature on an orbital shaker set at 800 +/- 50 RPM. By using a microplate magnetic device to ensure no loss of metallic micro particles, liquid from each well was discarded and washed 3 times by applying 100µL of 1 X wash

buffer to each well, incubating for 1 minute and then discarding all fluid from wells. Following washing, 50µL of diluted biotin antibody cocktail was added to each well, and the plate sealed and incubated for 1 hour at room temperature on an orbital shaker set at 800 +/- 50 RPM. The plate was then washed 3 times in the same conditions as described previously. 50µL of Streptavidin-PE was then added to each well followed by the plate being sealed and incubated for 30 minutes at room temperature on an orbital shaker set at 800 +/- 50 RPM. Following 3 more washes, micro particles were re-suspended in 100µL wash buffer per each well, and the plate incubated for 2 minutes at room temperature on an orbital shaker set at 800 +/- 50 RPM.

Concentrations of cytokines were then determined by reading the plate in a Luminex MAGPIX system with xPONENT software.

2.6 Phosphorylated-P65 ELISA

Levels of phosphorylated P65 (Ser536) were analysed using an NF-κB P65 (pS536) SimpleStep ELISA™ kit (ab176647, abcam).

2.6.1 Sample preparation

Cells were treated with cytokines or drug as described in prior sections. Following drug or cytokine treatment, cells were harvested and immediately placed on ice prior to lysate gathering. Harvested cells were centrifuged at 310 X g for 5 minutes at room temperature, the supernatant removed, and the pellet re-suspended with cold PBS and centrifuged once more at 310 x g at room temperature for 5 minutes. The PBS supernatant was removed and the resulting cell pellet was snap frozen on dry ice and stored at -80 ˚C until further analysis.

Cell pellets prepared as previously described were re-suspended in 30µL of 1x cell extraction buffer PTR, and incubated on ice for 30 minutes and the protein concentration of each sample was determined using a BCA assay as described previously.

2.6.2 ELISA Method

Following this, samples were diluted in 1x cell extraction buffer PTR to achieve a final protein concentration of 250µg/mL in 100µL. Lyophilized NF-κB P65 control lysate was reconstituted by adding 250µL of ultra-pure water, mixing thoroughly and incubating at room temperature for at least 1 minute. This serves as the stock lysate solution (the highest concentration of standard). A two-fold dilution was then performed by adding 125µL of stock lysate into 125µL of 1x cell extraction buffer, resulting in control '1'. This two-fold dilution series was continued until 7 control tubes were attained in addition to the stock lysate. Finally, control tube '8' was prepared which contained only 1x cell extraction buffer and served as a negative control. 50µL of either sample or standard lysates were added to a single well in the 96 well assay plate. Individual samples and standard lysates were run in technical duplicate resulting in two assay wells used per condition. To each of these wells, 50µL of antibody cocktail was added, and the plate was sealed and incubated at room temperature for 1 hour while shaking at 400 RPM. Wells were then washed by decanting and adding 350µL of 1x wash buffer PT into each well. This wash process was performed 3 times. Following this, 100µL of TMB substrate was added to each well and the plate was incubated in dark conditions for 15 minutes while shaking at 400 RPM. Subsequently, 100µL of stop solution was added to each well, and the plate was shaken for 1 minute at 400 RPM to allow sufficient mixing of reagents. Finally, optical density at 450nm was recorded for each well using a Wallac VICTOR^2 multilabel counter (PerkinElmer).

2.7 Patient derived xenograft models

2.7.1 Tumour growth and single cell isolation

Mice harbouring PDX tumours were maintained at the HuPrime animal facility (CrownBioscience), and underwent weekly monitoring of tumour growth. At the appropriate tumour size, mouse xenografts were harvested and minced in PBS on a tissue culture plate producing a cell suspension. This suspension was then filtered through a cell strainer (Falcon), with the nylon mesh being washed 3-5 times with PBS. The resulting cell suspension was centrifuged at 1000 RPM, washed with PBS and centrifuged again to pellet. If required, red blood cells were removed using a red blood cell lysis buffer and the cell suspension re-centrifuged at 1000 RPM for 5 minutes, and the resulting cell pellet washed

with PBS and centrifuged again at 1000 RPM for 5 minutes. Finally, the washed cell pellet was re-suspended in the appropriate volume of culture medium for the downstream application.

2.7.2 2D *ex vivo* viability assay

Following production of single cell suspensions, cell concentrations were adjusted to 1 x 10^5 per mL in media and 150µL of cell suspension was added per well of a 96-well plate in duplicate plates. Cells were then treated for 24 hours with varying concentrations of DMX3433 and viability relative to vehicle control (DMSO) was assessed by CTG assay.

2.7.3 Generation of PDX model cell pellets

Following single cell isolation (describe in prior section), 2 X 10^6 were seeded in 1900µL of X-vivo 15 basal growth medium (Cat#04-744Q, Lonza) per well of a 6 well plate. Cells were then incubated overnight in a humidified incubator at 37° C with 5% CO_2. The following day, 200µL of 20X DMX3433 or DMSO (vehicle control) was added to the wells and incubated for 24hrs in a humidified incubator at 37° C with 5% CO_2. Post incubation, cell supernatant was removed, and the cells were harvested and pelleted. The cell pellets were then stored at -80°C prior to shipping on dry ice.

2.8 Gene expression analysis

2.8.1 RNA isolation

RNA isolation was carried out using a PureLink® RNA Mini Kit (ThermoFisher scientific):

Previously obtained cell pellets were re-suspended in 1mL of Trizol reagent (ThermoFisher scientific), and incubated at room temperature for 5 minutes. To this, 200µL of chloroform was added per tube and each tube was shaken vigorously for 15 seconds and incubated at room temperature for 3 minutes. Tubes were then centrifuged at 12,000Xg for 15 minutes at 4 degrees, resulting in phase separation. Following this, 400µL of the colourless aqueous phase was transferred to an RNase free tube containing and equal volume of 70% ethanol and vortexed briefly. 700µL of each sample was then transferred to a spin cartridge and

centrifuged at 12,000 X g for 15 seconds at room temperature, and the flow through was discarded. To this column, 350µL of wash buffer 1 was added and centrifuged at 12,000 X g for 15 seconds and the flow-through discarded. Each spin cartridge was placed in a fresh collection tube and 80µL of 1 X PureLink® DNase mixture was added directly to the spin cartridge membrane and incubated at room temperature for 15 minutes. 350µL of wash buffer 1 was added to each spin cartridge and subsequently span at 12,000Xg for 15 seconds at room temperature, and flow-through discarded, and the spin cartridge inserted into a new collection tube. Next, 500µL of wash buffer 2 (supplemented with ethanol) was added to each spin cartridge which were then subsequently centrifuged at 12,000 X g for 15 seconds at room temperature, and the flow-through was discarded. This wash with wash buffer 2 was repeated once more and finally the spin cartridge was centrifuged at 12,000 X g for 1 minute in order to dry the membrane, and the spin cartridge was placed into a fresh collection tube. In order to recover the purified RNA form the spin cartridge, each spin cartridge was added to a recovery tube and 30µL of RNase free water was applied to the centre of each spin cartridge membrane and allowed to incubate at room temperature for at least 1 minute. Finally, the spin cartridge was centrifuged at 12,000 X g for 1 minute at room temperature, and the resulting isolated RNA was stored at -80°C until further application.

2.8.2 cDNA synthesis

RNA was isolated from treated/untreated Ly10 cells as described in section 2.8.1. RNA was quantified using a NanoDrop 2000 spectrophotometer (ThermoFisher Scientific).

Reverse transcription (RT) was then carried out with the SensiFAST^{TM} cDNA synthesis kit (Bioline, London, UK). Total RNA (up to 1µg) was added to 4µL TransAmp buffer and 1µL reverse transcriptase or dH_2O and the total volume made up to 20µL with dH_2O. This reaction was heated to 25 °C for 10 min (primer annealing), 42 °C for 15 min (reverse transcription), and then 85 °C for 5 min (inactivation). Reactions were then chilled on ice or stored at -20°C until further use.

2.8.3 Taqman assay

Taqman assays (Applied Biosystems, Foster City, CA, USA) were performed in 96-well plate format. The following reagents were added per 20µL reaction:

- 10μL TaqMan® Fast Advanced Master Mix (2X)
- 1μL TaqMan® Assay (20X) - *IL10* (Hs00961622_m1) or *HPRT* (Hs02800695)
- 2μL cDNA (100ng/mL)
- 7μL nuclease free H_2O

Plates were briefly centrifuged and then ran on a QuantStudioTM 6 Flex Real- Time PCR System (Applied Biosystems) with the following conditions:

- 50°C for two minutes
- 95°C for 20 seconds
- 40 cycles of (95°C for one second, 60°C for 20 seconds)

Each sample was run in triplicate and mean CT values were used to calculate relative gene expression in the samples tested using the delta-delta method (Pfaffl, 2001).

2.8.4 Agilent single colour microarray

Following RNA isolation, purified RNA was provided to the NUCLEUS genomics core facility at the University of Leicester. Subsequent microarray steps were carried out by Drs Nic Sylvius and Spencer Gibson.

RNA quality was checked on a Bioanalyzer 2100 (Agilent, UK). All the RNA samples had a RNA Integration Number (RIN) > 7. A total of 100ng of total RNA was reverse transcribed, converted into complementary RNA (cRNA) and labelled with Cy3 using the LowInput QuickAmp Labeling Kit One-Color according to manufacturer's protocol (Agilent, Stockport, UK). Labelled cRNA was then hybridized over night at 65 ˚C onto the SurePrint G3 Human Gene Expression v3 8x60K Microarray which permits the quantification of about 60,000 transcripts. Each microarray was scanned on an Agilent DNA microarray C-scanner. Extraction and quality check of the raw data was performed using the Agilent Feature extraction software 10.5.1.1. At this point, raw data was sent back to the author who carried out subsequent analyses.

Quantile normalization of data was performed using Partek Genomic Suite v6.6. Normalised data was then imported into Multiple Experiment Viewer (MeV), and a two-class unpaired significance analysis for microarrays (SAM) analysis was performed. Hierarchical clustering (distance metric selection by Pearson correlation, linkage by average linkage clustering) was carried out for significant genes.

2.9 Bioinformatic Methods

2.9.1 Analysis of the cancer genome atlas

Data from the cancer genome atlas (TGCA) was accessed and analysed using FIREBROWSE (Broad institute - http://firebrowse.org/) (Broad Institute of MIT and Harvard, 2018).

2.9.2 Gene set enrichment analysis

Gene expression values from untreated and treated PDX models was analysed in the desktop GSEA software v3.0 (Broad institute). The PDX expression set was interrogated for enrichment with hallmark gene sets in the Broad molecular signature database (MSigDB). Enrichment with pathways was determined using thresholds of a FDR q-value of <0.25, a normalised enrichment score <-1 or >1 and a nominal *P*-value of < 0.05.

2.9.3 Kaplan-Meir survival analysis

Survival data was generated using SurvExpress v2.0 (Aguirre-Gamboa et al., 2013, SurvExpress, 2015) and data from a gene expression data set profiling 420 DLBCL patients treated with either CHOP or R-CHOP regimens (GSE10846, Lenz *et al*. 2008). Where a gene had several probe sets, average values were used. Data was then subjected to Kaplan-Meir survival analysis using GraphPad Prism 5.0.

2.9.4 Statistical analysis

Statistical tests were carried out in GraphPad Prism 5.0 unless stated otherwise. Details of statistical tests used are displayed in the figure legends. Error bars indicate +/- SEM and asterisks on graphs represent the level of significance: * = P < 0.05, ** = P < 0.01, ** = P < 0.001.

Chapter 3 – The expression of IKKε and TBK1 in diffuse large B-cell lymphoma

3.1 Introduction

In normal physiological conditions TBK1 is thought to be ubiquitously expressed similar to IKKα and IKKβ. The expression of IKKε however has been shown to be restricted largely to lymphoid tissue, peripheral blood lymphocytes and the pancreas (Shimada et al., 1999, Tojima et al., 2000)

The expression of IKKε and TBK1 has also been studied in a variety of human cancer settings.

Boehm et al., (2007) identified elevated transcript and protein expression of *IKBKE* in primary breast cancer and breast cancer cell lines in comparison to their normal tissue counterparts. Overexpression of IKKε has also been reported in ovarian cancer (Guo et al., 2009) and glioma (Guan et al., 2011)

Elevated *TBK1* transcript expression was seen in a subset of colon cancers and breast cancers relative to normal tissue. This overexpression was also observed at the protein level by means of immunohistochemistry (IHC) in primary colon and breast tumour tissue (Korherr et al., 2006).

There have been several studies examining the prognostic value of IKKε/TBK1 expression in malignancy. High expression of IKKε protein was significantly associated with poorer overall survival in ovarian cancer (Guo et al., 2009). The expression of *IKBKE* has also been shown to be significantly associated with decreased overall survival in oesophageal squamous cell carcinoma (Yang et al., 2018). Additionally, high TBK1 protein expression, as determined by IHC, was significantly correlated with a shorter overall survival in pancreatic ductal adenocarcinoma (PDAC) patients (Song et al., 2015).

Despite the abundance of studies examining IKKε/TBK1 expression in human malignancies, there is no literature describing the expression of either kinase in DLBCL.

Gene expression profiling studies have classified DLBCL cases into two main sub-types, the GCB like and the ABC like DLBCL's, which have proven to be clinically useful. This classification separates DLBCL cases into those whose gene expression is thought to match that of a germinal centre B – cell, and those whose gene expression is similar to activated B-cells. Classification of this kind has prognostic value as patients diagnosed with ABC like DLBCL are thought to have a poorer prognosis (Alizadeh et al., 2000). Gene expression

profiling is the most comprehensive method of separating DLBCL cases into these subtypes but has the drawback of being relatively expensive to implement. To overcome this issue, an immunohistochemistry staining algorithm has been developed by Hans et al., (2004) which can stratify DLBCL cases into either GC or non-GC classifications by staining for the presence of CD10, BCL6 and MUM1.

This chapter aims to assess IKKε and TBK1 expression in DLBCL by utilising publically available gene expression databases and DLBCL cell lines. Additionally, IKKε and TBK1 protein levels will be assessed in primary human DLBCL and any correlation with GC or non-GC status will be determined.

3.2 Results

3.2.1 *IKBKE* and *TBK1* expression in the cancer genome atlas

In order to examine mRNA expression of *IKBKE* and *TBK1* in a range of human cancer types, data from the cancer genome atlas (TCGA) was interrogated. Mean RNA-Seq by expectation maximum (RSEM) (Li and Dewey, 2011) values from each cancer type represented in TCGA was obtained from the Broad institute FIREBROWSE (http://firebrowse.org/) (Broad Institute of MIT and Harvard, 2018), ranked and plotted for both *IKBKE* and *TBK1* (Figure 3:1).

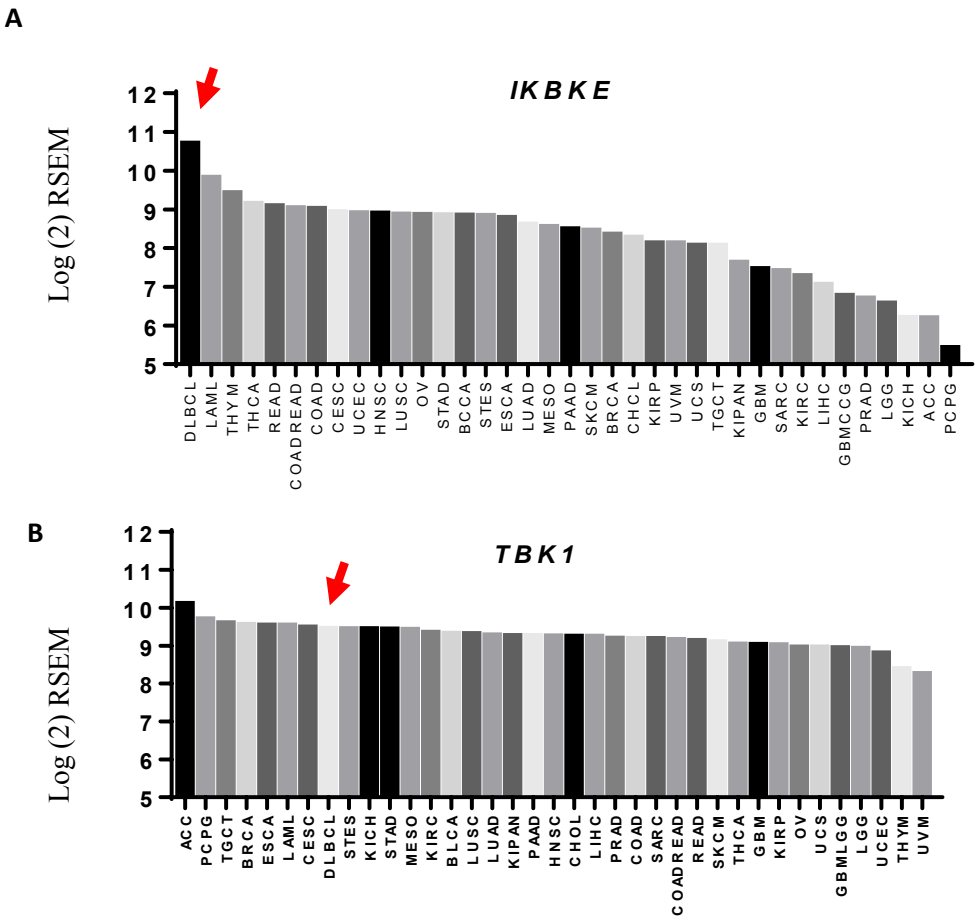

Figure 3:1: RSEM (log2) expression of *IKBKE* (A) and *TBK1* (B) across the 37 cancer types analysed in TCGA (Broad institute - http://firebrowse.org/). Red arrows indicate the position of DLBCL relative to other cancer types. A full key to abbreviations used for the cancer types included is provided in the Appendix (Table S1).

This reveals a variable expression of *IKBKE* across cancer types, compared to a more uniform high expression of TBK1. Notably, expression of *IKBKE* was highest in DLBCL cancer samples when compared to all other cancer types (1/37). With respect to *TBK1* expression, DLBCL ranked 8th out of the 37 cancer types recorded in TCGA.

3.2.2 *IKBKE* and *TBK1* levels with respect to survival in a DLBCL patient cohort

To then assess whether *IKBKE* and/or *TBK1* expression levels had any prognostic value in DLBCL, survival analysis was carried out from a DLBCL gene expression data set which was linked to clinical data. The TGCA dataset used to generate figure 3.1contains too few samples to generate a meaningful survival analysis, therefore an alternative, larger, dataset was used.

Lenz et al., 2008 performed a retrospective gene expression profiling experiment on a cohort of patients with DLBCL, with 181 samples from patients receiving solely CHOP chemotherapy, and 233 samples form patients who received an R-CHOP regimen. Using SurvExpress – a web resource for biomarker validation in cancer gene expression data sets (SurvExpress, 2015, Aguirre-Gamboa et al., 2013), the cohort could be divided into those with low or high *IKBKE*/*TBK1* expression.

The resulting high and low expression groups, and their accompanying survival data could be plotted in Kaplan-Meier curve format, and the resulting curves for *IKBKE* and *TBK1* are displayed in Figure 3:2.

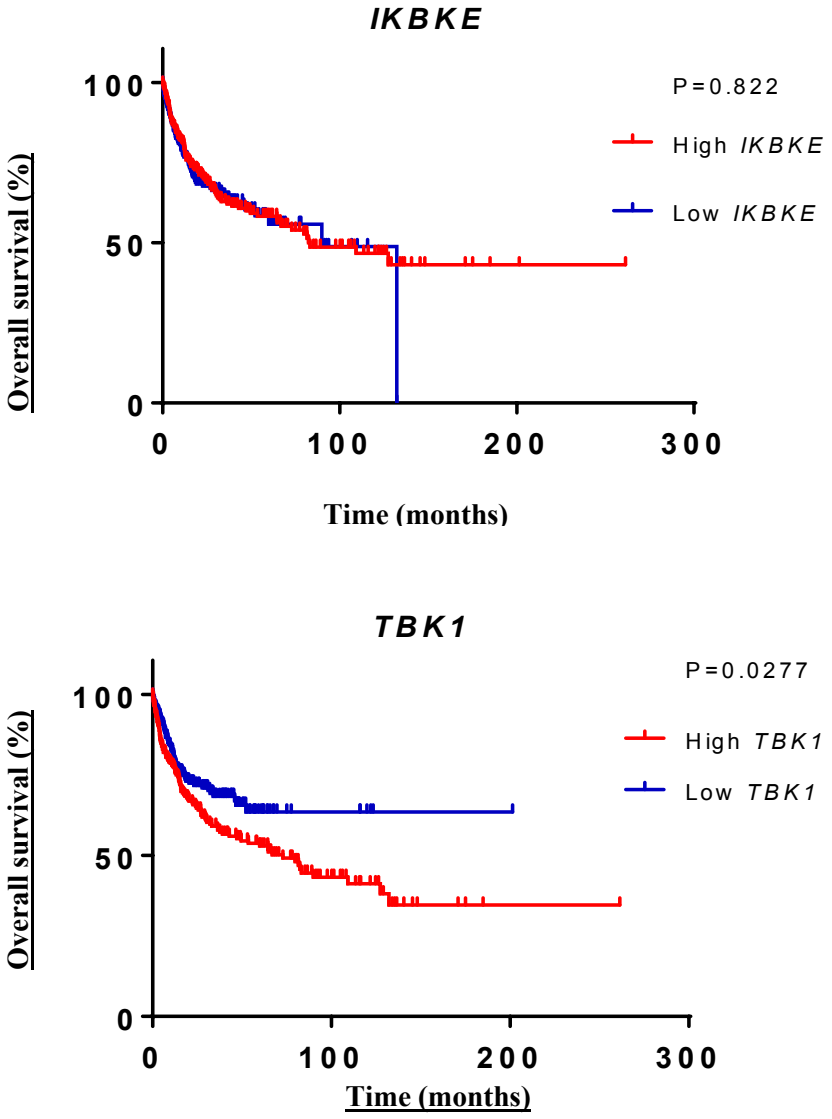

Figure 3:2: Kaplan Meier plots showing overall survival (%) by *IKBKE* (upper panel) and *TBK1* (lower panel) levels. For each plot the red line represents patients with mRNA levels greater than the median and the blue line those patients with levels less than the median. Data on expression and survival is from GSE10846 (Lenz et al., 2008).

This analysis showed that high *TBK1* expression was significantly (P = 0.027) associated with worse survival when compared with low *TBK1* expression. There was no significant difference between *IKBKE* high and *IKBKE* low expression with respect to overall survival in this dataset (Figure 3:3). There were approximately equal numbers of CHOP and R-CHOP

treated patients in the TBK1 high and TBK1 low groups which suggests that mode of treatment is not a confounding factor in this result.

3.2.3 IKKε and TBK1 protein expression in DLBCL cell lines

The protein levels of IKKe and TBK1 in DLBCL were next explored. As a first step, the relative protein amounts of each kinase was assessed in DLBCL cell lines. The protein expression of both IKKε and TBK1 was assessed in a panel of seven DLBCL cell lines, with cell lines representing both the GC and non-GC subtypes of DLBCL (Figure 3:4).

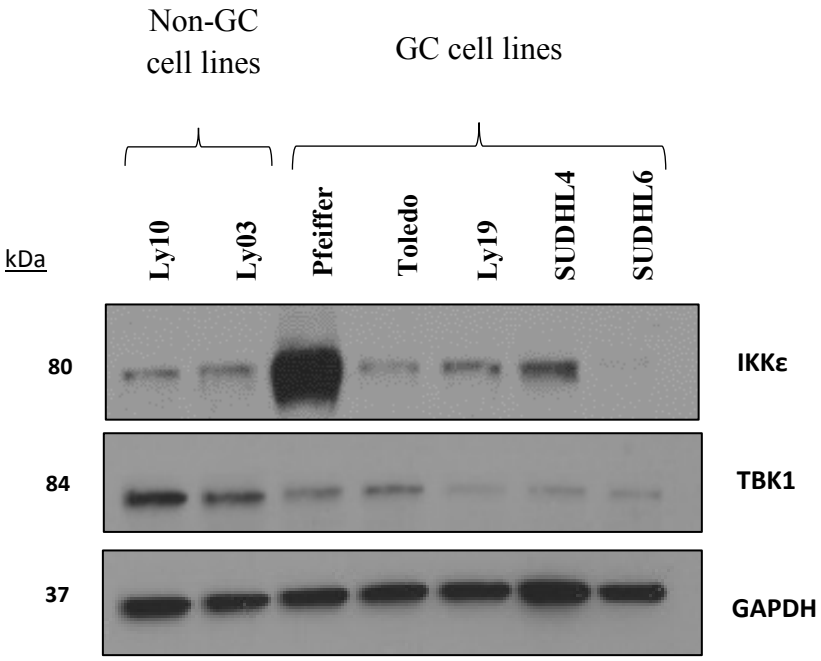

Figure 3:3: Western blots showing IKKε and TBK1 expression in a panel of DLBCL cell lines. Ly03 and Ly10 are representative of ABC-DLBCL and Ly19, Pfeiffer, Toledo, SUDHL4 and SUDHL6 of GC-DLBCL. GAPDH is shown as a loading control. Molecular weight (kDa) is indicated to the left.

The expression of IKKε was relatively constant in 5 out of the 7 cell lines. The two exceptions being Pfeiffer which had much more IKKε protein compared to the other cell lines, and SUDHL6 which had little to no IKKε expression. TBK1 expression appears higher in the non-GC cell lines, Ly10 and Ly03. GC cell lines on the whole had lower TBK1

expression, but within the GC group, Pfeiffer and Toledo had higher levels compared to Ly19, SUDHL4 and SUDHL6 (Figure 3:4). While DLBCL on the whole has high levels of expression of IKBKE and TBK1 mRNA, results presented in this section suggests that between cases of DLBCL there may well be variable protein expression of these kinases. The trend of TBK1 protein expression being higher in cell lines thought to be of non-GC origin suggests that this group of DLBCL cases may have higher TBK1 expression in comparison to GC DLBCL cases.

3.2.4 IKKε and TBK1 protein expression in human tonsil

Human tonsil tissue sections allow well-characterised compartments of normal lymphocytes i.e. germinal centre and extra-follicular, to be visualised. The expression of IKKε and TBK1 in human tonsil was determined by performing immunohistochemistry on paraffin embedded tonsil sections (Figure 3:5).

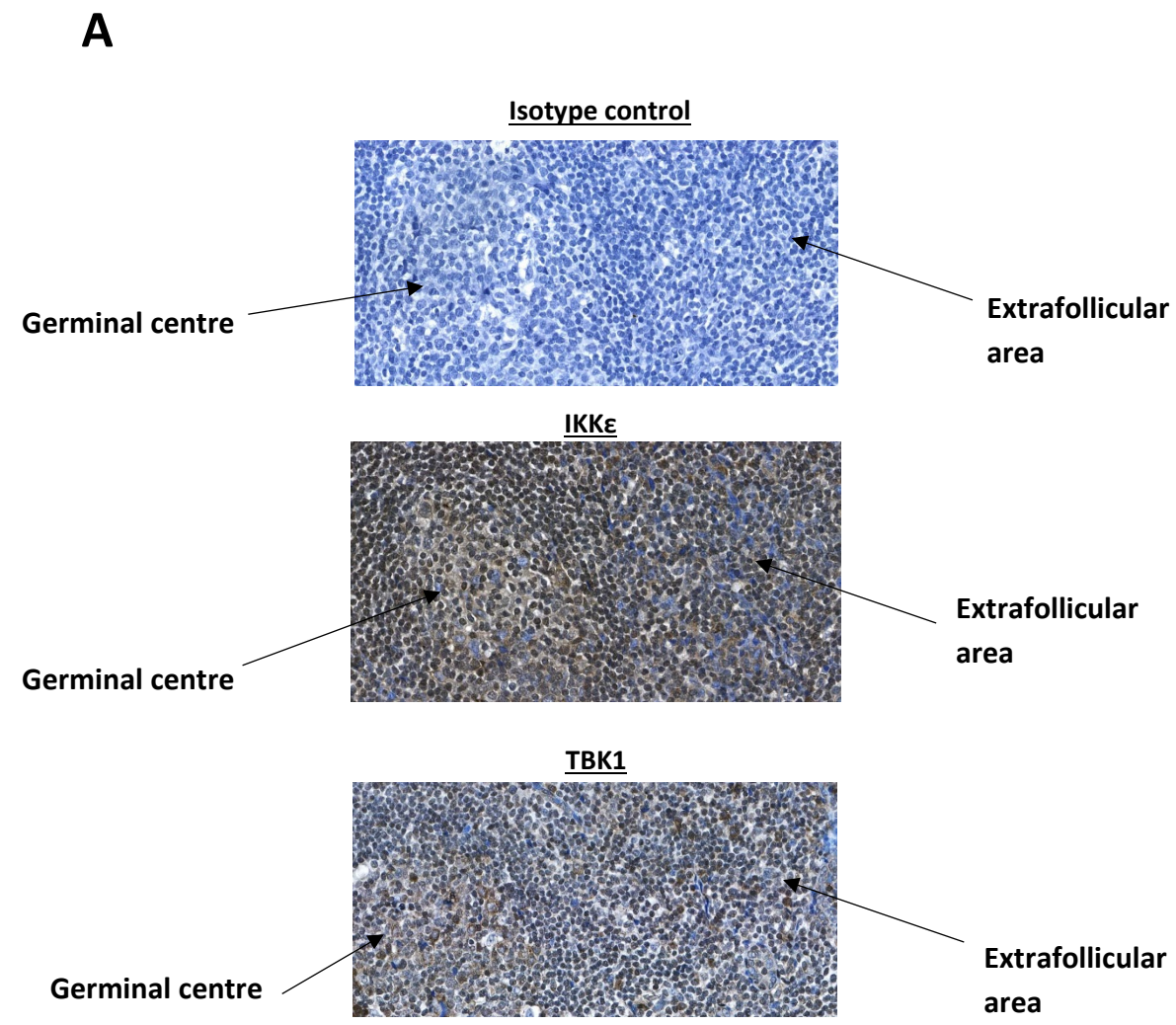

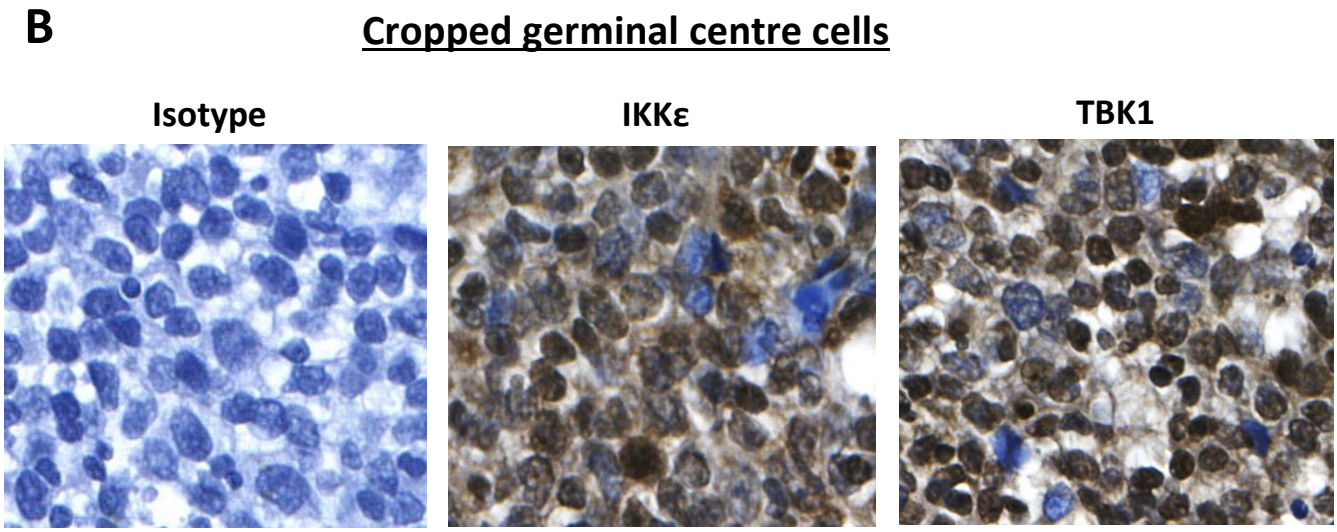

Figure 3:4: Immunohistochemical staining of human tonsil sections with antibodies specific for TBK1, IKKε or an isotype control. Staining of the germinal centre and extrafollicular region is shown (A). Cropped images of staining of germinal centre regions for each antibody are shown (B).

Specific IKKε and TBK1 protein expression was observed in the tonsil tissue examined. Germinal centres were largely positive for both IKKε and TBK1. There was also widespread IKKε and TBK1 expression in the T-cell rich extrafollicular areas outside the germinal centres suggesting that expression is not limited to just B-cells in the tonsil, but also T-cells. Positive staining was seen in the nucleus/cytoplasm of cells.

3.2.5 IKKε and TBK1 protein expression in human DLBCL

Following confirmation that both IKKε and TBK1 are indeed expressed at the protein level in human tonsil sections (Figure 3:4), the expression of both kinases was assessed patients diagnosed with DLBCL.

To achieve this, a tissue microarray consisting of tumour cores from 30 DLBCL patients (Appendix, Table S2) was analysed by co-immunofluorescence for the presence of IKKε (TRITC) and TBK1 (FITC), and counter stained with DAPI. Three cases were removed for technical reasons i.e. incomplete cores, leaving 27 cases which could then be scored as either positive or negative for the presence of IKKε, TBK1 or both. Examples of fluorescent staining (Figure 3:6) show that there are cases expressing one or the other kinase while other cases express both kinases, and some neither.

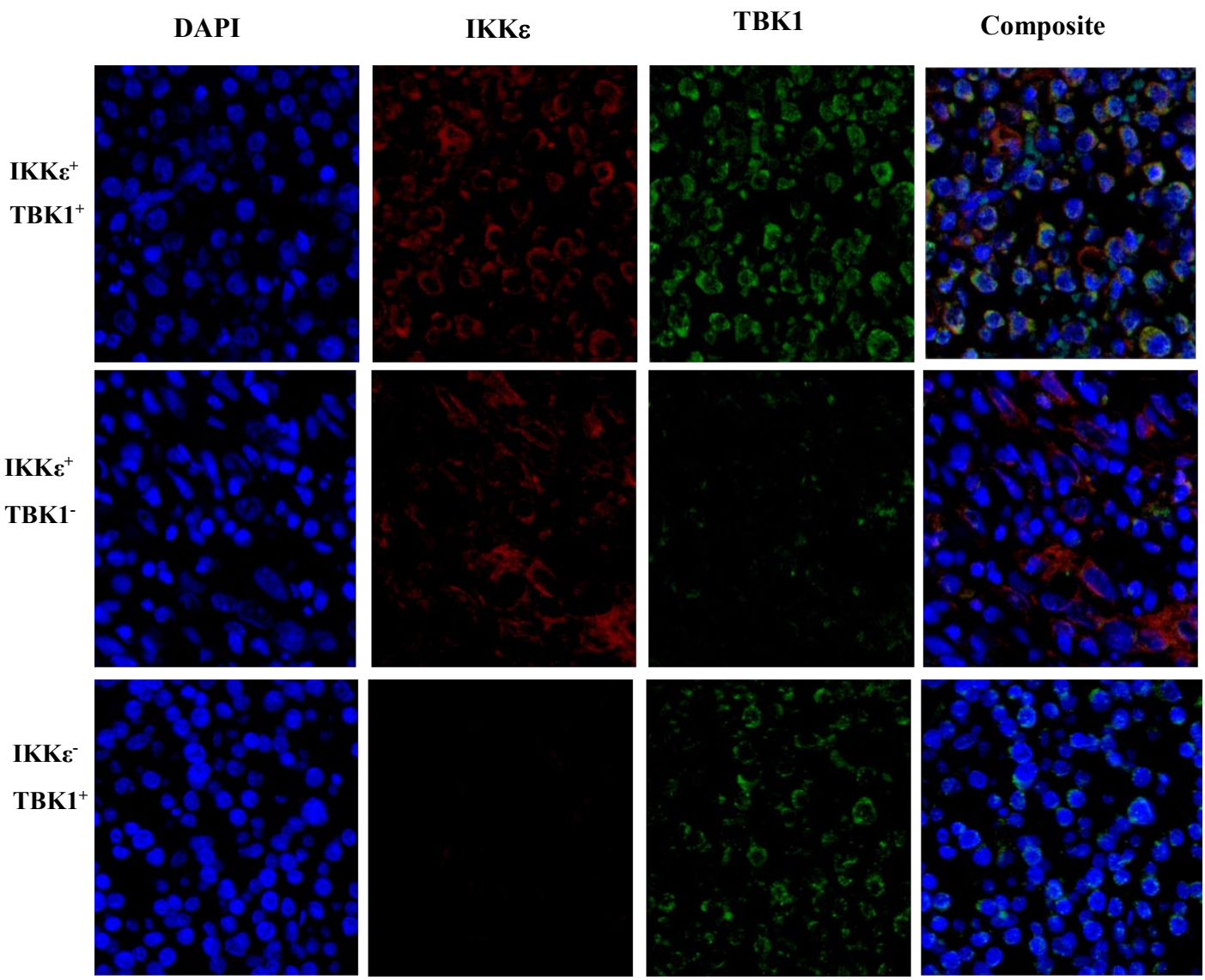

	IKKε$^-$ / TBK1$^-$	IKKε$^+$ / TBK1$^-$	IKKε$^-$/TBK1$^+$	IKKε$^+$ / TBK1$^+$
Number of cases	**9**	**3**	**5**	**10**

Figure 3:5: Representative immunofluorescence of cases of DLBCL stained with anti-TBK1 (green), anti-IKKε (red) and DAPI to define cell nuclei (blue). Merged images are shown to the right. Examples of IKKε$^+$TBK1$^+$, IKKε$^+$/TBK1$^-$, IKKε$^-$/TBK1$^+$ cases are shown, and frequencies of each case are shown in the Table.

The expression of IKKε is seen to be variable across primary human DLBCL cases. There was positive staining in 13 out of the 27 cases (48%) tested. Positive TBK1 expression was observed in 15 of 27 cases (56%) and co-expression of both IKKε and TBK1 was seen in 10 cases (37%) (Table 3:1). Analysis of staining images for IKKε and TBK1 in primary DLBCL tissue sections reveals that where positive staining is detected, staining is limited largely to the cytoplasm of cells (Figure 3:5).

These results demonstrate that, as seen in DLBCL cell lines, expression of IKKε and TBK1 is not uniform across primary DLBCL cases. The majority of cases had expression of at least one kinase, and the most common staining pattern was positive for both kinases. A third of cases were negative for both IKKε and TBK1 suggesting that there is a subset of DLBCL that do not involve these kinases.

3.2.6 IKKε and TBK1 association with GC/Non-GC status

Subsequent to confirmation of IKKε/TBK1 protein expression in primary human DLBCL, any association between kinase expression and GC/Non-GC status was determined. In order to do this, TMA slides containing the same tumour samples as those analysed in Figure 3:6 were stained by chromogen based immunohistochemistry for the presence of CD10, BCL6 and MUM1. This then allows tumours to be classified into GC or non-GC status by following the Hans algorithm (Hans et al., 2008). Example staining of CD10, BCL6 and MUM1, and the subsequent assignment of GC or non-GC status for the tumour samples contained on the TMA are shown in Figure 3:6.

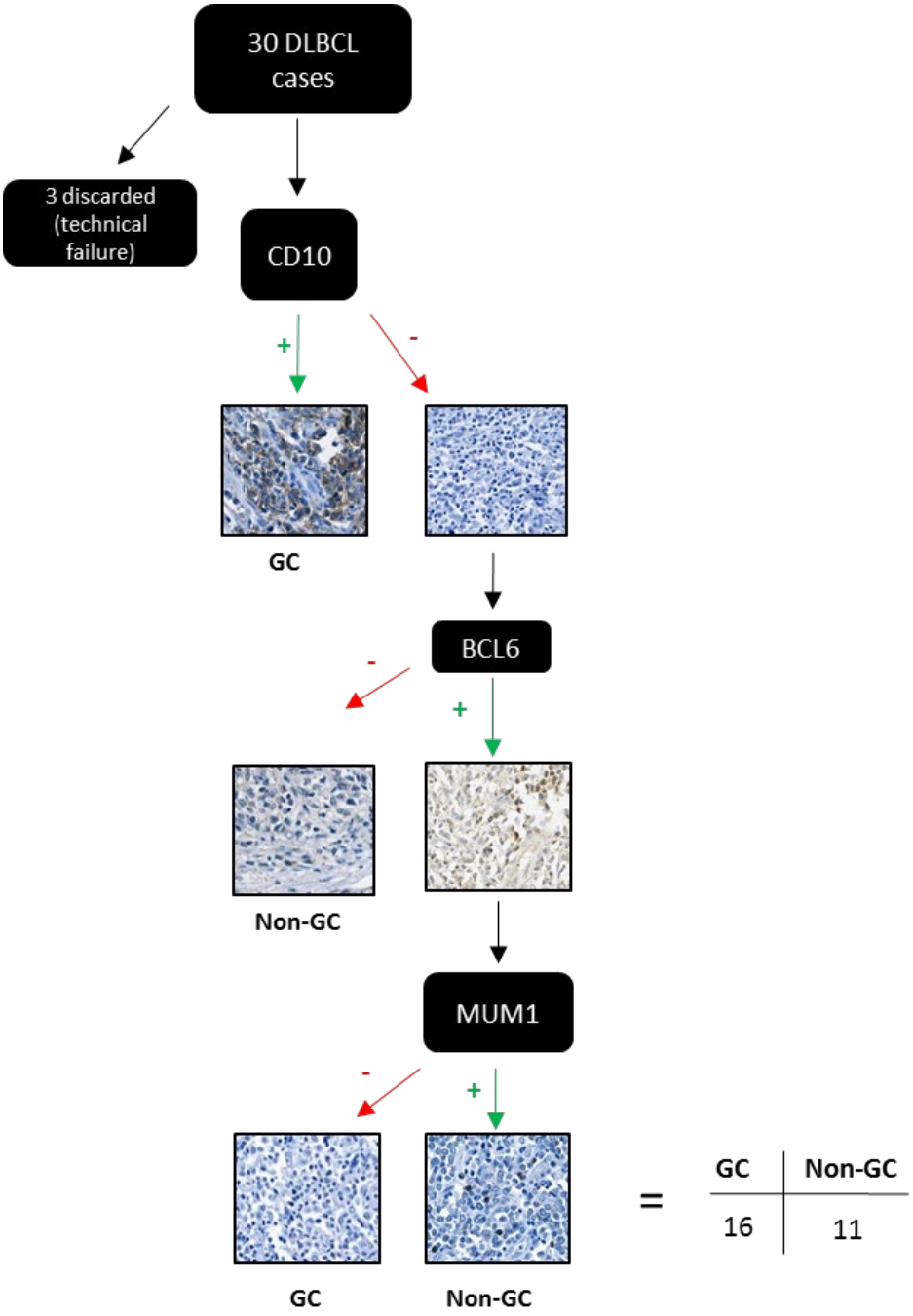

Figure 3:6: Application of the Hans algorithm in 27 primary DLBCL cases. Example positive and negative staining for each antibody is provided. Resulting numbers of cases classified as GC or non-GC are provided.

After application of the Hans algorithm, each tumour sample on the TMA was assigned a GC/non-GC status resulting in 16 GC and 11 non-GC DLBCLs. It was then possible to assess

whether or not IKKε or TBK1 expression has any association with GC/non-GC status (Figure 3:7).

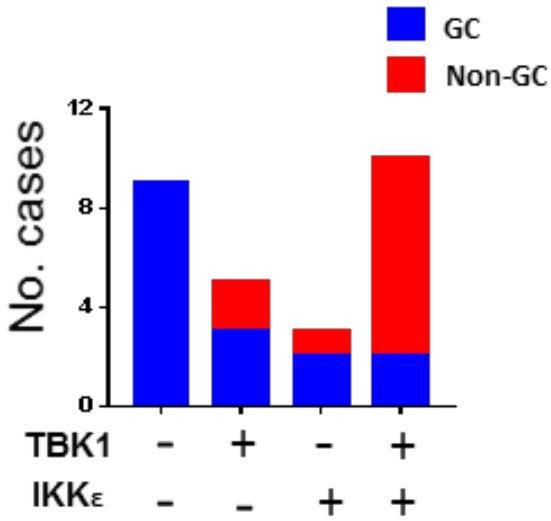

Association with non-GC status

TBK1 (P = 0.002)

IKKε (P = 0.004)

Figure 3:7: Histogram showing numbers of DLBCL cases (defined by expression of IKKε and TBK1) of GC (blue) or non-GC (red) type. Significant association to non-GC status was determined for IKKε (P = 0.004) and TBK1 (P = 0.002) by chi-squared analysis.

Figure 3:7 demonstrates a statistical association (chi-squared analysis) between both IKKε and TBK1 expression and non-GC status in primary DLBCL. All cases of DLBCL with no IKKε or TBK1 expression belonged to the GC category, and 8/10 cases with positive staining for both TBK1 and IKKε belonged to the non-GC status. These results suggest that IKKε and TBK1 are more preferentially expressed in non-GC DLBCL.

3.3 Discussion

In this chapter, the transcript and protein expression of IKKε and TBK1 was assessed in DLBCL. Additionally, association with IKKε/TBK1 expression and prognosis or GC/non-GC status was assessed in DLBCL patient cohorts.

3.3.1 *IKBK*E and *TBK1* transcript expression is high in DLBCL compared to other human cancer types

As an initial step, the transcript levels of *IKBKE* and *TBK1* were interrogated in a publically available database containing RNA-Seq values of gene expression across 37 types of human malignancy – the cancer genome atlas (TCGA). This analysis revealed variable expression of *IKBKE* across TCGA, with log(2) expression values ranging from 5.5 in PCPG, to ~ 10.5 in DLBCL. The highest ranked cancer types ranked by *IKBKE* expression are DLBCL, acute myeloid leukaemia (AML), being 1st and 2nd out of 37 cancer types, respectively. These malignancies are derived from lymphocytes, which fits with the described expression of *IKBKE* expression being largely restricted to lymphocytes and immune tissue (Shimada et al., 1999, Tojima et al., 2000).

The expression of *TBK1* transcript is consistently high with almost all cancer types having a log (2) expression between 9 and 10. This is consistent with previously reported data that *TBK1* is largely ubiquitously expressed in all tissue types (Shimada et al., 1999, Tojima et al., 2000). The *TBK1* expression value ranks DLBCL 8th out of 37.

3.3.2 TBK1 expression associates with poor prognosis in a DLBCL cohort

In order to determine whether there is any prognostic value to *IKBKE* or *TBK1* expression in DLBCL, a large patient cohort was examined (Lenz et al., 2008). Data for this cohort includes survival data and accompanying gene expression data for each patient. When patients were split into high or low *TBK1* groups, those with high *TBK1* expression had a significantly shorter overall survival (P = 0.027).

Song et al., (2015) found that high *TBK1* expression was associated with shorter overall survival in PDAC patients, albeit at the protein level.

There was no significant association between *IKBKE* expression and overall survival in this cohort. This is in contrast to findings in ovarian cancer (Guo et al., 2009) and squamous cell

carcinoma (Yang et al., 2018) where IKKε protein and *IKBKE* transcript were associated with poorer survival in each disease state, respectively.

The data presented in this chapter support the notion that *TBK1* expression, but not *IKBKE*, may be a useful prognostic indicator in the DLBCL setting.

3.3.3 IKKε and TBK1 protein expression in DLBCL

Initially, the expression of IKKε and TBK1 protein was assessed in a panel of seven DLBCL lines which are thought to represent a range of both GC and ABC like DLBCLs.

Expression of IKKε was relatively uniform in 5 out of 7 DLBCL cell lines. The two exceptions are the GC like cell lines Pfeiffer and SUDHL4. Pfeiffer cell lines had a very high expression level, whereas SUDHL4 was largely deplete of IKKε expression.

As TBK1 is thought to be ubiquitously expressed, it was somewhat surprising to observe variable expression between DLBCL cell lines. That said, Cooper et al., (2017) observed variable TBK1 expression across non-small cell lung cancer cell lines. TBK1 could therefore become either up or downregulated in during certain transformation events.

The variation seen in IKKε and TBK1 expression in DLBCL cell lines was reflected in primary human DLBCL. There were several cases (9/27) devoid of either IKKε or TBK1 expression, and several (10/27) cases with positive expression of both kinases. The remaining cases were split between those only positive for TBK1 (5/27) or IKKε (3/27). The absence of either kinase in a subset of cases suggests that the pathophysiology of these cases does not involve IKKε or TBK1 and therefore targeting these kinases may not be of use.

3.3.4 TBK1 and IKKε expression is associated with non-GC status in DLBCL

The Hans (2004) staining algorithm was applied to this set of patient tumour samples in order to first separate the DLBCL TMA cases into GC or non-GC status. This resulted in assignment of 16 tumours to GC status and 11 tumours to non-GC status.

This staining then allowed an assignment of GC/non-GC status to specimens previously stained for IKKε and TBK1. When this is done, there is a significant association between non-GC status and expression of IKKε or TBK1 ($P = 0.002$, $P = 0.004$, respectively.). These data show that IKKε and TBK1 are highly expressed at the mRNA and protein level in a subset of DLBCL cell lines and primary human DLBCL cases. The enzymes are often expressed together and are more likely to be expressed in non-GC DLBCLs which has a

worse prognosis. In the next chapter the effects of combined IKKε/TBK1 small molecule inhibitors will be explored.

Chapter 4 – Characterization of novel dual IKKε/TBK1 inhibitors effects on diffuse large B-cell lymphoma cell lines.

4.1 Introduction

Inhibition of IKKε and TBK1 has been suggested as a potential therapeutic avenue in obesity related dysfunctions (Reilly et al., 2013) inflammation (Yu et al., 2012), and multiple human malignancies (Shen and Hahn, 2011). IKKε and TBK1 are therefore attractive therapeutic targets in some non-malignant conditions and, several attempts have been made to establish inhibitors of these kinases.

One such inhibitor is Amlexanox. Amlexanox is currently used for the treatment of ulcers, (Bell, 2005), and has been shown to target both IKKε and TBK1 (Reilly et al., 2013). Oral et al., 2017 assessed the use of Amlexanox in a phase two clinical trial of obese patients with type-2 diabetes and non-alcoholic fatty liver disease. In this study, administration of Amlexanox was found to improve glucose control in a subset of patients, and exhibited only mild side effects (Oral et al., 2017). This is the only published clinical trial involving IKKε/TBK1 inhibitors. In the cancer setting, Amlexanox has been shown to reduce cell viability in glioblastoma cell lines (Liu et al., 2017) and increase sensitivity of MLL/AF4 positive acute lymphoblastic leukaemia to TNFα treatment (Tamai et al., 2017).

The IKKε/TBK1 inhibitors MRT67037, BX795 and CYT387 have also been explored as potential anti-cancer agents. BX795 was originally identified as a 3-phosphoinositide-dependent kinase-1 (PDK1) inhibitor (Feldman et al., 2005), but was later discovered to inhibit IKKε and TBK1 in the low nano molar range (Bain et al., 2007) BX795 treatment of human oral squamous carcinoma cells reduced cell proliferation and inhibited NF-κB and AKT signalling in these cells (Bai et al., 2015). Using NSCLC cells, Zhu et al, (2014) demonstrated that BX795, MRT67037 and CYT387 (a potent JAK/IKKε/TBK1 inhibitor) were selective against Kras dependent cell lines in reducing viability (Zhu et al., 2014)

There have been no prior studies investigating IKKε/TBK1 inhibitors in the DLBCL setting.

The drug discovery company Domainex (DMX), are currently developing highly selective dual IKKε/TBK1 inhibitors for potential use in the inflammatory disease setting. Several of these inhibitors were included on a small molecule panel that was used to screen a Burkitt lymphoma cell line – DG75 that had conditional BCL6 expression. The purpose of this screen was to identify compounds that had preferential activity against BCL6 negative DG75 cells when compared to BCL6 positive cells. This could then identify drug candidates that may have preferential activity against non-GC DLBCL (typically BCL6 deficient) compared

to GC – DLBCL. Amongst other small molecule inhibitors, three DMX IKKε/TBK1 inhibitors demonstrated preferential activity in BCL6 deficient DG75 cells.

The efficacy of DMX IKKε/TBK1 inhibitors against a panel of DLBCL cell lines was assessed, and forms the basis of this chapter.

4.2 Results

4.2.1 Pilot screening of DLBCL cell lines with a panel of Domainex IKKε/TBK1 inhibitors

As an initial step in examining DLBCL sensitivity to IKKε/TBK1 inhibition, a panel of six DMX dual IKKε/TBK1 inhibitors were used to treat a panel of six DLBCL cell lines for 48 hours at concentrations within the range of 13.7nM to 30μM. Following 48 hours of drug treatment, viability of the treated cells was assessed by CTG assay and a summary of the initial screening data is presented (Figure 4:1).

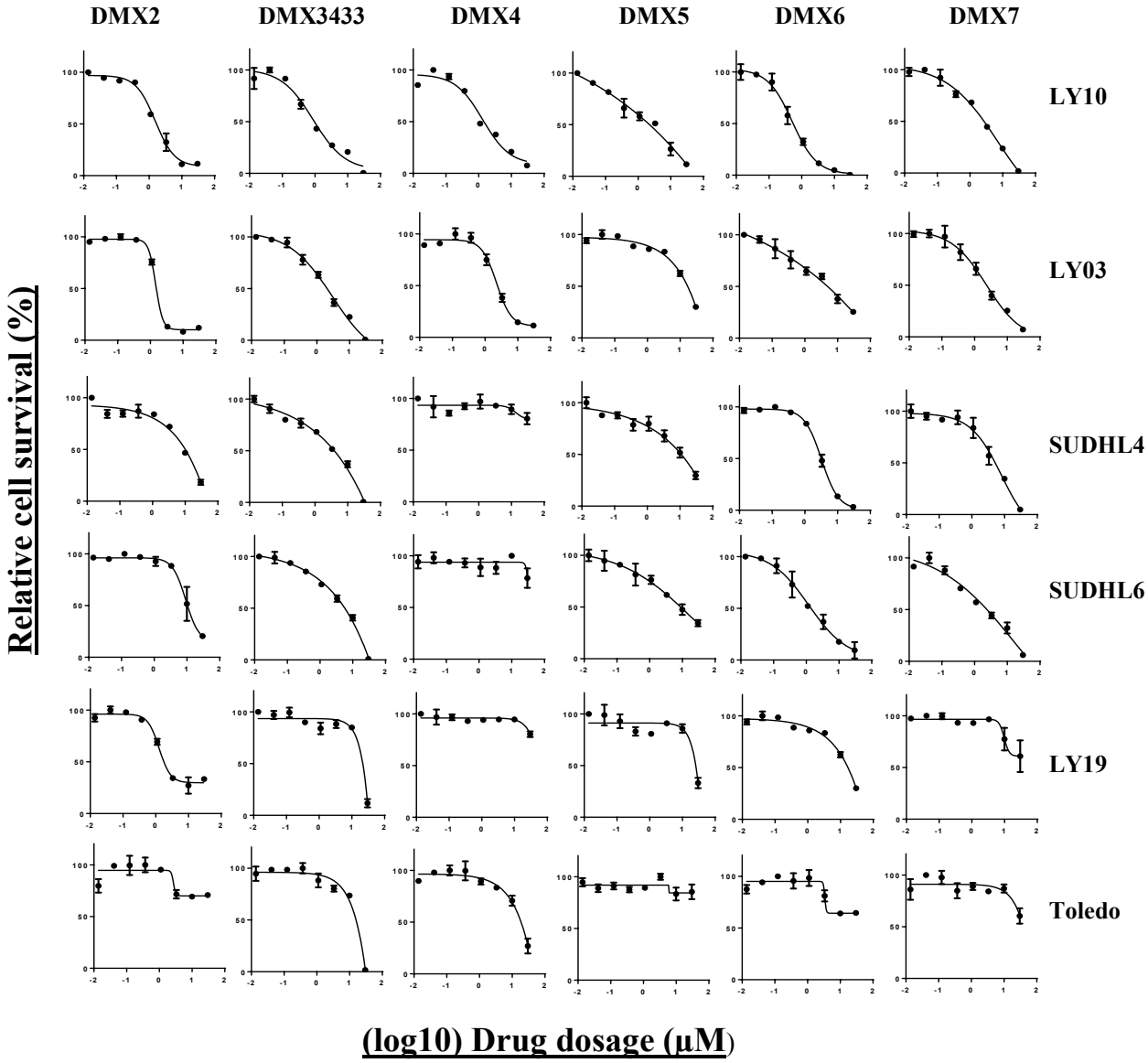

Figure 4:1. Dose effect curves of 6 DLBCL cell lines treated with 6 individual DMX IKKε/TBK1 inhibitors. Cells were treated with a range of DMX inhibitor dosages, and cell viability assessed after 48h treatment by CTG assay. Relative cell survival was calculated as a percentage of vehicle control (DMSO) treated cells. Error bars are Mean ± SEM, N=1.

The concentration at which cell viability was reduced to that of 50% of DMSO treated cells (EC50) was calculated for each drug/cell line combination and are shown in Table 4:1.

Cell line	DMX2 EC50	DMX3433 EC50	DMX4 EC50	DMX5 EC50	DMX6 EC50	DMX7 EC50
Ly10	2.2	1.0	1.8	2.4	0.6	3.1
Ly03	1.7	2.7	2.7	20.0	8.3	2.9
SUDHL4	12.4	5.4	>30.0	15.2	3.5	6.4
SUDHL6	12.2	6.9	>30.0	15.2	1.8	3.4
Ly19	1.7	22.3	>30.0	26.1	20.0	>30.0
Toledo	>30.0	18.3	23.3	>30.0	>30.0	>30.0

Table 4:1. EC50 values (µM) calculated from dose effect curves presented in Figure 4:1. Conditional formatting was applied to the values with lower values shaded green and higher values shaded red.

These pilot experiments revealed that the ABC cell lines, Ly10 and Ly03 were, on the whole, more sensitive to treatment with dual IKKε/TBK1 inhibitors. The EC50 values for these cell lines generally ranged from 1-3µM. The GCB cell lines, showed more resistance to inhibitor treatment with EC50 values exceeding 20µM for Ly19 and Toledo cells.

4.2.2 Correlating Domainex IKKε/TBK1 potency against cell lines with their selectivity against purified enzyme

The observed reduction in cell viability due to the DMX inhibitors could be due to effects on kinases other than IKKε and TBK1. In order to gain reassurance that the reduction in cell viability observed in sensitive DLBCL cell lines was due to on-target effects, the *in vitro* ability of each compound to inhibit IKKε/TBK1 kinase activity was plotted against the *in vitro* capacity to inhibit cellular viability. To aid in this, an additional three compounds with comparatively low *in vitro* selectivity for IKKε/TBK1 were screened against the sensitive Ly10 and Ly03 cells.

Due to the large difference in EC50 values against purified enzyme (low nano molar range) and cellular EC50 (low micro molar range), pEC50 values i.e $\log_{10}$ -(EC50), were used. Plots are presented (Figure 4:2).

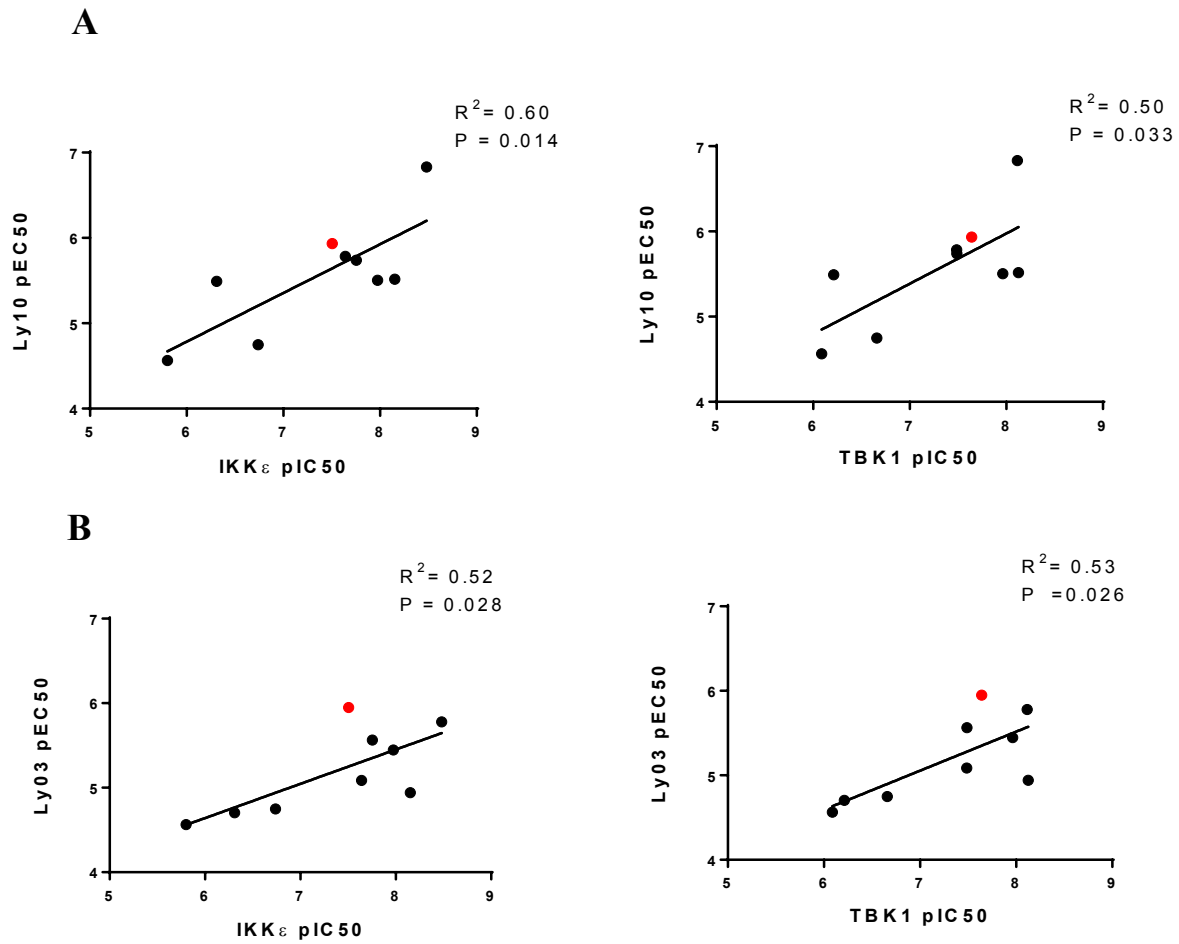

Figure 4:2. Nine IKKε/TBK1 small molecule inhibitors were assessed for effects on cell survival (determined by ATP luminescence) of the Ly10 cell line (left-hand panels) or Ly03 cell line (right-hand panels). pEC50 against the cell line (y-axis) is plotted against the concentration required for 50% inhibition of enzyme activity (pIC50), (N=1). Results for TBK1 are shown in the upper panel and IKKε in the lower panels. DMX3433 is indicated by the red dot.

4.2.3 Characterisation of DMX3433 – a dual IKKε/TBK1 inhibitor

From the initial pilot screen of DMX inhibitors (Figure 4.2.1), one compound, DMX3433, was selected for further, more detailed analysis. DMX3433 was selected as it produced the most reproducible data and was resistant to degrading following freezing and thawing.

A total of seven DLBCL cell lines were then treated with DMX3433 for 48 hours over a range of doses. Viability was then assessed by ATP luminescence, and the resulting survival curves are shown (Figure 4:3).

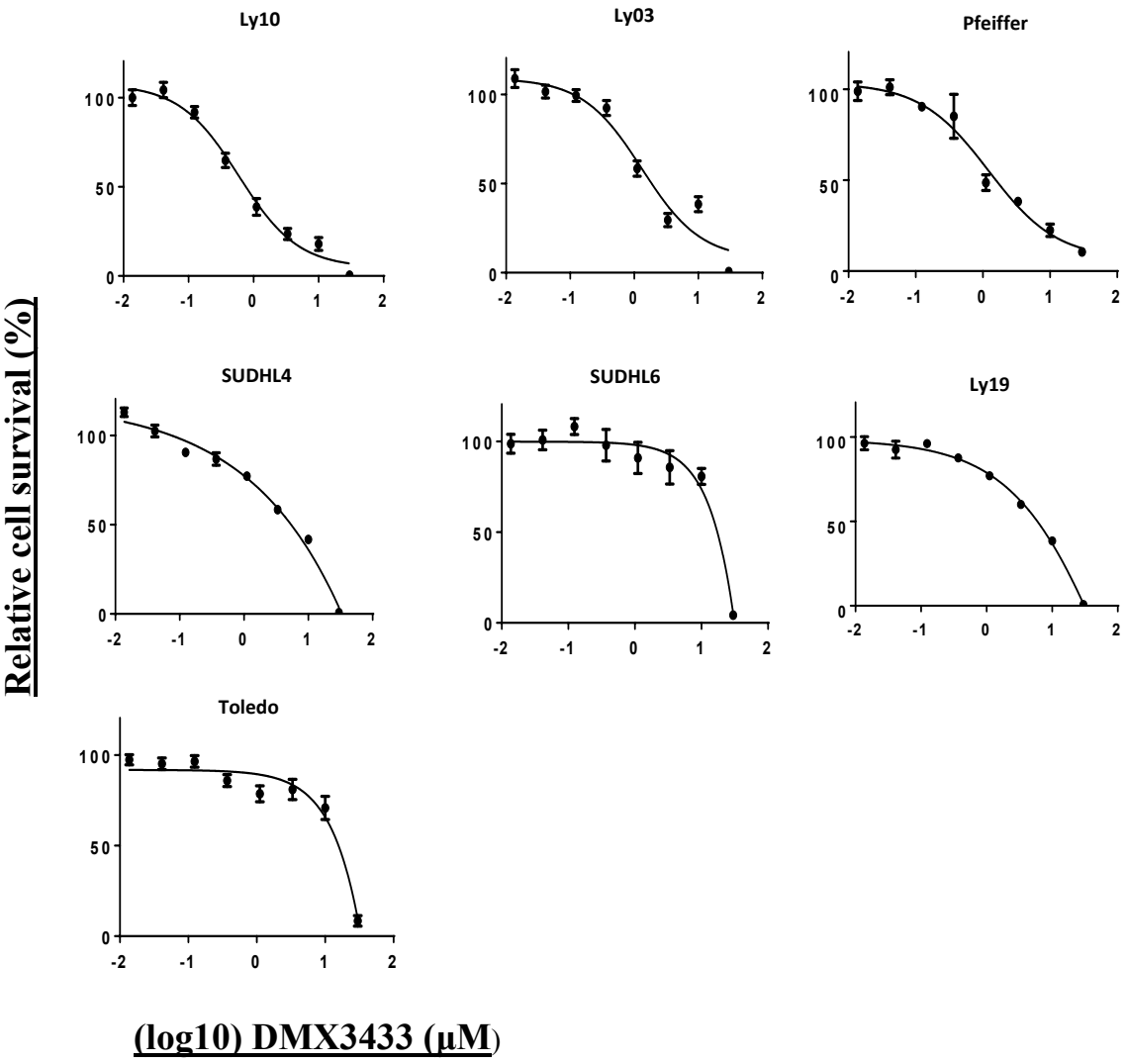

Figure 4:3. Dose response curves for cells treated with DMX3433 for 48 hours. For SUDHL4 N=1, but for other cell lines N=3. Viability was assessed by ATP luminescence and percentage survival calculated relative to DMSO treated cells. Error bars are Mean ± SEM.

The mean absolute EC50 values are summarised (Table 4:2). Ly10, Ly03 and Pfeiffer are the most sensitive while Ly19 and Toledo are the least sensitive with SUDHL4 and SUDHL6 having intermediate sensitivities.

Cell Line	DMX3433 EC50
Ly10	1.41
Pfeiffer	1.68
Ly03	1.71
SUDHL4	5.41
SUDHL6	6.04
Ly19	15.25
Toledo	15.54

Table 4:2. EC50 (μM) values calculated from the dose response curves shown in Figure 4:3.

4.2.4 Cellular consequences of DMX3433 treatment

4.2.4.1 DMX3433 treatment does not result in cell cycle arrest in Ly10 cells

As an initial step in determining cellular consequences of DMX3433 treatment, the effects on the cell cycle in treated Ly10 cells was examined (Figure 4:4).

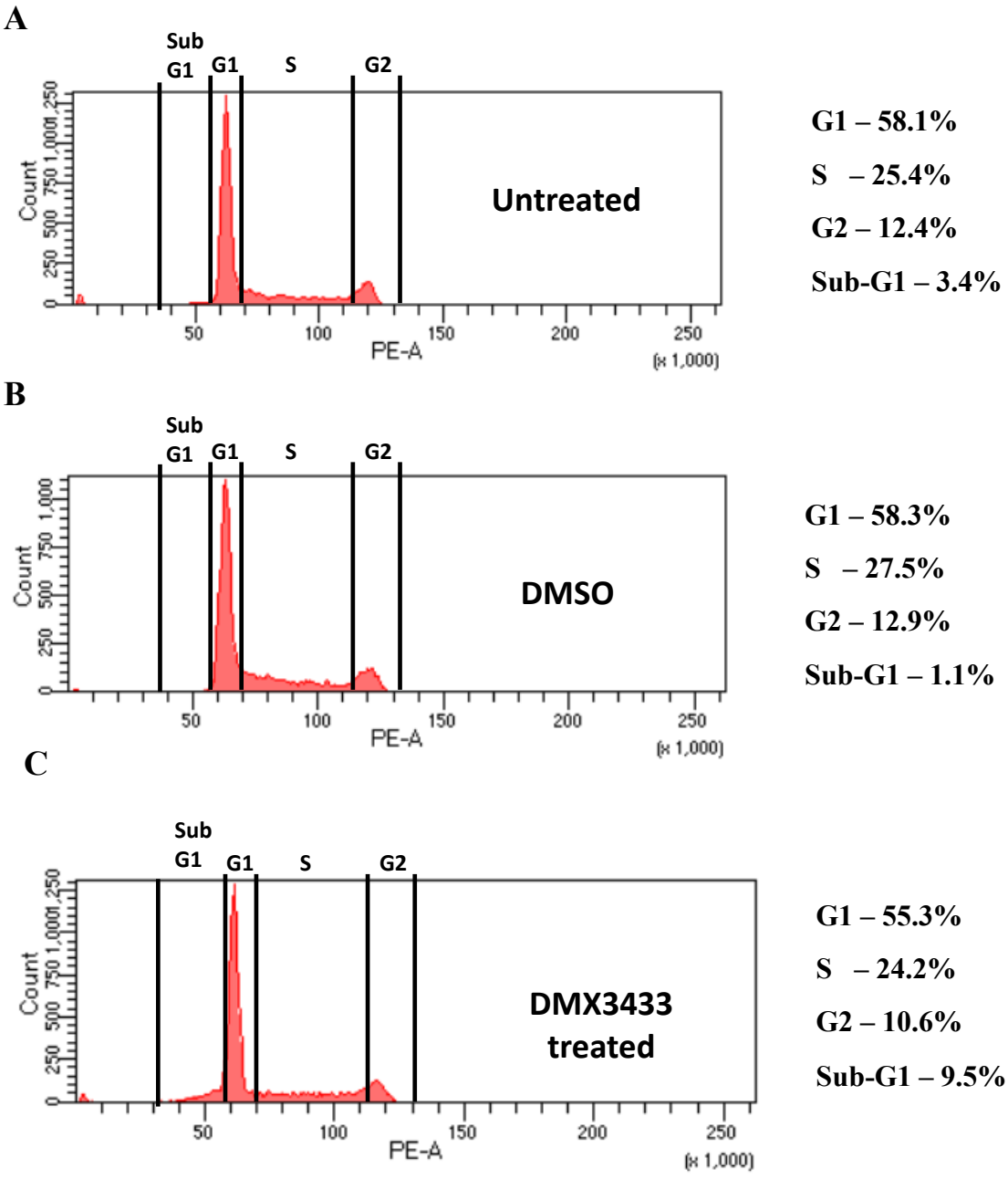

Figure 4:4. Cell cycle analysis of untreated Ly10 cells (A), DMSO treated Ly10 cells (B), or Ly10 cells treated with 2uM DMX3433 for 18h (C). Percentages of cells judged to be in either G1, S or G2 or sub-G1 phase are displayed to the right of each condition, N=1.

There appeared to be little effect on the cell cycle of Ly10 cells treated with DMX3433. Approximately equal proportions of G1 and S phase cells were seen between untreated, DMSO treated and DMX3433 treated cells. There was a very slight reduction in the proportion of cells in the G2 phase in DMX3433 treated Ly10 cells. This is suggestive that DMX3433 treatment has little effect on the cell cycle in the Ly10 cell line. There was however, an increase in the sub-G1 population in cells treated with DMX3433. The presence of a sub-G1 population is sometimes indicative of apoptotic cells (Riccardi and Nicoletti, 2006), and therefore I next set out to determine if Ly10 cells undergo apoptosis in response to DMX3433.

4.2.4.2 DMX3433 treatment triggers apoptosis in Ly10 cells

Ly10 cells were selected as they are sensitive to DMX3433 treatment and were more amenable to cell culture than the Ly03 or Pfeiffer cell lines.

A common method for the detection of apoptotic cells is the staining for the presence of AnnexinV on the cell surface (Vermes et al., 1995). This can be readily achieved through flow cytometry analysis. The abundance of AnnexinV positive cells in response to 2μM DMX3433 treatment for 24h is summarised in Figure 4:5.

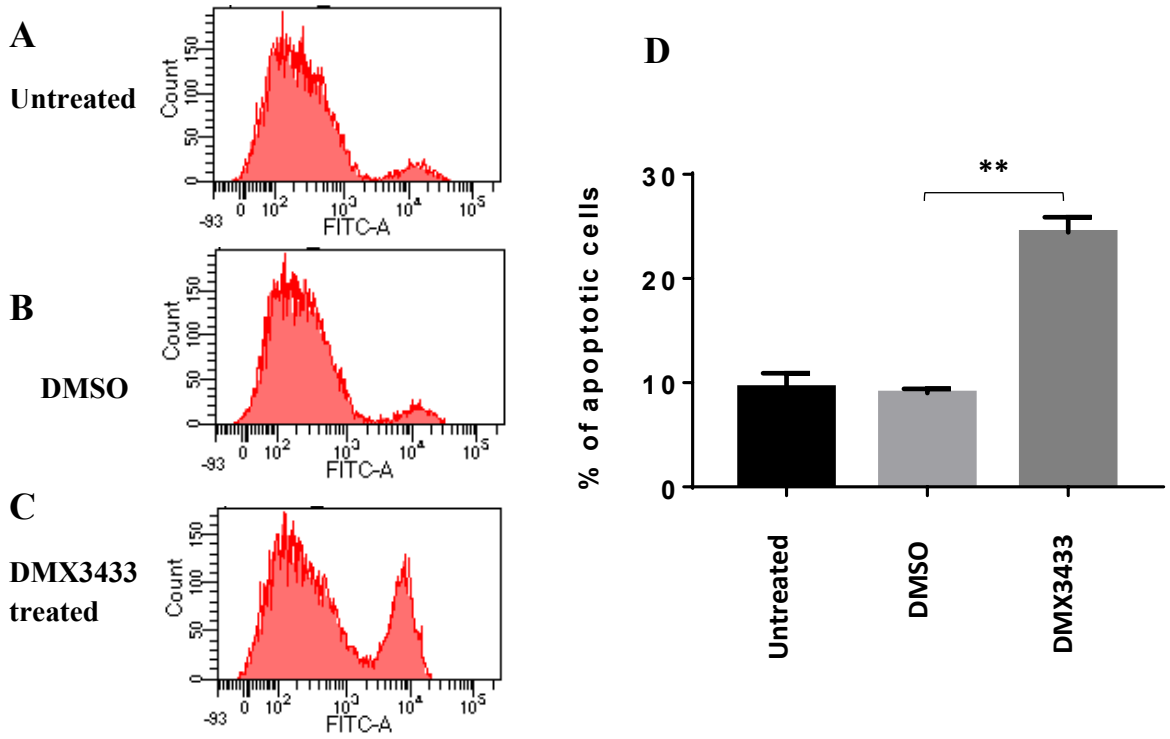

Figure 4:5. Representative Annexin V staining (FITC) of Ly10 cells either untreated (A), vehicle control treated (B) or DMX3433 treated for 24h (C). Percentages of apoptotic cells for each condition are presented in (C), there was a significant increase (paired t-test, P = 0.0031, N=3) in apoptotic cells in Ly10 treated with DMX3433.

Figure 4:5 demonstrates that Ly10 cells treated with DMX3433 for 24 hours show an increased percentage of apoptotic cells compared to those treated with DMSO only and this increase was significant (P = 0.0031).

Another marker of apoptosis is the presence of cleaved poly (ADP-ribose) polymerase 1 (PARP1). PARP is a 116 kDa protein that is cleaved by caspases upon the induction of apoptosis producing two subunits of 89 and 24 kDa in size (Oliver et al., 1998). To investigate this, a western blot was performed on lysates taken from Ly10 cells that were

untreated, treated with DMSO or treated with DMX3433 (2μM) for 24 hours. Membranes were then incubated with antibody for PARP1 (Figure 4:5).

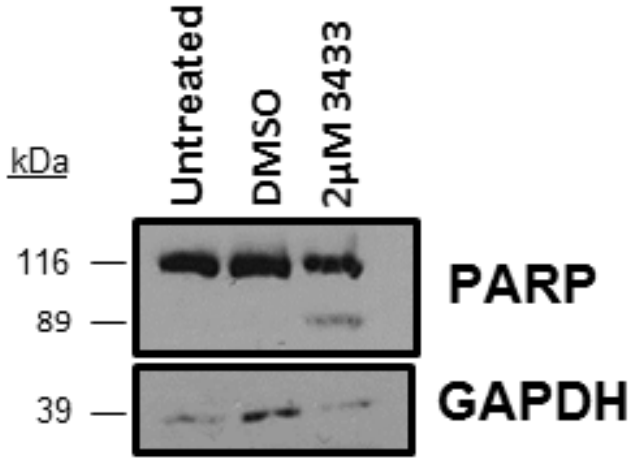

Figure 4:6. Western blot analysis of lysates taken from untreated, DMSO or 2uM DMX3433 treated Ly10 cells. Membranes were blotted for PARP and GAPDH was used as a loading control. Molecular weight (kDa) is indicated to the left.

The presence of a PARP1 subunit can be seen in lysates taken from Ly10 cells treated with DMX3433 for 24 hours. There is no detectable PARP1 cleavage in the untreated or DMSO treated Ly10 cells (Figure 4:5).

Overall, this evidence suggests that DMX3433 treatment induces apoptosis in Ly10 cells.

4.2.4.3 Markers for sensitivity of DLBCL cell lines to DMX3433 treatment

Work so far showed that not all DLBCL cell lines were equally sensitive to IKKε and TBK1 inhibitors and that differences in cell line sensitivity correlated with differences in potency of the small molecules against purified kinases. The cell lines Ly03 and Ly10 were most sensitive as compared with the other DLBCL cell lines (Table 4:2). In order to explore markers for sensitivity to DMX3433 treatment, which could be useful in considering targeting specific patient populations for clinical trials, the basal protein levels of known IKKε/TBK1 targets were examined by western blot across the seven DLBCL cell lines tested. This is shown in Figure 4:7.

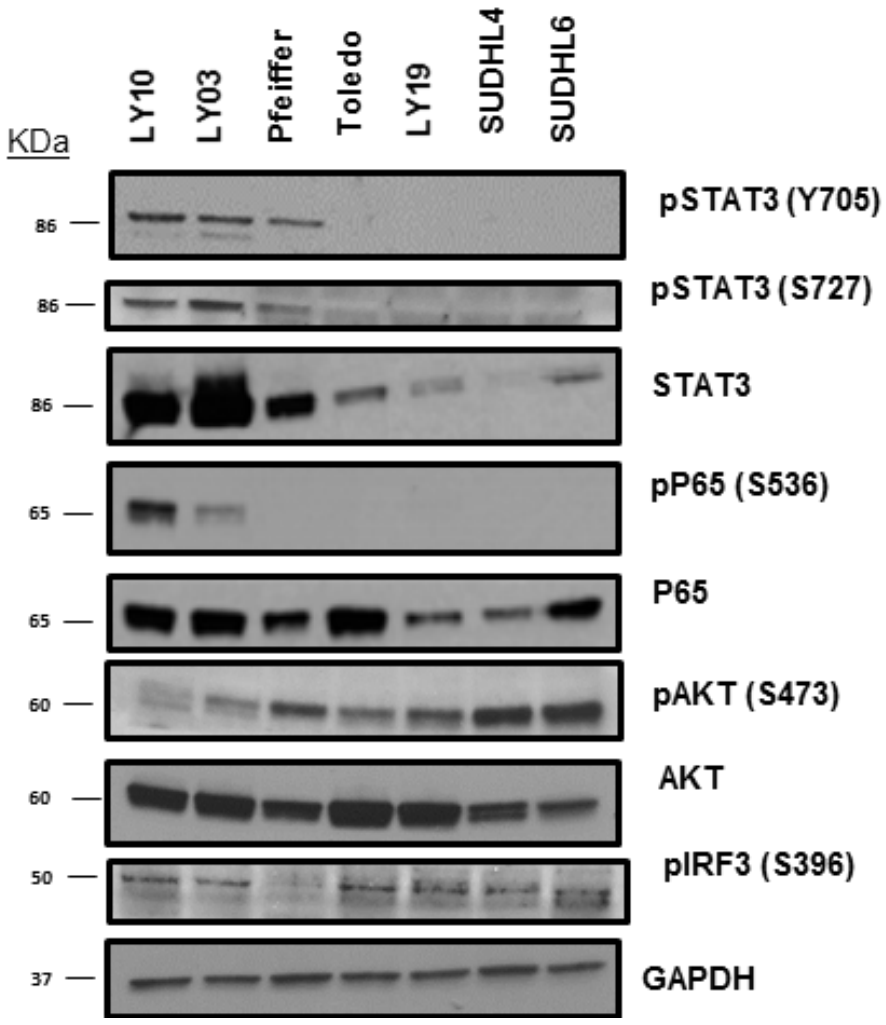

Figure 4:7. Western blot analysis of lysates taken from seven DLBCL cell lines. Membranes were blotted for pSTAT3 (Y705), pSTAT3 (S727), STAT3, pP65 (S536), P65, pAKT (S473), AKT and pIRF3 (S396). GAPDH was used as a loading control. Molecular weight (kDa) is indicated to the left.

A feature seemingly unique to cell lines sensitive to DMX3433 treatment is the presence of phosphorylated STAT3. Phosphorylation on both the tyrosine 705 and serine 727 residues is observable only in Ly10, Ly03 and Pfeiffer cell lines. Levels of total STAT3 are also elevated in these cells lines. This is indicative of active STAT3 signalling occurring in these cell lines, whereas those cell lines negative for phosphorylated STAT3 are not likely to harbour active STAT3 signalling.

NF-κB component, P65, is phosphorylated at serine 536 only in the ABC like DLBCL cell lines Ly10 and Ly03, whereas total P65 is seen in all cell lines, suggesting that only Ly10 and Ly03 have active NF-κB signalling.

Conversely, phosphorylated AKT (serine 473) is predominantly expressed in the GC like cell lines, with comparatively little expression in Ly10 and Ly03 cells.

Phosphorylated IRF3 (serine 396) is ubiquitously expressed across the DLBCL cell lines with the exception of Pfeiffer which shows little pIRF3 (Figure 4:7).

Overall it appears that the cell lines most sensitive to DMX3433, Ly03 and Ly10, are those with phosphorylated STAT3 and P65. However, Pfeiffer is also sensitive to DMX3433 and yet has no phosphorylated P65 suggesting that there are other factors that are important although phosphorylated STAT3 and P65 might be useful protein markers for sensitivity to DMX3433.

4.3 Discussion

This chapter demonstrates that a subset of DLBCL cell lines undergo apoptosis, as judged by an increase in AnnexinV positive cells (Figure 5:5) and further supported by the presence of cleaved PARP in Ly10 cells, when treated with DMX IKKε/TBK1 inhibitors.

4.3.1 DMX IKKε/TBK1 inhibitor screen

A panel of six DMX IKKε/TBK1 inhibitors was used in a pilot screen of six DLBCL cell lines. This demonstrated a stark contrast in sensitivity to DMX inhibitor treatment between subsets of DLBCL cell lines. On the whole, the non-GC cell lines Ly10 and Ly03 exhibited a greater degree of sensitivity to inhibit treatment then the GC cell lines SUDHL4, SUDHL6, Toledo and Ly19. This suggests that IKKε/TBK1 inhibition may be a potential therapeutic avenue in non-GC DLBCL, but perhaps not in GC DLBCL.

There was also considerable variation seen between the efficacies of DMX inhibitors within a single cell line. For example, in Ly10 cells, treatment for 48 hours with DMX6 achieves a 50% loss of cell viability at 600nM, whereas treatment of the same cells with DMX7 results in an EC50 value of 3μM. It was hypothesised that the variation of inhibitor efficacy in reducing cell viability was correlated with their potency in inhibiting kinase activity of the purified IKKε and TBK1 enzymes. This was shown to be largely true, as a significant ($P = 0.0014$, $P = 0.026$) positive correlation between pEC50 against Ly10 cell viability and pEC50 against purified IKKε and TBK1, respectively and is an important piece of evidence confirming that the observed reductions in cell viability are due to on-target effects.

The addition of the Pfeiffer cell line into subsequent DMX3433 screening resulted in surprising levels of sensitivity of this cell line to DMX3433 treatment. This is evidence that there may be subsets of GC DLBCL that are dependent on IKKε/TBK1 function.

4.3.2 Markers of sensitivity to DMX3433 treatment

In order to determine signalling correlates with sensitivity to IKKε/TBK1 inhibitors western blots for the major pathways known to be altered by IKKε/TBK1 i.e. STAT3, NF-κB, AKT and IRF3, were carried out.

TBK1 has previously been shown to directly phosphorylate AKT (Ou et al., 2011), and phosphorylated AKT is present in ~ 50% of DLBCL cases (Xu et al., 2013). However, while being sensitive to DMX3433 treatment, Ly10 and Ly03 cells exhibited comparatively little phosphorylated AKT. Phosphorylated AKT was associated with GC cell line status, which is likely to be a reflection of primary GC like DLBCL having a higher association with PI3K/AKT signalling (Pfeifer et al., 2013). There was also little correlation between DMX3433 sensitivity and levels of IRF3 phosphorylation. This suggests that in DLBCL neither AKT nor IRF3 are suitable biomarkers for sensitivity to IKKε/TBK1 inhibition, and the mechanism of action that leads to cell death following DMX3433 treatment is unlikely to involve these proteins.

There was however, a correlation between P65 and/or STAT3 expression and DMX3433 sensitivity. The observation that pP65 is seen only in non-GC cell lines (Figure 4:7) is consistent with the published findings that constitutive NF-κB signalling is a hallmark of non-GC DLBCL (Staudt, 2010). The presence of phosphorylated STAT3 in the non-GC cell lines Ly10 and Ly03 is supported by findings that these two cell lines exhibit phosphorylated STAT3 on both the tyrosine 705 and serine 727 residues (Ding et al., 2008). Figure 4:7 also

shows that both tyrosine 705 and serine 727 phosphorylation is also observable in the GC like DLBCL cell line Pfeiffer. This is supported by the same observation in another study using Pfeiffer cells (Jiang et al., 2016). While active STAT3 signalling is generally associated with non-GC DLBCL (Ding et al., 2008), there are several studies identifying pSTAT3 in GC like DLBCL also. It is therefore not totally unexpected to observe pSTAT3 in GC like DLBCL cell lines. Indeed, Ding et al. (2008) show Y705 phosphorylation of STAT3 in the GC like cell lines Ly1 and Val – although S727 phosphorylation was absent in these cell lines (Ding et al., 2008).

However, the correlations with sensitivity to IKKε/TBK1 inhibitors are likely to be complex. For example, Pfeiffer did not have detectable phosphorylated P65 and therefore may not use NF-κB signalling. Pfeiffer does however bear an EZH2 mutation (Knutson et al., 2014) and the widespread changes in chromatin methylation caused by this aberration may modify the effects of IKKε/TBK1 inhibitors.

Collectively, it was shown here that cell lines sensitive to DMX3433 treatment were those which displayed active STAT3 signalling and/or active NF-κB signalling, as determined by the presence of phosphorylated STAT3 and P65, respectively. It is therefore a possibility that the mechanism of action of DMX3433 involves perturbation of these pathways. Analysis of this hypothesis will form the basis of Chapter 5.

Chapter 5– Analysis of the function of IKKε/TBK1 in diffuse large B-cell lymphoma

5.1 Introduction

It was demonstrated that small molecule inhibitors of IKKε/TBK1 are effective in causing apoptosis in a subset of DLBCL cell lines (Chapter 4). This subset appeared to be characterised by high-level expression of phospho-STAT3 and phospho-P65, but even this small group of cell lines did not show uniformity. Pfeiffer, one of the sensitive cell lines, did not have detectable phospho-P65 whereas Ly10 and Ly03 did show expression of this protein and all three cell lines expressed phospho-STAT3. Both the STAT3 and NF-κB pathways have been shown to be important for the survival of subsets of DLBCL (Davis et al., 2001, Ding et al., 2008, Lam et al., 2008) , which raises the possibility that DMX3433 leads to loss of cell viability in these cells through interruption of one or both of these pathways.

The importance of STAT3 signalling in the survival of a subset of DLBCL is well documented (Ding et al., 2008, Lam et al., 2008, Huang et al., 2013). STAT3 is activated by Janus kinase (JAK) signalling, which in turn is activated by cytokine receptor activation. Small molecule inhibitors of JAK2 have been developed for the treatment of myeloproliferative disorders such as myelofibrosis (Cervantes et al., 2013). Inhibition of STAT3 signalling by JAK inhibitors has been shown to be effective in pre-clinical models of DLBCL (Beguelin et al., 2015), however use of these drugs for the treatment of DLBCL has yet to enter clinical practice.

It is known that the ABC-like-DLBCL subset is reliant on constitutive NF-κB signalling (Davis et al., 2001). There have been several studies showing that targeting the NF-κB pathway in DLBCL is effective in reducing cell viability. For example there have been pre-clinical studies of small molecule inhibitors of IKKα and IKKβ (Deng et al., 2015, Lam et al., 2008). In clinical practice, the proteasome inhibitor bortezomib is used for the treatment of multiple myeloma, and inhibits NF-κB nuclear translocation (Leaonard et al., 2017). Despite several efforts to introduce bortezomib treatment for ABC like DLBCL patients, the use of this drug is yet to enter widespread clinical practice.

In DLBCL the NF-κB and STAT3 signalling pathways interact with one another. Lam et al., (2008) identified co-operative signalling between NF-κB and STAT3. These authors

suggested that NF-κB signalling drives the expression of IL-6 and 10, which can then signal through STAT3.

Although IKKε and TBK1 have roles in NF-κB signalling in several human cancers (Boehm et al., 2007, Guan et al., 2011) no studies have described functions for either kinase in DLBCL pathophysiology. In this chapter the function of IKKε and TBK1 in DLBCL will be analysed through investigation of drug treatment and siRNA knockdown in Ly10 cells which are sensitive to DMX3433 treatment.

5.2 Results

5.2.1 The effects of DMX3433 treatment on STAT3 in Ly10 cells

It was observed that the cell lines most sensitive to DMX3433 treatment (Ly10, Ly03 and Pfeiffer) expressed high levels of phosphorylated STAT3 whereas the insensitive cell lines (Toledo, Ly19) had undetectable levels of this protein. This suggests the hypothesis that the mechanism of action of DMX3433 involves directly or indirectly altering phosphorylated STAT3 levels.

To investigate this, lysates from Ly10 cells treated with DMX3433 (2 μM) for varying lengths of time (0.5 to 8 hours) were immunoblotted with antibodies directed against phosphorylated (Y705 and S727) and total STAT3 (Figure 5:1).

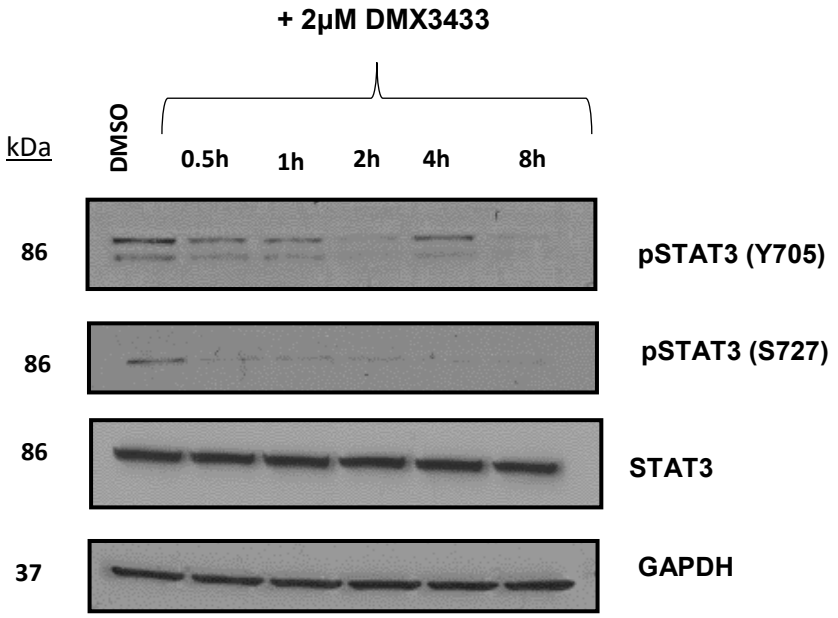

Figure 5:1. Western blot showing expression of phosphorylated and total STAT3. Lysates from Ly10 cells treated with 2μM DMX3433 for either 0.5, 1, 2, 4 or 8 hours or DMSO for 8hours were blotted for pSTAT3 Y705, pSTAT3 S727, or total STAT3. GAPDH was used as a loading control. Molecular weight (kDa) is indicated to the left.

There is an observable decrease in phosphorylated STAT3 on the tyrosine 705 residue from two hours post treatment with DMX3433 (2 μM). This reduction appears to be bi-phasic with an increase observed at the 4 hour time point, followed by a further reduction at 8 hours. This effect was reproducible (N=3). The serine 727 residue of STAT3 undergoes rapid and persistent de-phosphorylation (from 0.5 hours to 8 hours) after DMX3433 treatment. Levels of total STAT3 remain unchanged following DMX3433 treatment at these time points. These results suggest that the regulation of STAT3 phosphorylation in Ly10 cells by IKKε/TBK1 is complex with potentially different mechanisms regulating the two phosphorylation sites.

5.2.2 DMX3433 effects on NF-κB signalling

Two out of the three cell lines sensitive to DMX3433 treatment were also judged to have active NF-κB activity marked by the presence of phosphorylated P65 at residue serine 536. In order to establish if DMX3433 alters phosphorylated P65 pathway in Ly10 cells, western blots were carried out (Figure 5:2).

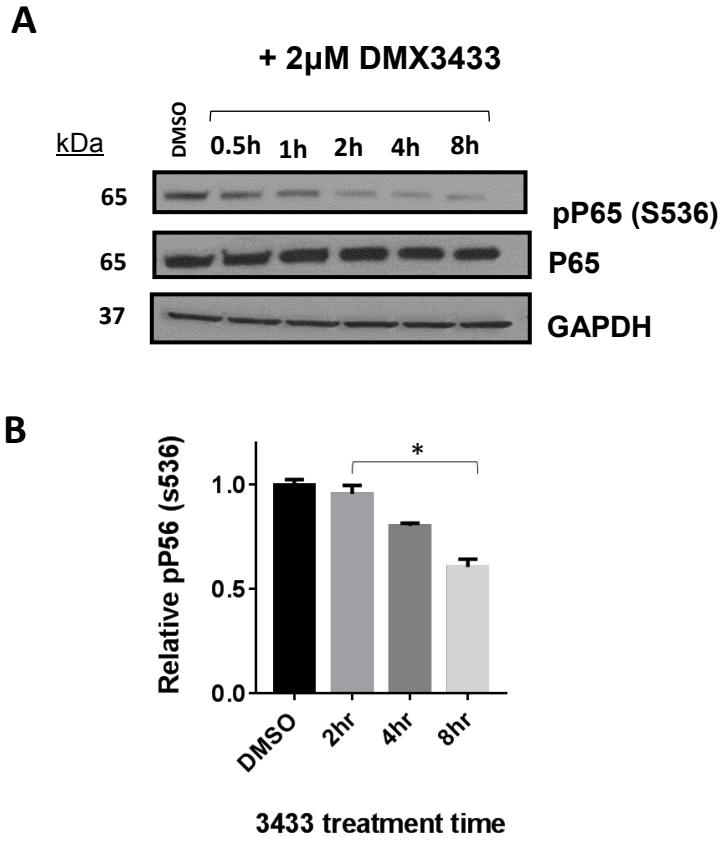

Figure 5:2 (A) Western blot taken from lysates of Ly10 cells treated with 2uM DMX3433 for either 0.5, 1, 2, 4 or 8 hours or DMSO for 8hrs. Lysates were blotted for pP65 (S536) or whole P65. GAPDH was used as a loading control. Molecular weight (kDa) is indicated to the left. (B) Expression of pP65 relative to DMSO treated cells from a pP65 S536 specific ELSIA for Ly10 cells treated with 2μM DMX3433 for 2, 4 or 8h. There was a significant difference (paired t-test) between pP65 levels at 2h and 8h post DMX3433 treatment (P = 0.03) Mean±SEM (N=3, outliers excluded).

There is minimal reduction of phosphorylated (S536) P65 at the 0.5 hour and 1 hour time points, but this becomes more apparent after 2 hours of drug treatment. Levels of total P65 remain unchanged throughout the treatment time course (Figure 5:2 (A)). Reduction in pP65 (S536) levels in Ly10 cells treated with DMX3433 were observed by means of ELISA (Figure 5:2 (B)), although only reaching statistical significance between the 2 and 4hr time points, and not between DMSO and 8hr treated samples. This is presumably due to the omission of a DMSO treated replica on account of it being an obvious outlier. Together, these results suggest that IKKε/TBK1 are required for P65 phosphorylation in Ly10 cells.

5.2.3 DMX3433 treatment alters cytokine secretion in Ly10 cells.

Both IKKε and TBK1 are serine/threonine kinases and, therefore, the tyrosine 705 residue of STAT3 cannot be a direct target of these kinases. The hypothesis suggested by the work of others is that NF-kB signalling drives cytokine production (Lam et al., 2008), which is in turn responsible for phosphorylation of tyrosine 705 of STAT3 (Béguelin et al 2015, Hodge et al., 2005). This view focuses attention on molecules secreted by the lymphoma cell lines and the question of whether levels are perturbed by administration of IKKε/TBK1 inhibitors. Based on the literature (Ghia et al., 2002, Husson et al., 2002, Lund, 2008, Yang et al., 2012, Takahashi et al., 2015) multiplex ELISAs for a panel of cytokines and chemokines was designed. IFNβ was tested for by ELISA as there was cross-reactivity on the multiplex ELISA with its inclusion (Table 5:1).

Cytokine	Chemokine
TNFα	CXCL6
IFNβ	CXCL13
IL-2	CCL3
IL-4	CCL4
IL-6	CCL17
IL-10	CCL22
IL-13	
IL-19	

Table 5:1. Cytokines and chemokines tested for their presence in Ly10 growth supernatant.

From this panel four – CCL3, CCL4. CCL22, IL-10 - were detectable in the supernatants of untreated Ly10 cells. There detectable levels at 8, 24 and 48 hours post cell seeding are shown in Figure (Figure 5:3).

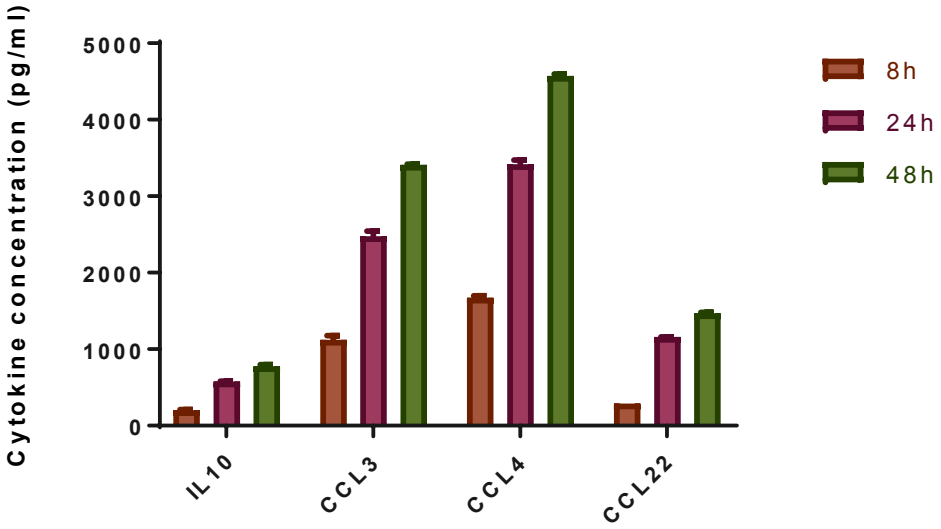

Figure 5:3. Concentration (pg/mL) of IL-10, CCL3, CCL4 or CCL22 released into the supernatants of untreated Ly10 cells cultured for 8, 24 or 48 hours. N=1 Mean ± SEM.

Next, it was investigated which cytokines became repressed upon treatment with DMX3433. A time point of 24 hours post drug treatment was chosen as at this time point, most cells are likely to still be viable and therefore producing cytokine. Of the four cytokines identified in Figure 5:3 as being secreted by Ly10 cells, three, IL-10. CLL3 and CCL4 underwent dose dependent reduction upon DMX3433 treatment. This is summarised in Figure 5:4.

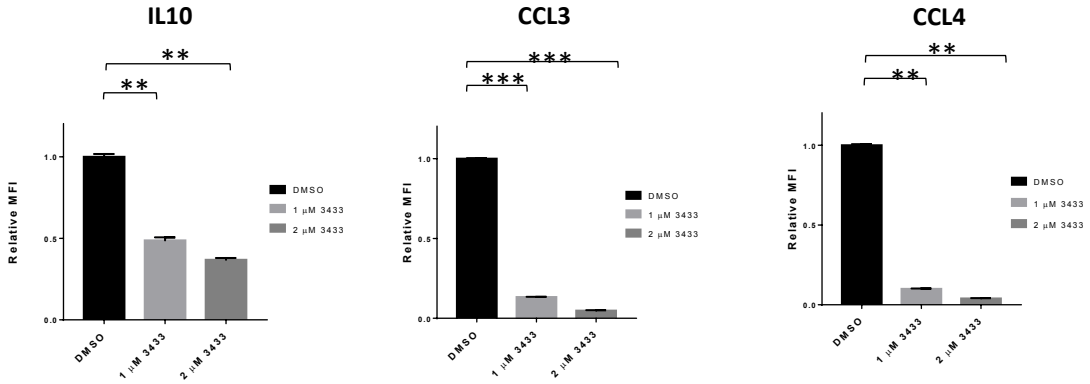

Figure 5:4. Mean fluorescence intensity (MFI) of CCL3 and CCL4 and IL-10 determined by multiplex ELISA in response to DMX3433 at concentrations of 1 μM and 2 μM relative to vehicle control (DMSO) treated cells. Drug treatment causes significant repression (paired t-test) of IL-10 ($P = 0.0013$ at 1 μM and $P = 0.0018$ at 2 μM), CCL3 ($P = 0.0001$ at 1 μM and $P < 0.0001$ at 2 μM) and CCL4 ($P = 0.0013$ at 1 μM and $P = 0.0017$ at 2 μM). Mean±SEM. N=2.

Levels of IL10, CCL3 and CCL4 undergo a dose-dependent reduction in secreted levels upon treatment with either 1 μM or 2 μM DMX3433 for 24 hours (Figure 5:4). Treatment of Ly10 cells with DMX3433 (2 μM) reduced IL10 secretion to ~ 60% of the levels seen in cells treated with DMSO alone. The reduction in CCL3 and CCL4 secretion is much more pronounced with a ~90% reduction in the secretion of both cytokines upon DMX3433 (2μM) treatment.

As levels of IL10, CCL3 and CCL4 were shown to be reduced upon DMX3433 treatment, it was next determined whether this could contribute to the mechanism by which DMX3433 reduces STAT3 phosphorylation in Ly10 cells. To accomplish this, Ly10 cells were treated with DMX3433 (2 μM) for 8hours, conditions that were previously found to abolish STAT3 phosphorylation (Figure 5:1). Subsequently, exogenous IL10, CCL3 or CCL4 was added to the media of Ly10 cells pre-treated with DMX3433, and cells harvested and lysed after 30 minutes exposure to cytokine.

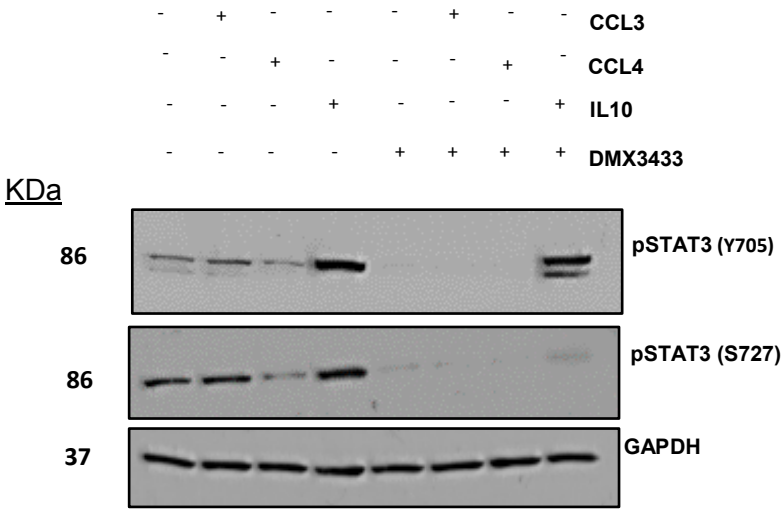

Figure 5:5. Western blots showing effects of added growth factors (CCL3 100 ng/mL, CCL4 100 ng/mL and IL-10 50 ng/mL) on STAT3 phosphorylation in the presence and absence of DMX3433 in Ly10. Antibodies directed against phosphorylated STAT3 (Y705 and S727) were employed. GAPDH was used as a loading control. Molecular weight (kDa) is indicated to the left.

As expected, the treatment of Ly10 cells with 2μM DMX3433 (2μM) for 8 hours abolished STAT3 phosphorylation on both the Y705 and S727 residues (Figure 5:5). The addition of CCL3 into the media of untreated Ly10 cells had no effect on the phosphorylation levels on either Y705 or S727, and addition of CCL3 could not rescue the loss of phosphorylation caused by DMX3433. The addition of CCL4 appears to diminish phosphorylation levels on both Y705 and S727 in untreated Ly10's and did not rescue DMX3433 mediated loss of phosphorylation on either residue. Conversely, the addition of IL-10 enhanced Y705 phosphorylation of STAT3 in untreated cells, but did not enhance levels of S727 phosphorylation. IL-10 addition was sufficient to rescue DMX3433 mediated loss of Y705 phosphorylation, but not S727 phosphorylation of STAT3 (Figure 5:5).

This experiment suggests that in the absence of DMX3433 exogenous IL-10 increases STAT3 phosphorylation especially at tyrosine 705 but also at serine 727 and that in the presence of DMX3433 the addition of IL-10 is sufficient to rescue STAT3 phosphorylation but only at tyrosine 705. Exogenous CCL3 and CCL4 did not alter STAT3 phosphorylation.

Therefore, a further hypothesis derived from this experiment is that DMX3433 interrupts phosphorylated P65 signalling, which in turn suppresses *IL10* transcription and consequently reduced IL-10 secretion to reduce phosphorylation of STAT3 phosphorylation on tyrosine 705.

Therefore, to further support the notion that DMX3433 supresses Y705 STAT3 phosphorylation through IL10 suppression, *IL10* mRNA levels were assessed at 8 hours after DMX3433 treatment – a time point where Y705 phosphorylation of STAT3 is reduced post DMX3433 treatment.

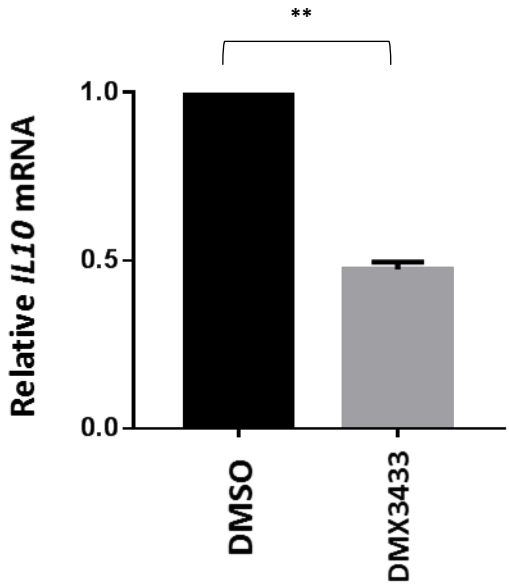

Figure 5:6. Levels of *IL10* mRNA in Ly10 in response to DMX3433 (2 μM). There is a significant reduction (paired t-test, P = 0.0017). Mean±SEM (N=3).

The transcript levels of *IL10* were significantly reduced (paired t-test, P = 0.0017) in Ly10 cells after 8 hours treatment with DMX3433 (2 μM) (Figure 5:6). Together with the effects on P65 phosphorylation this suggests that DMX3433 supresses the transcription of *IL10* which is likely required for the reduction seen in secreted IL-10.

5.2.4 siRNA mediated knockdown of IKKε/TBK1

Small molecule inhibitors can have off-target effects and, therefore, to validate the proposed roles of IKKε/TBK1 in P65/STAT3/IL-10 signalling, each kinase was knocked down in Ly10 cells.

Initially, the protein levels of whole and phosphorylated P65 and STAT3 were assessed by western blot at 48 hours after transfection (Figure 5:7).

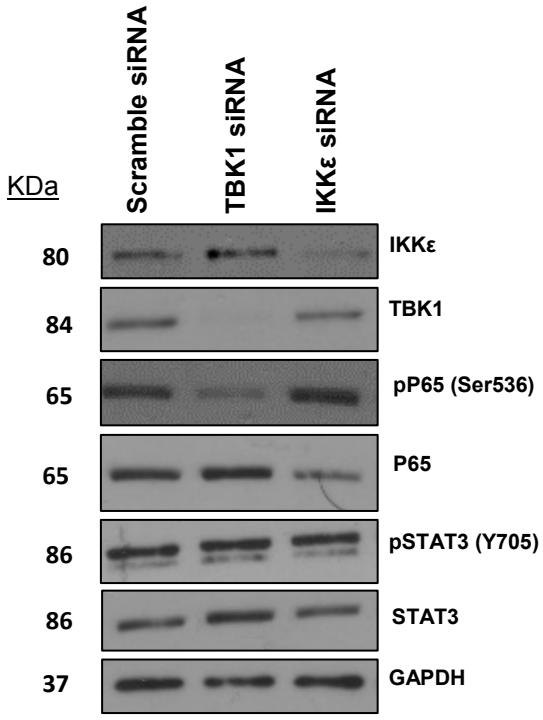

Figure 5:7. SiRNA knockdown of IKKε and TBK1. Western blots showing levels of IKKε and TBK1 in response to transfection of Ly10 with scrambled control siRNA and siRNAs directed against IKKε and TBK1. Corresponding levels of phosphorylated (S536) and total P65 and phosphorylated (Y705) and total STAT3 are shown. GAPDH was used as a loading control. Molecular weight (kDa) is indicated to the left.

Knockdown of IKKε and TBK1 was detectable at the protein level 48 hours post-transfection with siRNAs specific for each kinase. Negative control siRNA had no observable effect on the expression of either kinase. At the 48 hour time point, TBK1 knockdown was sufficient to reduce S536 phosphorylation of P65, while levels of whole P65 remain unchanged. IKKε knockdown had no observable effect on P65 phosphorylation, but levels of total P65 appear reduced at this time point. There was no observable difference in total or Y705 phosphorylated STAT3 upon knockdown of either kinase at this time point.

It was next assessed whether knockdown of IKKε/TBK1 had any effects on the secretion of the cytokines identified as being downregulated upon DMX3433 treatment. To achieve this, supernatants of Ly10 cells were taken 48 hours after transfection with IKKε/TBK1 siRNAs and interrogated by multiplex ELISA assay for the presence of IL-10, CCL3 and CCL4.

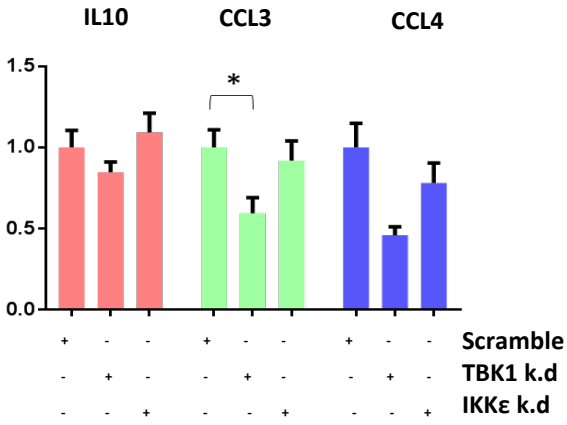

Figure 5:8. Multiplex ELISA for IL-10, CCL3 and CCL4 in Ly10 cells following siRNA knockdown of IKKε and TBK1. Knockdown of TBK1 causes a significant (paired t-test) reduction in CCL3 levels (P = 0.02). Mean±SEM. N=2.

The secreted levels of IL-10 were not significantly reduced in TBK1 knockdown cells, although a modest reduction was observed with secreted IL-10 levels reduced to ~80% of baseline levels. TBK1 knockdown also resulted in a significant reduction of CCL3 ($P = 0.02$) and an observable but non-significant reduction in CCL4. Knockdown of IKKε did not cause a change in IL-10 secretion but did cause slight reductions in CCL3 and CCL4 secretion, although this did not reach statistical significance. These data suggest that TBK1, and not IKKε, is the principle enzyme governing CCL3, CCL4 and IL-10 secretion in these cells.

5.3 Discussion

In this chapter the mechanism of action of DMX3433 has been explored by utilising an ABC like DLBCL cell line, Ly10.

5.3.1 DMX3433 inhibits IL-10/STAT3 signalling in Ly10 cells

Building on the previous discovery (Chapter 4) that cell lines that are sensitive to DMX3433 treatment are also express high levels of phosphorylated STAT3, work in this chapter demonstrated that DMX3433 treatment impairs STAT3 phosphorylation in Ly10 cells. Phosphorylation of the S727 residue on STAT3 is reduced within 0.5 hours of DMX3433 (2 μM) treatment and remains reduced throughout the treatment course investigated (0.5 to 8 hours). The introduction of IL-10 into the media of DMX3433 treated cells was not sufficient to rescue the loss of S727 phosphorylation of STAT3 suggesting that this phosphorylation is independent of IL10. As IKKε and TBK1 are serine/threonine kinases, this raises the possibility that STAT3 S727 is a novel target of these kinases. Serine phosphorylation on STAT3 is not thought to affect it's DNA binding capacity, but rather it's transcriptional capacity (Decker and Kovarik, 2000).

The treatment of Ly10 cells also reduced levels of phosphorylation at tyrosine 705 of STAT3 in a bi-phasic manner with an initial reduction seen at 2 hours after treatment, a restoration of phosphorylation at 4 hours post treatment, and then a further reduction at the 8 hour time point. As both IKKε and TBK1 are serine/threonine kinases, the observed reduction in tyrosine phosphorylation cannot be a direct effect, and therefore alternative mechanisms were explored. Others have suggested that autocrine or paracrine signalling by cytokines or other growth factors can be altered by mutation and drug action in DLBCL (Yang et al., 2012). To investigate the effects of DMX3433 on levels of B-cell specific secreted molecules multiplex ELISA was carried out. Secretion of IL-10 was reduced to ~ 40% of the levels seen in DMSO treated cells after 24 hours treatment with DMX3433 (2 μM). At the 8 hour time point, *IL10* mRNA was significantly reduced consistent with the notion that DMX3433 repressed IL10 transcription through reducing activation of P65. A prediction of this model is that the addition of IL-10 to the medium will activate JAK2 and STAT3 signalling. This was indeed the case and addition of IL-10 to DMX3433 treated cells proved sufficient to restore STAT3 tyrosine 705 phosphorylation. These data suggest that the mechanism for DMX3433-induced STAT3 tyrosine 705 de-phosphorylation is through inhibition of IL-10 secretion.

Béguelin et al., 2015 demonstrated that interruption of IL-10 signalling leading to subsequent repression of STAT3 phosphorylation leads to cell death in ABC DLBCL. Therefore, DMX3433 mediated suppression of IL-10 secretion and consequently STAT3phosphorylation contributed to the loss of cell viability seen with Ly10 cells.

While disruption of IL-10 secretion may explain the reduction in STAT3 phosphorylation at 8 hours post treatment, it is unlikely to explain the reduction in tyrosine 705 STAT3 phosphorylation seen at earlier time points. One potential explanation of this phenomenon is an off-target effect. For example, DMX3433 might inhibit members of the JAK family. However this is unlikely as the *in vitro* EC50's of the JAK1, JAK2 and JAK3 are relatively high compared to the selectivity towards IKKε and TBK1.

The levels of STAT3 tyrosine 705 phosphorylation did not alter upon knockdown of either TBK1 or IKKε at the 48 hour time point. This is somewhat surprising as DMX3433 treatment reduced STAT3 tyrosine 705 in a reproducible manner. There are several potential explanations for this. Firstly, although IL-10 secretion was slightly reduced by TBK1

knockdown, this reduction was only by ~ 20%. This means there will still be ~80% of baseline levels of IL-10 in the media of these cells which may be sufficient to maintain Y705 STAT3 signalling. The reason behind the failure of TBK1 knockdown failing to reach the levels of IL-10 reduction seen in DMX3433 treated cells could well be transfection efficiency whereby a proportion of cells remain un-transfected with siRNA and secrete normal levels of IL-10. It also remains a possibility that DMX3433 is targeting molecules in these cells other than IKKε/TBK1, and that these molecules are unaffected by the transfection of IKKε/TBK1 specific siRNAs.

5.3.2 DMX3433 inhibits P65 phosphorylation in Ly10 cells

By both western blot and ELISA, it can be seen that treatment of Ly10 cells with DMX3433 reduces serine 536 phosphorylation of P65. This suggests that this residue of P65 is a target for phosphorylation by IKKε/TBK1 in these cells, which is supported by previous work that has shown that both IKKε and TBK1 can phosphorylate the serine 536 residue of P65 in HeLa cells (Adli and Baldwin, 2006) and in the setting of breast cancer (Deng et al., 2014).

Levels of P65 serine 536 phosphorylation were markedly reduced upon TBK1 knockdown, whereas IKKε knockdown had little effect at 48 hours after transfection. This suggests that TBK1 is the principal enzyme involved in P65 phosphorylation in this DLBCL cell line.

Furthermore, Lam et al., (2008) demonstrated that NF-κB activity drives *IL10* transcription and IL-10 secretion specifically in Ly10 cells. This raises the possibility that DMX3433 represses IL-10 secretion by directly inhibiting TBK1 mediated phosphorylation of P65 and subsequent transcription of *IL10* in Ly10 cells.

5.3.3 DMX3433 supresses the secretion of CCL3 and CCL4

It was also found that treatment with DMX3433 (2 μM) almost completely abolished secretion of CCL3 and CCL4. Contrary to IL-10, the addition of CCL3 or CCL4 into the media of either untreated or DMX3433 treated Ly10 cells failed to enhance phosphorylation of STAT3 on either the serine 727 or tyrosine 705 residues. This suggests that CCL3 or CCL4 secretion is not required for functional STAT3 signalling in these cells.

The mechanism for repression of CCL3 and CCL4 levels by DMX3433 could well be a direct effect of IKKε/TBK1 inhibition. In a prostate cancer model, the transcription factor C/EBPβ has been shown to be directly phosphorylated by IKKε, which then induces C/EBPβ nuclear translocation (Péant et al., 2017). Binding motifs for C/EBPβ are found in the promotor regions of both *CCL3* and *CCL4*, and in human chondrocytes, transcription of *CCL3* and *CCL4* is dependent on C/EBPβ (Zhang et al., 2010). Suppression of IKKε by DMX3433 could, therefore, lead to C/EBPβ suppression and the subsequent down regulation of CCL3 and CCL4 in Ly10 cells. Additionally, Zhang et al., 2010 found *CCL3* and *CCL4* expression to not only be dependent on C/EBPβ, but also on NF-κB. This raises the possibility that the suppression of P65 phosphorylation by DMX3433 could contribute directly to CCL3 and CCL4 reduction. Indeed, the secretion of CCL3 and CCL4 was more obviously reduced by TBK1 knockdown but not by IKKε, suggesting that TBK1 is the principal enzyme involved in the regulation of CCL3 and CCL4 production as it also appeared to be the principal enzyme responsible for P65 activation. As TBK1 knockdown was sufficient to reduce P65 phosphorylation, and NF-κB activity is known to be necessary for the production of CCL3 and CCL4, the TBK1 mediated regulation of P65 phosphorylation could well be the mechanism behind CCL3 and CCL4 secretion in these cells.

Both of these secreted chemokines are thought to be involved in the recruitment of other immune cells to B-cells, and in the CLL setting have been shown to foster beneficial interactions between malignant B-cells and monocytes/macrophages (Zucchetto et al., 2009). As Ly10 cells were grown as a monoclonal population where there is no interaction with other immune cells, the suppression of CCL3 or CCL4 is unlikely to be contributing to the

loss of cell viability seen with DMX3433 by this mechanism of action. Speculatively, suppression of CCL3 and CCL4 secretion by DMX3433 could show enhanced reductions in tumour cell viability *in vivo*, where tumour-immune cell interactions are likely to occur.

Both CCL3 and CCL4 have been shown to be indicative of poor prognosis in DLBCL (Takahashi et al., 2015). It may well be that CCL3 and CCL4 could serve as bio markers not only for prognosis, but for sensitivity to DMX3433 treatment.

A summary diagram outlining the proposed pharmacodynamics of DMX3433 in Ly10 cells is presented in figure 5:9.

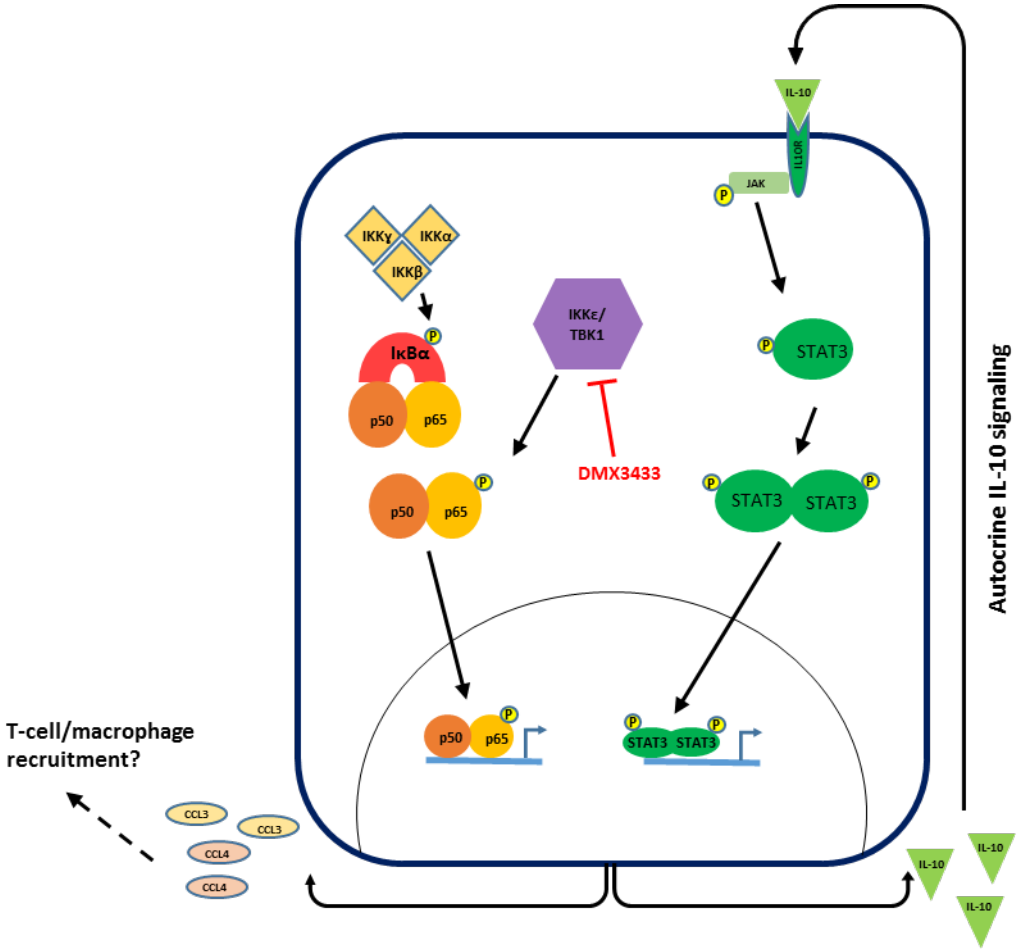

Figure 5:9. Summary wiring diagram of the proposed mechanism of action of DMX3433 (in red) in Ly10 cells. Flat ended red arrows represent inhibition.

5.3.4 The need for the use of primary DLBCL cells

The use of cell lines is a valuable tool and has provided many insights into the biology of DLBCL. However, use of cell lines is not without its drawbacks. Due to the need to immortalize cells to allow for indefinite propagation in culture, cancer cell lines often have a mutational burden distinct from that seen in the primary counterpart of the disease. To overcome this potential issue in the context of this thesis, the effects of DMX3433 treatment on primary human DLBCL cells was examined in the form of patient derived xenograft (PDX) models. This work forms the basis of Chapter 6.

Chapter 6 – Assessing drug inhibition of IKKε/TBK1 in primary human DLBCL

6.1 Introduction

Immortalized cell lines derived from patients with DLBCL have been the workhorse of DLBCL research for many years. While many discoveries regarding the fundamental principles of the disease have been made through utilizing these cell lines, they have key caveats.

For example, cells taken from a human and cultured in supplemented media cannot propagate indefinitely, even with stimulation. To generate a cell line capable of indefinite propagation, cells must be immortalized through the acquirement of mutations which will undoubtedly alter the biology of the cells relative to their non-immortalized counterparts. This can lead to cell lines becoming dependent on mechanisms that when disrupted are lethal to immortalized cells, but may not be required for the survival of non-immortalized cells – such as *TP53* in the case of DLBCL (Chapuy et al., 2016).

In an effort to circumvent these issues, a mouse based patient derived xenograft (PDX) technique has been developed. In short, primary human tumour tissue is implanted into an immunocompromised recipient mouse, and allowed to engraft. Once established, these tumours can then be passaged over future generations of mice. Mice bearing patient derived tumours can then be subjected to in vitro experiments or tumour tissue may be resected and *in vitro* experiments performed on the isolated tumour cells (Hidalgo et al., 2014). An overview of the generation of PDX models is presented in Figure 6:1.

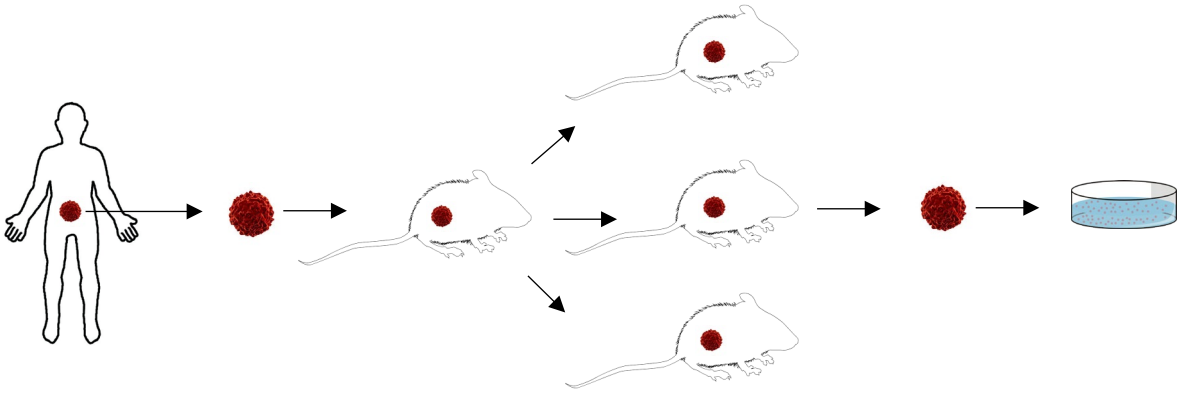

Figure 6:1 – A visual description of the generation of PDX mouse models

In this chapter, PDX technology has been utilised to assess the effects of DMX3433 treatment on primary human DLBCL.

6.2 Results

6.2.1 Selection of PDX models

PDX models were provided by CrownBiosciences and four DLBCL PDX models were selected for treatment with DMX3433.

The models were chosen in order to capture a range of DLBCL entities. PDX model LY0257 and PDX model LY2345 were derived from patients diagnosed with the non-GC subtype of DLBCL, whereas PDX models LY2214 and LY2318 were from patients with GC like DLBCL diagnoses. Genotypic data was available for each model, and a summary of the known mutations of each PDX model is displayed in Table 6:1.

PDX model	GC/Non-GC status	Known genetic lesions
LY0257	Non-GC	*MYD88* (L273P), *KMT2D* (L2808fs), *PIM1* (L2V, K249, K29N, S75F, L80M, L106I, E141Q, G45D), *PRDM1* (S429N), *SOCS1* (C111Y), *TNFRSF14* (K17R), *BCL6* translocation.
LY2214	GC	*CREBBP* (R1730C), *KMT2D* (P2382S, M3349V), *PIM1* (T23I), *SOCS1* (M1V, A17P, P25S), *TP53* (P72R), *MYC* translocation.
LY2345	Non-GC	*CARD11* (A687V), *EZH2* (D185H), *TNFAIP3* (F127C, I194T), *PRDM1* (G74S), *TNFRS14* (K17R), *TP53* (P72R).
LY2318	GC	*TNFRSF14* (K17R), *TP53* (P72R).

Table 6:1 – Characteristics of the four selected PDX models. Diagnostic and mutational data was acquired from the HuBase database (CrownBio).

6.2.2 PDX *in vitro* treatment

At CrownBio, tumour cells from PDX models were isolated and cultured *in vitro*. Cells were then treated with a range of DMX3433 concentrations or vehicle (DMSO) control for 24 hours, and their viability assessed by CTG assay. Luminescence values were recorded and sent to Leicester for dose-curve analysis. The dose-curves for the four treated PDX models and their corresponding EC50 values are displayed (Figure 6:2).

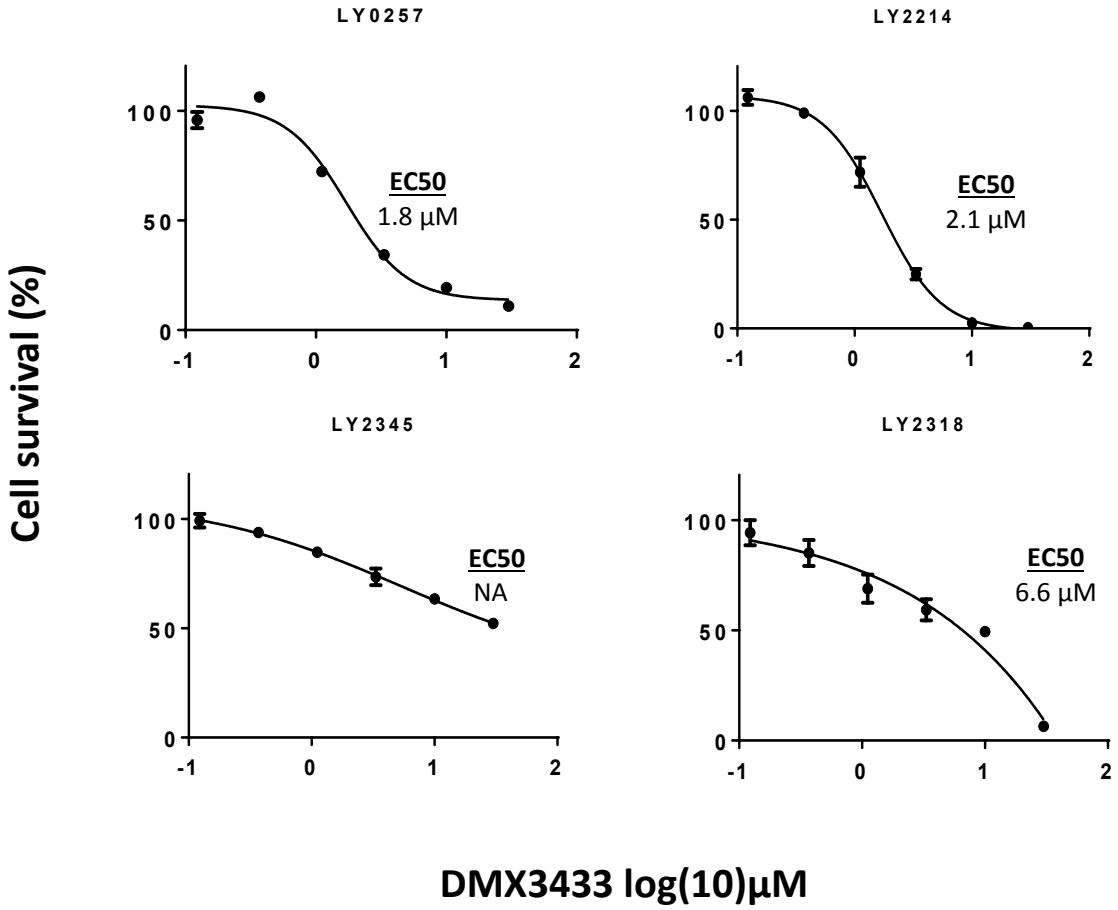

Figure 6:2 – Sigmoidal dose response curves of the four PDX models treated with a range of dosages of DMX3433. Mean values are plotted. Error bars are SEM (N=3). Absolute EC50 values are shown for each PDX model.

As for DLBCL cell lines, there are both sensitive and insensitive PDX models (Figure 6:2). LY0257 and LY2214 displayed EC50's in the range of 2µM, whereas LY2318 had an EC50 of 6.6µM. LY2345 did not reach a 50% reduction in viability even at the top dosage of DMX3433 after 24 hours treatment.

As the PDX models mirrored the differential sensitivity to DMX3433 that was seen in the cell lines, it was next determined whether sensitive PDX models shared characteristics with sensitive cell lines.

6.2.3 Markers of DMX3433 sensitivity in DLBCL PDX models

Cell pellets from untreated PDX models were shipped to Leicester on dry ice. Once here, cell lysates were generated and western blots performed. Western blot of lysates from the four treated PDX models, showed expression of IKKε, TBK1, STAT3, pSTAT3 (Y705) (Figure 6:3).

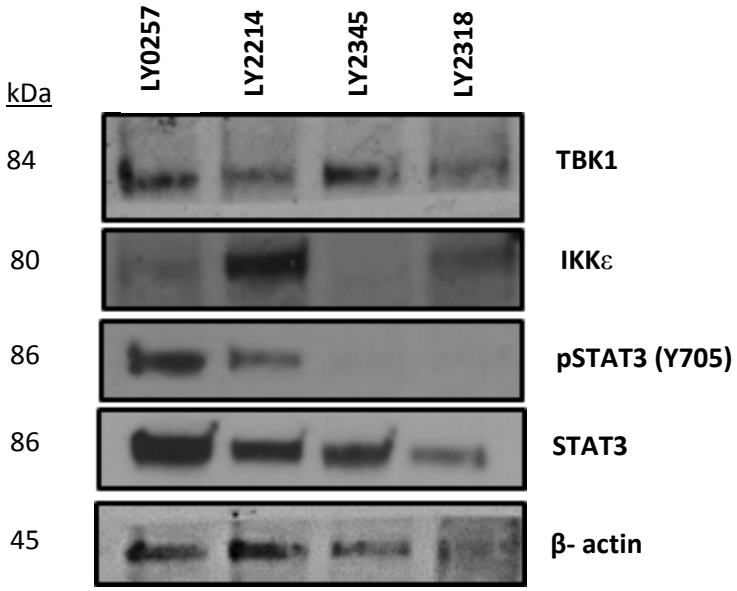

Figure 6:3 –Western blots of TBK1, IKKε, pSTAT3 (Y705) and STAT3 protein expression in the four PDX models. B-actin was used as a loading control. Molecular weight (kDa) is indicated to the left

Similar to the DLBCL cell lines, non-GC PDX models (0257 and 2345) had a higher protein expression of TBK1 relative to the GC models. IKKε expression appears to show no association with GC/non-GC status, but, like the cell lines, its expression was variable in PDX models with two (LY2214 and LY2318) having relatively higher protein expression.

While levels of STAT3 were detectable in all four models, phosphorylated STAT3 was only detectable in the two PDX models that were sensitive to DMX3433 treatment (LY0257 and LY2214). This result suggests that STAT3 signalling is marker for sensitivity in these PDX models. To explore this hypothesis further, RNAseq data from the CrownBio HuBase database of PDX model information was interrogated. While STAT3 expression itself was independent of DMX3433 sensitivity, the expression of *IL10* mRNA was much higher in the sensitive models in comparison to the more resistant models (Figure 6:4):

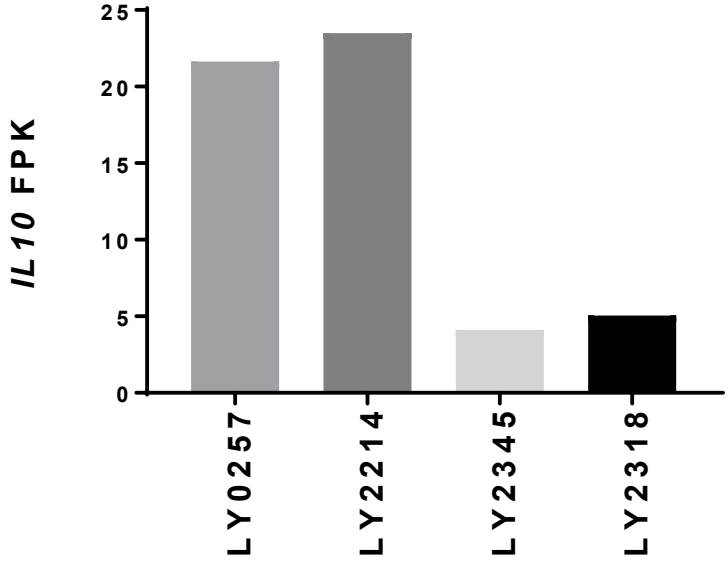

Figure 6:4 – RNA-seq transcript expression (FPKM) of *IL10* across the four PDX models.

6.2.4 Protein changes upon DMX3433 treatment

Lysates from LY0257 and LY2214, the two models most sensitive to DMX3433 treatment, were used to analyse effects on STAT3 and P65 protein after 24 hours of treatment. These downstream effects are shown (Figure 6:5).

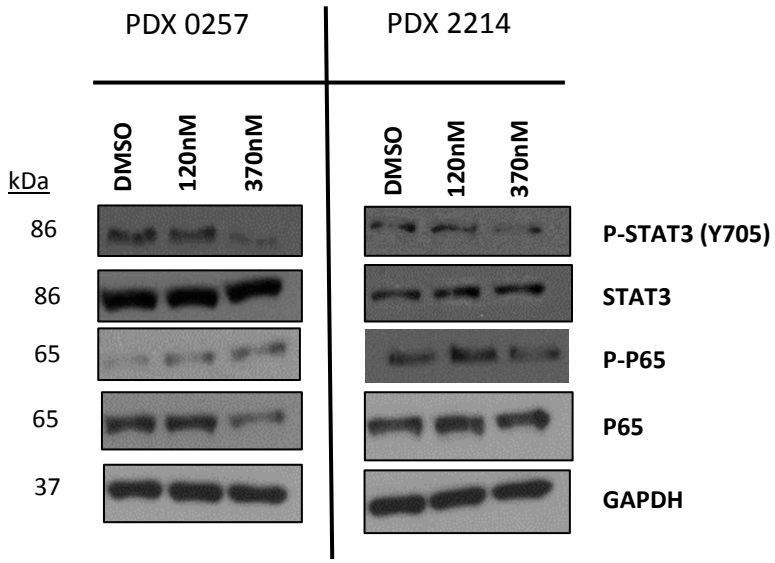

Figure 6:5 –Western blots of pSTAT3 (Y705), STAT3, pP65 (S536), and P65 protein expression in PDX0257 and PDX2214 upon treatment with DMSO, 120nM DMX3433 or 370nM DMX3433. GAPDH was used as a loading control. Molecular weight (kDa) is indicated to the left

The levels of pSTAT3 (Y705) were decreased relative to DMSO treated cells in PDX0257 and PDX2214 after treatment with DMX3433 (370 nM) for 24 hours, while levels of total STAT3 remained unchanged. PDX2214 also exhibited a reduction in pP65 levels at this concentration, whereas PDX0257 showed little change although there seemed to be a reduction in whole p65 levels (Figure 6:5).

6.2.5 Analysis effects of IKKε/TBK1 drug inhibition in primary human DLBCL at the transcriptional level

In order to gain further insight into the cellular consequences of drug mediated IKKε/TBK1 inhibition in DLBCL, the transcriptional alterations following drug treatment were analysed. In order to do this, a DNA microarray analysis was performed on PDX models comparing gene expression of models before and after treatment with DMX3433 for 24 hours. Pellets of untreated and treated cells were sent on dry ice to Leicester, and once here, pellets were lysed and RNA was isolated and sent to the core genomics facility for cDNA synthesis and hybridisation onto DNA microarray slides. Once the array was performed, unprocessed raw data was returned and analysed.

A total of 7 samples (4 biological control replicates and 3 treatment replicates) could be analysed which were as follows:

LY0257 – treated with vehicle control for 24h

LY0257 – treated with ~ 1μM DMX3433 for 24h

LY2214 – treated with vehicle control for 24h

LY2214 – treated with ~ 1μM DMX3433 for 24h

LY2318 – treated with vehicle control for 24h

LY2318 – treated with ~ 1μM DMX3433 for 24h

LY2345 – treated with vehicle control for 24h

Raw data were uploaded into Partek Genomics Suite and subjected to quantile normalization. Following this, normalized expression values for each sample could be uploaded into Mev for subsequent statistical analysis.

6.2.5.1 Gene set enrichment analysis of PDX microarray data

Gene set enrichment analysis (GSEA) takes an unbiased approach to determining if an expression data set is enriched for any previously established gene sets. In this case gene expression data from *untreated* PDX models were assigned as one group (group A) and data from the *treated* PDX models was assigned as a second group (group B). GSEA software was then used to determine if either group was enriched for genes associated with distinct biological pathways.

'Hallmark' gene sets in the Molecular Signatures database (MSigDB) were interrogated with the treated PDX data set. 'Hallmark' gene sets are a collection of 50 gene sets that represent genes associated with specific biological functions.

For this analysis, a nominal P-value cut off of <0.05 was used, alongside a normalized enrichment score threshold of <-1 to >1. For the purpose of this exploratory analysis, a relaxed false discovery rate (FDR) of <0.25 was used. Using these parameters, an untreated (group A) versus treated (group B) analysis was interrogated for enrichment in hallmark gene sets. The summary of this is shown (Table 6:2).

Hallmark gene set name	Normalized enrichment score	Nominal p-value	FDR q-value	Enriched in group
Allograft rejection	1.77	<0.001	0.002	A
Hypoxia	1.52	<0.001	0.141	A
Apical junction	1.50	0.006	0.116	A
UV response downregulated	1.46	0.004	0.136	A
Androgen response	1.39	0.043	0.179	A
Estrogen response	1.36	0.018	0.202	A
Inflammatory response	1.34	0.035	0.220	A
IL2/STAT5 signalling	1.31	0.021	0.215	A

TNFα signalling via NF-kB	1.308	0.021	0.199	A
Oxidative phosphorylation	1.29	0.044	0.200	A
Epithelial-mesenchymal transition	1.28	0.036	0.196	A
UV response upregulated	1.27	0.048	0.193	A
IFNA response	-1.76	<0.001	0.005	B

Table 6:2 – Hallmark gene sets which show significant enrichment (NES <-1>1, nominal P-value <0.05, FDR <0.25) with either untreated (group A) or treated (group B) PDX model gene signatures.

12 hallmark pathway gene sets showed enrichment for untreated PDX model gene expression (group A), while 1 pathway gene set showed enrichment for the PDX treated with DMX3433 gene signature (Group B) (Table 6:2). While several of these pathways have no known association with IKKε/TBK1 or the pathogenesis of DLBCL, four pathways (highlighted in green) do. These pathways were subsequently subjected to leading edge analysis – a method of determining which genes contribute the most to the observed enrichment of one gene set to another – the leading-edge subset. Enrichment plots for each of the pathways highlighted (Table 6:2) are shown (Figure 6:6). Heat maps of the leading-edge subset of genes and their respective expression levels in each sample are displayed beneath each enrichment plot. This analysis supports the hypothesis that the small molecule IKKε/TBK1 inhibitor perturbs NF-κB and interferon gene expression in primary human DLBCL.

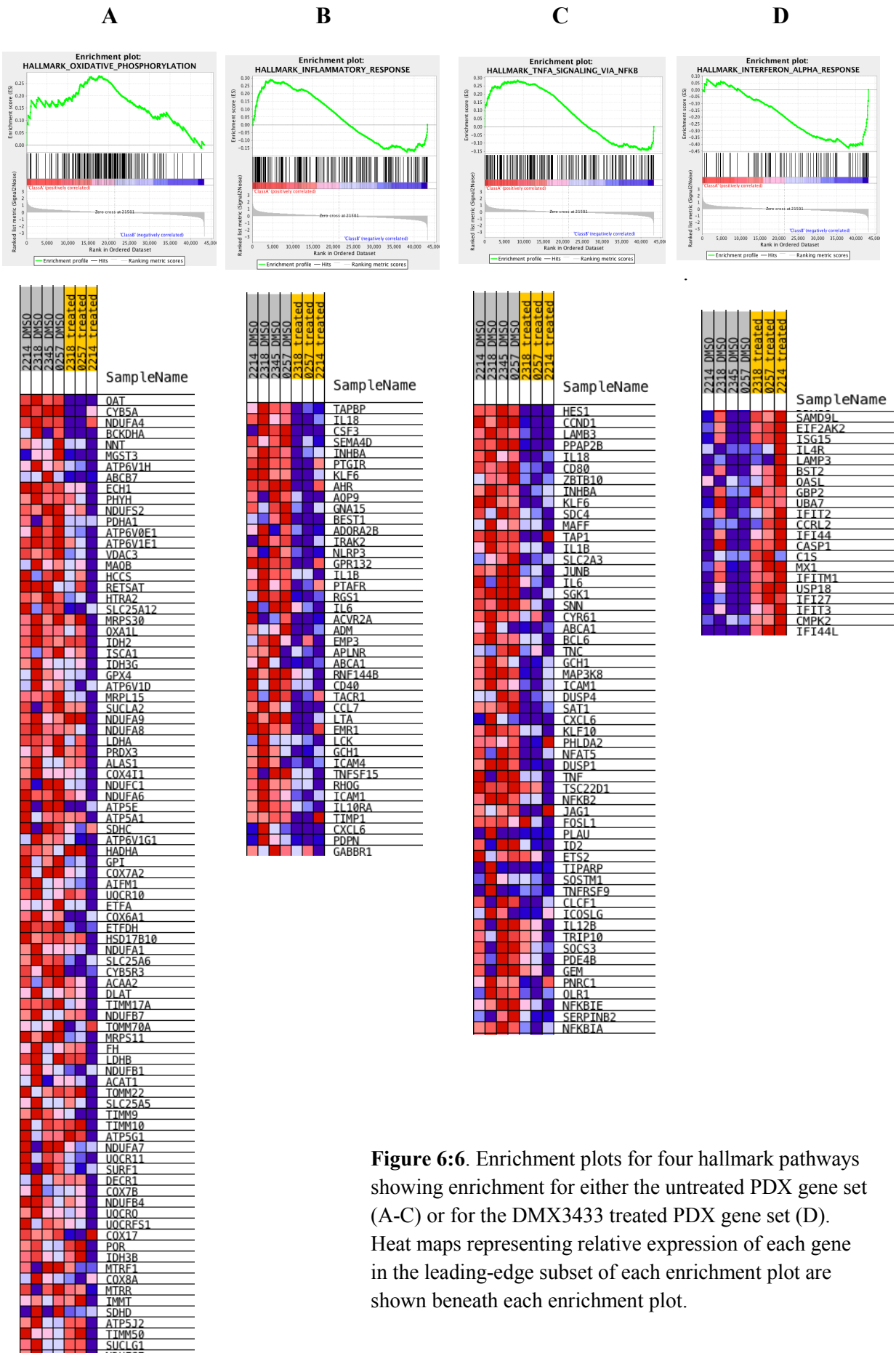

Figure 6:6. Enrichment plots for four hallmark pathways showing enrichment for either the untreated PDX gene set (A-C) or for the DMX3433 treated PDX gene set (D). Heat maps representing relative expression of each gene in the leading-edge subset of each enrichment plot are shown beneath each enrichment plot.

6.2.5.2 Discovery of differentially expressed genes between untreated and treated PDX models

To extend the hypothesis and discover the individual altered genes normalized expression data was subjected to significance analysis of microarrays (SAM) analysis in MeV. SAM analysis allows for the manual threshold of false discovery rate (FDR), and for this analysis, a delta value of 1.2 was used, producing a false discovery rate of 0.0024. While rather stringent, this delta value was used in order to keep the number of significantly differentially expressed genes at a manageable size of ~500. The SAM plot of treated versus untreated PDX models is shown (Figure 6:7).

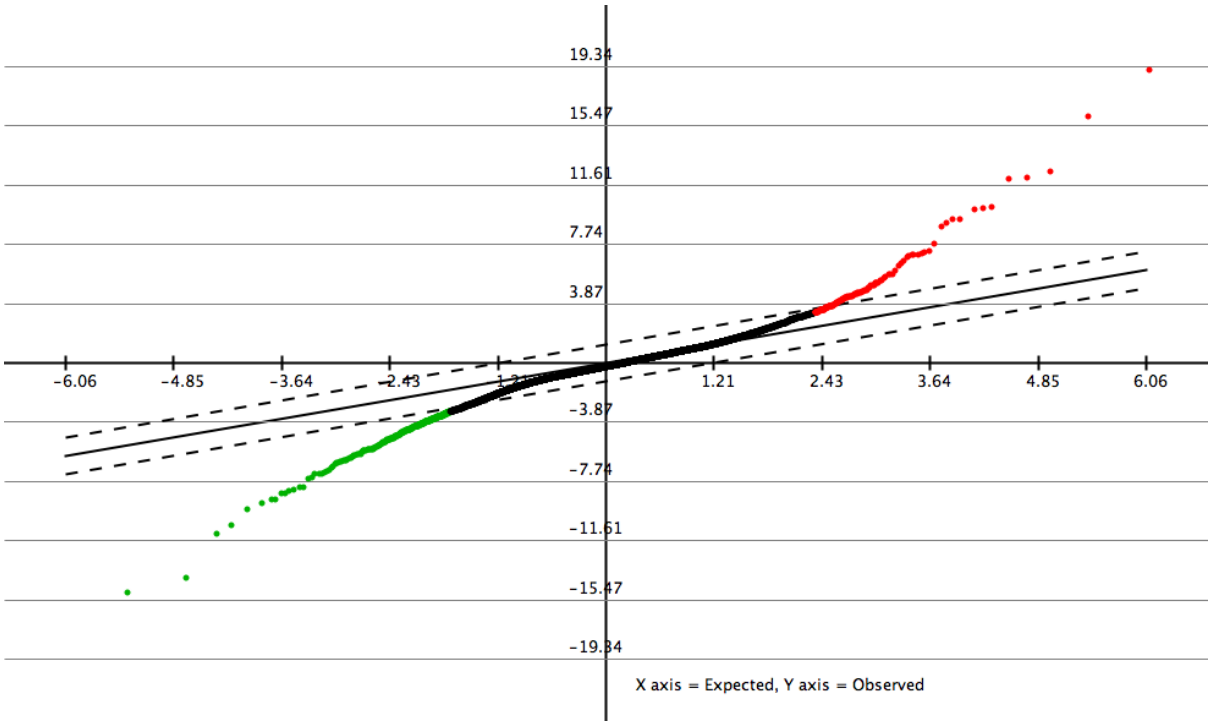

Figure 6:7– The SAM plot of grouped untreated PDX models (N=4) vs grouped treated PDX models (N=3). Each dot represents a single gene. Those in green are those that are downregulated in the treated PDX group, whereas those in red are upregulated. The solid line runs through Y=X, and the dotted lines represent a delta value of 1.2. Genes that fall outside of these dotted lines are judged to be significantly differentially expressed between the two groups.

Figure 6:7 is a visualisation of all genes in the dataset post normalization. Here, gene expression values from the 'treated' group are plotted against values from the 'untreated' group. If there was no difference between the two groups, a straight line with the formula y=x would be visible. This is true for the vast majority of genes with 39406 (99%) showing no significant difference with these parameters. This demonstrates that DMX3433 treatment significantly affects only 1% of the genes in total. With these parameters, 515 genes are judged to be significantly differentially expressed between treated and untreated PDX groups. Of these, the majority (393) are downregulated upon treatment with DMX3433, leaving 122 genes that are significantly upregulated in treated PDX models upon DMX3433 treatment.

This list of differentially expressed genes could then be split into those whose expression reduces upon DMX3433 treatment (downregulated) and those whose expression increases upon DMX3433 treatment (upregulated). These gene lists could then be subjected to hierarchical clustering and are presented in Figures 6:8 and 6:9, respectively.

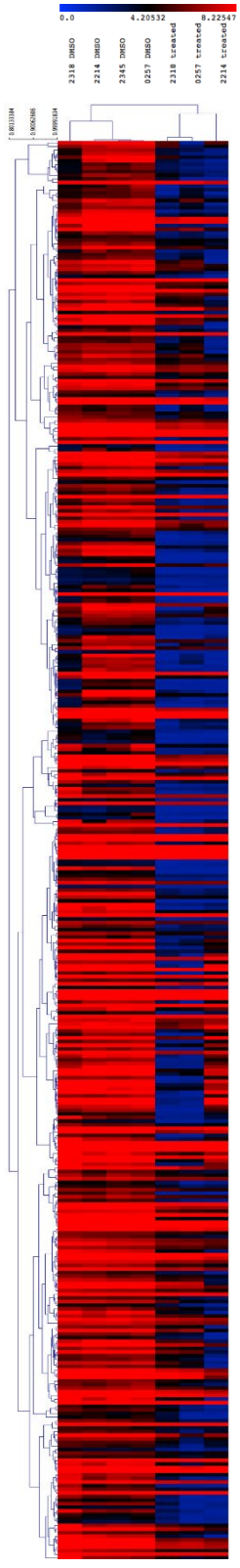

Figure 6:8 – Hierarchical clustering of the 393 significantly downregulated genes in treated PDX models.

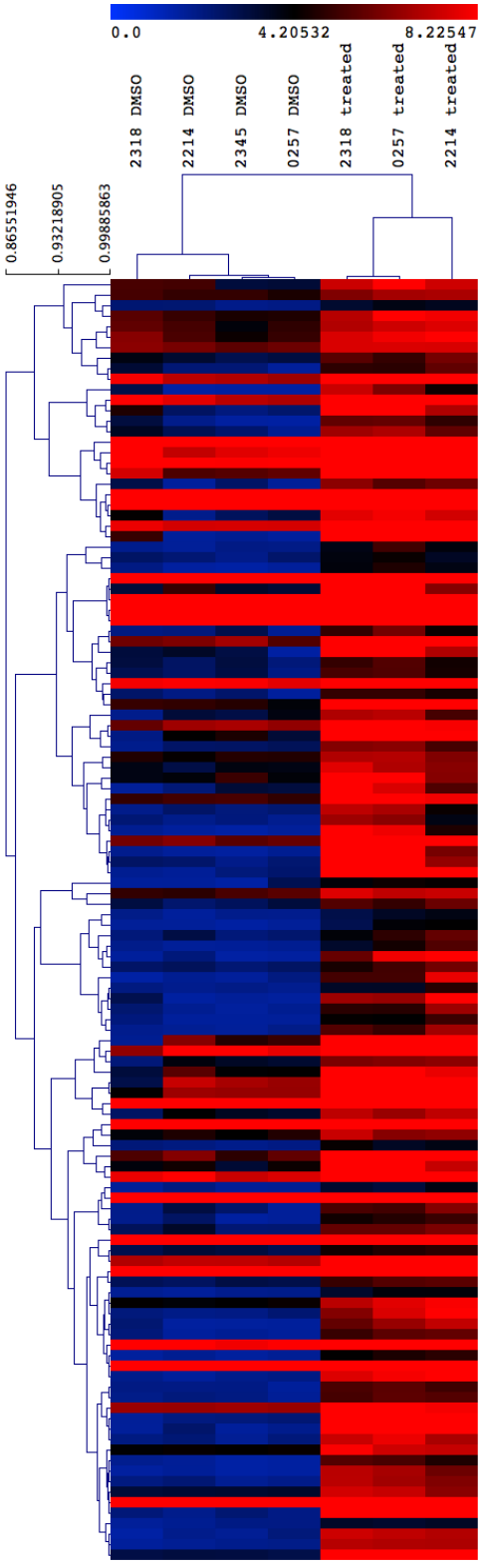

Figure 6:9 – Hierarchical clustering of the 122 significantly upregulated genes in treated PDX models.

Figure 6:8 and 6:9 also demonstrate that when the gene expression values of the differentially expressed genes between untreated and treated PDX groups are subjected to hierarchical clustering, the untreated PDX models cluster together, as do the treated PDX models. This supports the idea that DMX3433 has consistent effects on gene expression across different lymphomas and different individuals.

6.2.5.3 Analysis of differentially expressed genes between untreated and treated PDX models

Now a limited number of genes that are either up or downregulated upon DMX3433 treatment have been identified, it is possible to interrogate these genes to see if they are enriched for biological pathways.

The lists of up and downregulated genes upon DMX3433 treatment were uploaded into the MSigDB, and overlaps with gene sets within the 'hallmark' gene set collection were computed. Taking into account the total number of genes in the genome, this software calculates the likelihood of overlap between the gene list uploaded by the user and the gene lists contained within the MSigDB collection. This provides an output which can inform the user if their gene list is likely enriched for specific biological pathways. In calculating enrichment, a stringent FDR rate of <0.001 was used in order to limit the number of enriched pathways discovered. The output of computed overlaps between the genes downregulated or upregulated by DMX3433 in PDX models and those in the 'hallmark' collection of the MSigDB are shown in Tables 6:3 and 6:4, respectively.

Downregulated gene enrichment:

Gene Set Name	p-value	FDR q-value	Overlapping genes
IL2 STAT5 signaling	1.23E-04	6.14E-03	*IRF8, LTB, CA2, FGL2, NCOA3, PLIN2, SYNGR2, CYFIP1*
Allograft rejection	7.20E-04	9.00E-03	*IRF8, LTB, CD80, TAPBP, CD96, CRTAM, TAP2*
Early estrogen response	7.20E-04	9.00E-03	*CCND1, HES1, WFS1, SEC14L2, ZNF185, CBFA2T3*
TNFα signaling via NF-κB	7.20E-04	9.00E-03	*CD8, CCND1, HES1, SAT1, SGK1, DUSP1, LAMB3*

Table 6:3 – Enrichment with hallmark pathways in the MsigDB for the downregulated genes identified in PDX models treated with DMX3.

Upregulated gene enrichment:

Gene Set Name	p-value	FDR q-value	Overlapping genes
TNFα signaling via NF-κB	2.29E-07	1.14E-05	*TNFAIP6, SPHK1, KYNU, PHLDA1, KLF2, EGR1, IER2*

Table 6:4 – Enrichment with hallmark pathways in the MSigDB for the upregulated genes identified in PDX models treated with DMX3.

Table 6:3 shows that in this analysis, significantly downregulated genes in DMX3433 treated PDX models are enriched for genes implicated in four hallmark pathways including TNFα-mediated NF-κB signalling and IL-2/STAT5 signalling. Interestingly, genes that are significantly upregulated upon DMX3433 are enriched for a subset of NF-κB signalling genes (Table 6:4), which may be similar to the effects of TNFα. Overall the SAM and GSEA analyses support an effect of DMX3433 on NF-κB and other inflammatory pathways in human DLBCL.

6.3 Discussion

This chapter has utilised PDX DLBCL models to investigate the use of DMX3433 in primary DLBCL. The four DLBCL PDX models used in this chapter each represent distinct models of DLBCL with distinct mutational profiles.

6.3.1 DMX3433 treatment of PDX models

When the four PDX models were treated with DMX3433 for 24 hours, two models (0257 and 2214) displayed relative sensitivity with absolute EC50 values of 1.8μM and 2.1μM, respectively. This in contrast to the two relatively resistant PDX models 2345 (failed to reach EC50) and 2318 (EC50 of 6.6μM). There are no obvious genetic mutations that predict sensitivity to DMX3433 in these PDX models, likely due to the fact that 0257 and 2214 are of non-GC and GC classification, respectively, and are therefore driven by distinct mutations.

Protein levels of TBK1 and IKKε varied in these PDX models, as was also seen in the DLBCL cell lines (Chapter 3). Consistent with the expression patterns found in the DLBCL TMA, TBK1 expression appeared highest in 0257 and 2345 – the two non-GC models. This is supportive of the correlation seen between TBK1 expression and non-GC status seen in DLBCL cell lines and also in a small cohort of primary DLBCL tumours (Chapter 3). The expression of TBK1 or IKKε at the protein level did not correlate with sensitivity to DMX3433.

Only the sensitive PDX models displayed pSTAT3 (Y705), despite all models having detectable levels of total STAT3. This is suggestive that these sensitive models are those that harbour active STAT3 signalling. This is a confirmation of the same finding that was made in DLBCL cell lines (Chapter 4), and provides further support to the notion that pSTAT3 (Y705) may be a suitable biomarker for DMX3433 sensitivity. While no data on the cytokine secretion profile of these PDX models was obtained, analysis of the PDX model database reveals that PDX models sensitive to DMX3433 treatment have considerably higher *IL10* mRNA as detected by RNAseq - further support that these models are engaging in active STAT3 signalling.

There was sufficient material to analyse the protein effects on STAT3 and P65 following DMX treatment in the two sensitive PDX models. At 24 hours, both 0257 and 2214 displayed reduced pSTAT3 (Y705) levels upon treatment with 370nM DMX3433. Conversely, levels of pP65 (S536) seem to increase upon DMX3433 treatment at 24h. A possible explanation for this seemingly contradictory finding is that 24h may not be an appropriate time point to asses P65 phosphorylation, as phosphorylation reduction occurred much earlier in Ly10 cells (Chapter 5). Indeed, at 24 hours, levels of whole P65 are reduced, suggesting transcriptional repression of P65 may have occurred by this time point. Unfortunately, PDX material was only available at this time point and therefore earlier time points could not be analysed. Interestingly, 2214, a GC PDX model, shows detectable levels of pP65, suggesting that this model is not devoid of active NF-kB signalling. However, there is little alteration in phospho or whole p65 levels upon DMX3433 treatment. This could be attributable to the 24h time point being too late to detect phospho changes, or simply that P65 is not targeted by IKKε/TBK1 in these cells.

6.3.2 Gene expression analysis of DMX3433 treated PDX models

It was also possible to perform a gene expression microarray on untreated and treated PDX models. This allowed an unbiased approach to be taken to analyse changes seen on the transcriptional level of PDX models treated with DMX3433.

Initially, GSEA was performed on untreated versus treated PDX gene expression data. For the purpose of this analysis, a relaxed FDR of <0.25 was used as a threshold. This is the threshold recommended by the Broad institute for GSEA (Mootha et al., 2003, Subramanian et al., 2005) and because of the small sample size used here, a more stringent FDR would not have produced any significant enrichment. With this FDR and a nominal P-value cut off of <0.05, untreated PDX gene expression showed enrichment with 12 hallmark gene sets, while the treated PDX gene expression set showed enrichment with just one hallmark gene set.

Several of the pathway gene sets (unshaded pathways in Table 6:2) identified as being enriched in untreated PDX models have no known association to IKKε/TBK1 or DLBCL pathophysiology. This raises the possibility that these pathways represent novel functions for IKKε/TBK1 in DLBCL cells. It is however likely that DMX3433 is inhibiting numerous other off target kinases, and the inhibition of these unidentified kinases may well be contributing to downregulation of genes associated with the pathways in question.

The alteration of genes associated with the inflammatory response upon DMX3433 treatment is less surprising, as IKKε/TBK1 have well documented roles in regulating inflammatory responses (Yu et al., 2012). When the leading-edge subset of this enrichment is analysed, it can be noted that many of genes that contribute the most towards enrichment are those that code for cytokines and/or their receptors - *IL-18, IL-1ß, IL-6, CCL7, LTA, IL10RA* and *CXCL6*. This is in keeping with the hypothesis suggested in Chapter 5 that at least part of DMX3433's mechanism of action in DLBCL involves alteration of the cytokine profile in these cells. Both IL-6 and IL-10RA play pivotal roles in STAT3 signalling in DLBCL (Lam et al., 2008, Beguelin et al., 2015), and suppression of these genes may, in part, be contributing to the loss of STAT3 phosphorylation observed upon DMX3433 treatment in sensitive PDX models (Figure 6:5). IL10 is known to activate STAT3 via JAK2, and interestingly, JAK2 can also activate STAT5 (Hexner et al., 2008). This could potentially explain the identification of STAT5 associated genes as being downregulated by DMX3433.

NF-kB associated genes were also found to be enriched in untreated PDX samples demonstrating that these genes become downregulated upon DMX3433 treatment. This is supportive of published roles for both IKKε and TBK1 in positive regulation of the NF-kB

pathway (Shen and Hahn, 2011) and evidence provided in this thesis that IKKε/TBK1 inhibition by DMX3433 results in decreased levels of the phosphorylated NF-kB subunit P65.

A further finding was the downregulation of oxidative phosphorylation related genes upon DMX3433 treatment. Monti et al., (2005) have identified a sub-group of DLBCL with gene expression signatures enriched for oxidative phosphorylation related genes – termed 'OxPhos' DLBCL. It was subsequently shown that tumours belonging to this sub-group exhibited enhanced mitochondrial metabolism, and that fatty acid oxidation and glutathione synthesis is required for the survival of these cells (Caro et al., 2012). IKKε/TBK1 have been shown to be essential for the increase in glycolytic metabolism required for the successful activation of dendritic cells (Everts et al., 2014)This raises the intriguing possibility that targeting IKKε/TBK1 may be a therapeutic option for OxPhos DLBCL. That said, the aforementioned paper (Caro et al., 2012) identified the DLBCL cell lines Pfeiffer and Toledo (amongst others) as OxPhos, and while Pfeiffer cells are sensitive to IKKε/TBK1 inhibition, Toledo cells are not. Furthermore, Caro et al., (2012) identified Ly03 and Ly10 cells as being OxPhos independent DLBCL, while both these cell lines show IKKε/TBK1 inhibition sensitivity (Chapter 4). Overall, therefore, it seems that markers of intermediate metabolism are not a useful guide to sensitivity to IKKε/TBK1 inhibitor sensitivity.

Despite the majority of enriched pathways being downregulated upon DMX3433 treatment, one pathway – the interferon alpha response – was shown to be upregulated upon DMX3433 treatment in PDX models (Figure 6:6). The leading-edge subset of these genes includes multiple interferon induced genes (*IFI44, IFIT2, IFI27, IFIT3, IFI44L* and *ISG15*), which seems counterintuitive given the established role of IKKε/TBK1 in the induction of the interferon response. However, Ng et al., (2011) showed that while positively regulating the type-1 interferon response, IKKε actively down regulates the type- 2 interferon response through the inhibition of STAT1 homodimer formation. Therefore, inhibition of IKKε may well result in both the downregulation and upregulation of different subsets of the interferon response in DLBCL. In addition there are lineage differences in the role of TBK1: interferon responses are normal in macrophages from TBK1 deficient mice but not in embryonic fibroblasts (Perry et al., 2004). Others have shown that B-cell interferon responses are

independent of TBK1 (Oganesyan et al., 2008). It is therefore possible that TBK1 has a redundant role in interferon responses in DLBCL.

In order to determine significantly differentially expressed genes between untreated and treated PDX samples, a SAM and clustering analysis was performed on the PDX gene expression dataset. SAM was developed as a specific tool for the detection of significantly differentially expressed genes in microarray datasets (Tusher et al., 2001). For the purpose of this analysis, a delta value of 1.2 was used to select only the top ~ 500 differentially expressed genes in the dataset. This delta threshold results in a FDR of 0.0024 meaning that genes judged to be significant are highly unlikely to be a result of false discovery. The ~500 differentially expressed genes could be split into those which are downregulated upon DMX3433 treatment, and those that are upregulated. When these genes were assessed for enrichment with the same hallmark pathways used for the GSEA, four pathways, including NF-kB signalling, were found to be enriched in the downregulated PDX gene set. These pathways were also identified by the GSEA, and having been identified by two independent statistical analyses, this supports a major role (especially for NF-kB) mediating IKKε/TBK1 effects in DLBCL.

Chapter 7–Discussion and future work

7.1 The expression of IKKε and TBK1 in diffuse large B-cell lymphoma

This thesis has described the expression of IKKε and TBK1 in DLBCL, both in cell lines and primary DLBCL specimens. The expression of both IKKε and TBK1 was found to be significantly associated with non-GC status in primary DLBCL. Furthermore, *TBK1* transcript expression was found to be a predictor of poorer overall survival in a publically available dataset from a DLBCL cohort.

While detection of expression of these kinases may have important prognostic value in the clinical setting, it does not strictly predict sensitivity to drug based inhibition of IKKε/TBK1 as discussed in Chapter 4. A potential explanation for this is that antibodies used in this study were specific for total IKKε or TBK1 and not 'active' forms of these kinases. Both IKKε and TBK1 are activated by phosphorylation on serine 172 found within their activation loops (Peters et al., 2000, Kishore et al., 2002). Therefore, detection of whole IKKε and TBK1, as in this study, could be detecting inactive kinases which may not be functionally important.

Most, if not all, commercially available antibodies are unable to distinguish between phosphorylated IKKε and TBK1, presumably due to their structural similarity. However, it may be useful for future studies to determine if expression of S172 phosphorylation on IKKε *and* TBK1 is a useful predictor for sensitivity to IKKε/TBK1 inhibition.

The finding that *TBK1* expression levels are associated with a poor prognosis suggests that it might be involved, directly or indirectly, with the biology of DLBCL. Expression studies also raise the issue of whether IKKε is biologically important because IKKε expression levels do not appear to be associated with clinical outcome. Therefore, the functions of IKKε and TBK1 in DLBCL were addressed by characterising cell lines and primary DLBCL.

7.2 The function of IKKε and TBK1 in diffuse large B-cell lymphoma

This study has gone some way in identifying a functional role for IKKε and TBK1 in DLBCL.

7.2.1 The mechanism of action of DMX3433 on Ly10 cells and PDX models

To gain insight into the function of IKKε and TBK1 in DLBCL cells, Ly10 cells, representative of ABC-DLBCL, were treated with DMX3, a specific IKKε/TBK1 inhibitor. This revealed that drug inhibition of IKKε/TBK1 results in diminished P65 and STAT3 phosphorylation compatible with reduced NF-κB and JAK/STAT3 signalling respectively. JAK/STAT signalling is downstream of cytokine receptors and there is previous work to demonstrate that IL-10, specifically, is important (Béguelin et al., 2015) and others have suggested a role for interferon signalling (Yang et al., 2012). Secreted factors including interleukins, chemokines and interferons might be a route for both autocrine and paracrine regulation of DLBCL. Secretion of chemokines CCL3, CCL4 and IL-10 was reduced upon treatment with DMX3. Interestingly CCL3 and CCL4 are also established prognostic markers in DLBCL (REF). The reduction of IL-10 specifically was shown to be responsible for the reduction of STAT3 Y705 phosphorylation linking IKKε/TBK1 effects to previously established biology of DLBCL. Furthermore, treatment of cells derived from two PDX models sensitive to DMX3433 treatment also resulted in reduction of STAT3 phosphorylation.

Turning to NF- κB signalling; comparison of the gene expression profiles of treated and untreated PDX models revealed downregulation of NF-κB associated genes.

NF- κB is known to drive interleukin gene transcription (Lam et al., 2008) and this suggests a circuit in which IKKε/TBK1 suppresses NF- κB signalling, which in turn reduces interleukin gene transcription and STAT3 signalling. It has been established that STAT3 signalling is critically important for a group of ABC-DLBCL (Lam et al., 2008) and the work in this thesis

prompts the question of whether IKKε/TBK1 and especially TBK1 expression are a component of this subtype of high grade lymphoma. These data support a role for IKKε and TBK1 in promoting STAT3 and NF-κB signalling in DLBCL cells.

7.2.2 Knockdown of IKKε and TBK1 in Ly10 cells

In an effort to validate the proposed functions of IKKε/TBK1 in Ly10 cells, IKKε and TBK1 were knocked down separately in Ly10 cells. This knockdown was performed by transfection with siRNAs specific for the transcripts of *IKBKE* and *TBK1*. The resulting reduction in translated IKKε and TBK1 protein was detected by western blot. Knockdown of IKKε and TBK1 revealed distinct roles for the two kinases in Ly10 cells. TBK1, but not IKKε knockdown led to a reduction in P65 phosphorylation at the serine 536 residue at 48 hours after transfection. Knockdown of neither IKKε nor TBK1 kinase resulted in a decrease in STAT3 phosphorylation, likely due to only minor reductions in IL-10 secretion. While significant, the reduction in IL-10 upon TBK1 knockout was only modest and this could be due to poor transfection efficiency in these cells or the kinetics of IL-10 production and decay. Un-transfected cells will continue to secrete IL-10 and this could be sufficient to maintain STAT3 signalling.

A potential avenue for future work which may aid in elucidating the functional differences between IKKε and TBK1 in DLBCL would be the use of clustered, regularly interspaced, short palindromic repeat (CRISPR)/Cas9 technology. In brief, CRISPR/Cas9 involves the transfection of RNA guided nucleases to achieve stable knockout of a gene in question (Sander and Joung, 2014). This has recently been applied in DLBCL cell lines, with a CRISPR/Cas9 screen used to identify essential genes (Phelan et al., 2018), demonstrating that use of this technology is feasible in DLBCL cell lines. This could then allow production of stable knockout DLBCL cell lines of IKKε and TBK1 individually or in combination, which could then be functionally characterised.

A further avenue for future work could be the *in vivo* characterisation of mechanism of action for IKKε and TBK1 in DLBCL. There are several murine models which spontaneously develop B-cell lymphomas such as models based on Eμ-Myc – where the oncogene *Myc* is constitutively expressed in the B-cell lineage (Mori et al., 2008). Alternatively, DLBCL-like mouse models have been achieved by constitutive expression of BCL6 in B-cells (Cattoretti et al., 2005). These mouse models could theoretically be crossed with *IKBKE*$^{-/-}$ knockout mice to determine if IKKε function is necessary for lymphomagenesis in these models. Investigation of TBK1$^{-/-}$ knockout mice is hampered by the fact that homozygous knockout of *TBK1* causes embryonic lethality (Bonnard et al., 2000). To overcome this, conditional knockout could be used or low level expression of a mutant form of the kinase (Marchlik et al., 2010).

7.2.3 Summary

Collectively the data on mechanism suggests a scheme (Figure 7:1) that places IKKε and TBK1 downstream of MYD88 in a signalling complex, downstream of Toll-like receptors, that has been defined in both previous work on DLBCL (Ngo et al., 2011) and normal B-cells (Neves et al., 2010). Work described in this thesis, therefore, integrates well with previous models of ABC-DLBCL and, in addition, ideas about STAT3 expressing DLBCL are refined (Lam et al., 2008, Huang et al., 2013) to suggest that this subtype associates with active IKKε or TBK1 signalling. There may be several routes that still have to be defined in detail by which IKKε/TBK1 signalling alters factors secreted by DLBCL but these are likely to include indirect suppression of STAT3 signalling through inhibition of NF-κB driven cytokine expression, particularly IL-10. Although others have suggested that interferon signalling is a route to cell death in DLBCL (Yang et al., 2012) recent work (Lu et al., 2018) demonstrated that STAT3 suppresses interferon levels in DLBCL in accord with findings presented here.

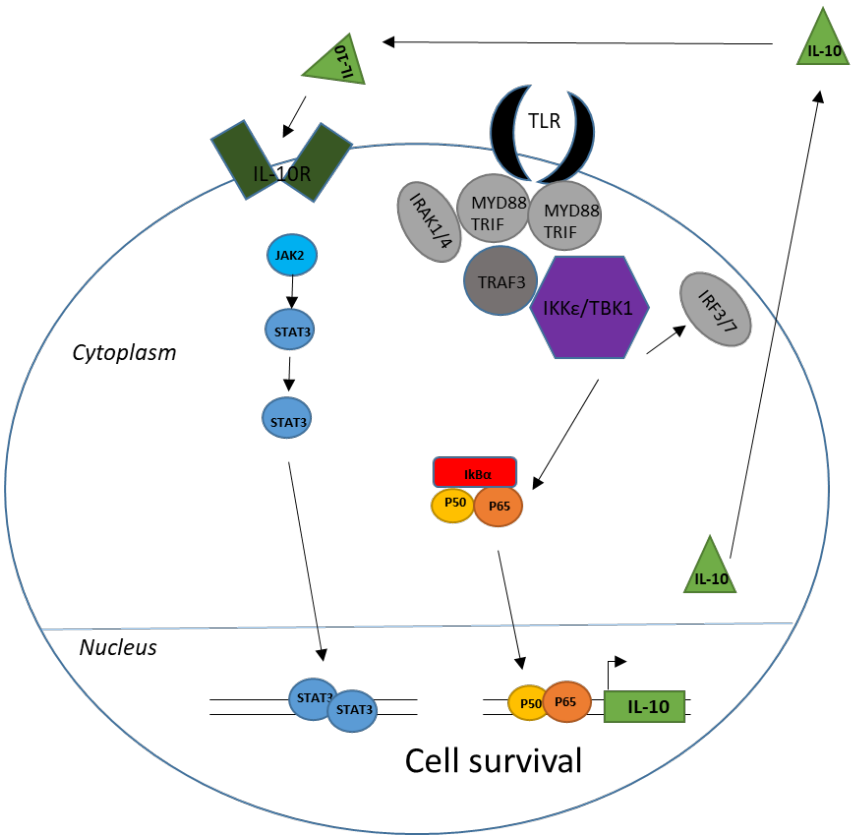

Figure 7:1. Summary wiring diagram of the proposed function of IKKε/TBK1 in DLBCL

7.3 The clinical use of dual IKKε/TBK1 inhibitors

The ultimate goal of translational studies is to reach an outcome that will lead to benefit in the clinical setting. While a majority of patients (50 to 60 %) can be cured of their DLBCL with R-CHOP combination chemotherapy, the remainder cannot and will ultimately relapse and succumb to their disease. This overall figure hides the fact that the clinical outlook for the elderly is much worse than for younger patients and also there are very few effective options for patients with relapsed DLBCL of whom only ~10% will be long-term survivors. There is therefore still a need to develop novel therapeutics for use in DLBCL and data

presented in this thesis suggest that the use of dual IKKε/TBK1 inhibitors may be of use in this setting.

7.3.1 Stratification of patients likely to benefit from IKKε/TBK1 inhibitor treatment

In both cell line and PDX models of DLBCL, there was a correlation between TBK1 protein expression and sensitivity to DMX3433 treatment, however there were models, which demonstrated both TBK1 protein expression and relative resistance to DMX3433 treatment. There were however no models which exhibited low TBK1 expression and sensitivity. These results suggest that while TBK1 protein expression is a necessary pre-requisite to DMX3433 sensitivity, there are DLBCL cases that express TBK1 but its drug inhibition is not lethal. Perhaps these models express TBK1 but do not rely on its function for their survival. There was no correlation between IKKε expression and DMX3433 sensitivity in the models examined.

A more robust predictor of sensitivity to DMX3433 treatment was the detection of STAT3 phosphorylated at the tyrosine 705 residue. In the DLBCL cell lines tested, the three cell lines that exhibited relative sensitivity to DMX3433 treatment – Ly10, Ly03 and Pfeiffer - were the only ones that had detectable levels of pSTAT3 Y705. The same pattern was observed in PDX models, with the two models relatively sensitive to DMX3433 treatment – PDX2214 and PDX0257 - being the only PDX models to express pSTAT3 Y05. While there were no exceptions to this correlation, a relatively small sample size was used (7 cell lines, 4 PDX models), and therefore larger numbers of pre-clinical models are likely to be needed to validate this association. Others have demonstrated that detection of pSTAT3 in DLBCL is achievable through immunohistochemistry (Ding et al., 2008, Gupta et al., 2012), and therefore if the association between pSTAT3 expression and IKKε/TBK1 drug sensitivity holds true, IHC analysis of pSTAT3 may be a useful predictor of sensitivity in DLBCL cohorts.

Furthermore, this study examined the secretion of cytokines in a cell line sensitive to DMX3433 treatment - Ly10 cells, before and after treatment with DMX3433. Interleukin 10 (IL-10) and the chemokines CCL3 and CCL4 were shown to be secreted into the media of resting Ly10 cells and their levels become significantly reduced upon treatment with DMX3433. Both CCL3 and CCL4 have been shown to be predictors of poor prognosis in ABC- DLBCL (see above) (Takahashi et al., 2015), and circulating levels of IL-10 are also associated with poor prognosis in DLBCL (Gupta et al., 2012).

Overall this study has demonstrated that DLBCLs characterised by TBK1 expression and phosphorylated STAT3 expression are sensitive to drug treatment with DMX3433, whereas others, without high level expression of these proteins, exhibit relative resistance. If use of DMX3433 or a similar compound were to enter clinical testing, it will be important to stratify patients based on those likely to respond to IKKε/TBK1 inhibitor use and results presented here together with the work of others suggests that CCL3, CCL4 and IL-10 levels in plasma may be biomarkers to predict response.

7.4 Final conclusions

The work in this thesis has shown that IKKε and TBK1 are expressed in a subset of DLBCL and their expression is significantly associated with the poor prognosis non-GC DLBCL sub-type.

Several DLBCL cell lines and PDX models are sensitive to treatment with a dual IKKε/TBK1 inhibitor – DMX3433. Sensitivity to DMX3433 treatment can be predicted by the presence of phosphorylated STAT3. Functional analysis of IKKε and TBK1 suggests a role for IKKε/TBK1 in maintaining pSTAT3 signalling in DLBCL cells via the production of IL-10. Treatment with DMX3433 also leads to reduced levels of P65 phosphorylation – a potential mechanism for reduced IL-10 secretion. Treatment of DLBCL cells with DMX3433 also leads to a reduction in the chemokines CCL3 and CCL4 and a reduction in NF-κB related genes in PDX DLBCL cells. Together, these data suggest that targeting IKKε/TBK1 by the use of dual inhibitors alone, or in combination with other small molecule inhibitors,

may be a potential therapeutic avenue for DLBCL patients especially those with poor prognosis and STAT3 expressing disease.

8. Appendix

Table S1

Disease Name	Cohort abbreviation	Cases
Adrenocortical carcinoma	ACC	92
Bladder urothelial carcinoma	BLCA	412
Breast invasive carcinoma	BRCA	1098
Cervical and endocervical cancers	CESC	307
Cholangiocarcinoma	CHOL	51
Colon adenocarcinoma	COAD	460
Colorectal adenocarcinoma	COADREAD	631
Lymphoid Neoplasm Diffuse Large B-cell Lymphoma	DLBC	58
Esophageal carcinoma	ESCA	185
FFPE Pilot Phase II	FPPP	38
Glioblastoma multiforme	GBM	613
Glioma	GBMLGG	1129
Head and Neck squamous cell carcinoma	HNSC	528
Kidney Chromophobe	KICH	113
Pan-kidney cohort (KICH+KIRC+KIRP)	KIPAN	973
Kidney renal clear cell carcinoma	KIRC	537
Kidney renal papillary cell carcinoma	KIRP	323
Acute Myeloid Leukemia	LAML	200
Brain Lower Grade Glioma	LGG	516
Liver hepatocellular carcinoma	LIHC	377
Lung adenocarcinoma	LUAD	585
Lung squamous cell carcinoma	LUSC	504
Mesothelioma	MESO	87
Ovarian serous cystadenocarcinoma	OV	602
Pancreatic adenocarcinoma	PAAD	185
Pheochromocytoma and Paraganglioma	PCPG	179
Prostate adenocarcinoma	PRAD	499
Rectum adenocarcinoma	READ	171
Sarcoma	SARC	261
Skin Cutaneous Melanoma	SKCM	470
Stomach adenocarcinoma	STAD	443
Stomach and Esophageal carcinoma	STES	628
Testicular Germ Cell Tumors	TGCT	150
Thyroid carcinoma	THCA	503
Thymoma	THYM	124
Uterine Corpus Endometrial Carcinoma	UCEC	560
Uterine Carcinosarcoma	UCS	57
Uveal Melanoma	UVM	80

Table S1. A key to the cohort abbreviations used in the cancer genome atlas with accompanying numbers of cases for each disease type.

Table S2

Position	Age	Sex	Organ/Anatomic site	Pathology diagnosis
A1	72	F	Lymphoma	Diffusive large B-cell lymphoma
A2	74	F	Lymphoma	Diffusive large B-cell lymphoma
A3	50	M	Lymphoma	Diffusive large B-cell lymphoma
A4	60	M	Lymphoma	Diffusive large B-cell lymphoma
A5	38	M	Lymphoma	Diffusive large B-cell lymphoma
A6	64	F	Lymphoma	Diffusive large B-cell lymphoma
B1	73	M	Lymphoma	Diffusive large B-cell lymphoma
B2	55	M	Lymphoma	Diffusive large B-cell lymphoma
B3	53	M	Lymphoma	Diffusive large B-cell lymphoma
B4	73	F	Lymphoma	Diffusive large B-cell lymphoma
B5	50	F	Lymphoma	Diffusive large B-cell lymphoma
B6	81	F	Lymphoma	Diffusive large B-cell lymphoma
C1	72	M	Lymphoma	Diffusive large B-cell lymphoma
C2	55	M	Lymphoma	Diffusive large B-cell lymphoma
C3	58	M	Lymphoma	Diffusive large B-cell lymphoma
C4	81	F	Lymphoma	Diffusive large B-cell lymphoma
C5	57	M	Lymphoma	Diffusive large B-cell lymphoma
C6	61	M	Lymphoma	Diffusive large B-cell lymphoma
D1	52	F	Lymphoma	Diffusive large B-cell lymphoma
D2	65	M	Lymphoma	Diffusive large B-cell lymphoma
D3	78	M	Lymphoma	Diffusive large B-cell lymphoma
D4	32	F	Lymphoma	Diffusive large B-cell lymphoma
D5	60	M	Lymphoma	Diffusive large B-cell lymphoma
D6	73	M	Lymphoma	Diffusive large B-cell lymphoma
E1	47	M	Lymphoma	Diffusive large B-cell lymphoma
E2	65	F	Lymphoma	Diffusive large B-cell lymphoma
E3	64	M	Lymphoma	Diffusive large B-cell lymphoma
E4	75	M	Lymphoma	Diffusive large B-cell lymphoma
E5	58	M	Lymphoma	Diffusive large B-cell lymphoma
E6	56	M	Lymphoma	Diffusive large B-cell lymphoma

Table S2. Details of each tumour core on the tissue microarray used.

Chapter 9: Bibliography

ABRAMSON, J. S. & SHIPP, M. A. 2005. Advances in the biology and therapy of diffuse large B-cell lymphoma: moving toward a molecularly targeted approach. *Blood,* 106**,** 1164-1174.

ADLI, M. & BALDWIN, A. S. 2006. IKK-i/IKKε Controls Constitutive, Cancer Cell-associated NF-κB Activity via Regulation of Ser-536 p65/RelA Phosphorylation. *Journal of Biological Chemistry,* 281**,** 26976-26984.

AGUIRRE-GAMBOA, R., GOMEZ-RUEDA, H., MARTÍNEZ-LEDESMA, E., MARTÍNEZ-TORTEYA, A., CHACOLLA-HUARINGA, R., RODRIGUEZ-BARRIENTOS, A., TAMEZ-PEÑA, J. G. & TREVIÑO, V. 2013. SurvExpress: An Online Biomarker Validation Tool and Database for Cancer Gene Expression Data Using Survival Analysis. *PLOS ONE,* 8**,** e74250.

AKIRA, S. & TAKEDA, K. 2004. Toll-like receptor signalling. *Nat Rev Immunol,* 4**,** 499-511.

AKIRA, S., UEMATSU, S. & TAKEUCHI, O. 2006. Pathogen Recognition and Innate Immunity. *Cell,* 124**,** 783-801.

ALIZADEH, A. A., EISEN, M. B., DAVIS, R. E., MA, C., LOSSOS, I. S., ROSENWALD, A., BOLDRICK, J. C., SABET, H., TRAN, T., YU, X., POWELL, J. I., YANG, L., MARTI, G. E., MOORE, T., HUDSON, J., JR., LU, L., LEWIS, D. B., TIBSHIRANI, R., SHERLOCK, G., CHAN, W. C., GREINER, T. C., WEISENBURGER, D. D., ARMITAGE, J. O., WARNKE, R., LEVY, R., WILSON, W., GREVER, M. R., BYRD, J. C., BOTSTEIN, D., BROWN, P. O. & STAUDT, L. M. 2000. Distinct types of diffuse large B-cell lymphoma identified by gene expression profiling. *Nature,* 403**,** 503-11.

ARMITAGE, J. O., GASCOYNE, R. D., LUNNING, M. A. & CAVALLI, F. 2017. Non-Hodgkin lymphoma. *The Lancet,* 390**,** 298-310.

BAEUERLE, P. A. & BALTIMORE, D. 1996. NF-κB: Ten Years After. *Cell,* 87**,** 13-20.

BAI, L.-Y., CHIU, C.-F., KAPURIYA, N. P., SHIEH, T.-M., TSAI, Y.-C., WU, C.-Y., SARGEANT, A. M. & WENG, J.-R. 2015. BX795, a TBK1 inhibitor, exhibits antitumor activity in human oral squamous cell carcinoma through apoptosis induction and mitotic phase arrest. *European Journal of Pharmacology,* 769**,** 287-296.

BAIN, J., PLATER, L., ELLIOTT, M., SHPIRO, N., HASTIE, C. J., MCLAUCHLAN, H., KLEVERNIC, I., ARTHUR, J. SIMON C., ALESSI, DARIO R. & COHEN, P. 2007. The selectivity of protein kinase inhibitors: a further update. *Biochemical Journal,* 408**,** 297-315.

BARBIE, D. A., TAMAYO, P., BOEHM, J. S., KIM, S. Y., MOODY, S. E., DUNN, I. F., SCHINZEL, A. C., SANDY, P., MEYLAN, E., SCHOLL, C., FROHLING, S., CHAN, E. M., SOS, M. L., MICHEL, K., MERMEL, C., SILVER, S. J., WEIR, B. A., REILING, J. H., SHENG, Q., GUPTA, P. B., WADLOW, R. C., LE, H., HOERSCH, S., WITTNER, B. S., RAMASWAMY, S., LIVINGSTON, D. M., SABATINI, D. M., MEYERSON, M., THOMAS, R. K., LANDER, E. S., MESIROV, J. P., ROOT, D. E., GILLILAND, D. G., JACKS, T. & HAHN, W. C. 2009. Systematic RNA interference reveals that oncogenic KRAS-driven cancers require TBK1. *Nature,* 462**,** 108-112.

BECK, D., ZOBEL, J., BARBER, R., EVANS, S., LEZINA, L., ALLCHIN, R. L., BLADES, M., ELLIOTT, R., LORD, C. J., ASHWORTH, A., PORTER, A. C. & WAGNER, S. D. 2016. Synthetic Lethal Screen Demonstrates That a JAK2 Inhibitor Suppresses a BCL6-dependent IL10RA/JAK2/STAT3 Pathway in High Grade B-cell Lymphoma. *J Biol Chem,* 291**,** 16686-98.

BEG, A. A., SHA, W. C., BRONSON, R. T., GHOSH, S. & BALTIMORE, D. 1995. Embryonic lethality and liver degeneration in mice lacking the RelA component of NF-κB. *Nature,* 376**,** 167.

BEGUELIN, W., SAWH, S., CHAMBWE, N., CHAN, F. C., JIANG, Y., CHOO, J. W., SCOTT, D. W., CHALMERS, A., GENG, H., TSIKITAS, L., TAM, W., BHAGAT, G., GASCOYNE, R. D. & SHAKNOVICH, R. 2015. IL10 receptor is a novel therapeutic target in DLBCLs. *Leukemia,* 29**,** 1684-1694.

BELL, J. 2005. Amlexanox for the Treatment of Recurrent Aphthous Ulcers. *Clinical Drug Investigation,* 25**,** 555-566.

BLAY, J. Y., BURDIN, N., ROUSSET, F., LENOIR, G., BIRON, P., PHILIP, T., BANCHEREAU, J. & FAVROT, M. C. 1993. Serum interleukin-10 in non-Hodgkin's lymphoma: a prognostic factor. *Blood,* 82**,** 2169-74.

BOEHM, J. S., ZHAO, J. J., YAO, J., KIM, S. Y., FIRESTEIN, R., DUNN, I. F., SJOSTROM, S. K., GARRAWAY, L. A., WEREMOWICZ, S., RICHARDSON, A. L., GREULICH, H., STEWART, C. J., MULVEY, L. A., SHEN, R. R., AMBROGIO, L., HIROZANE-KISHIKAWA, T., HILL, D. E., VIDAL, M., MEYERSON, M., GRENIER, J. K., HINKLE, G., ROOT, D. E., ROBERTS, T. M., LANDER, E. S., POLYAK, K. & HAHN, W. C. 2007. Integrative genomic approaches identify IKBKE as a breast cancer oncogene. *Cell,* 129**,** 1065-79.

BONNARD, M., MIRTSOS, C., SUZUKI, S., GRAHAM, K., HUANG, J., NG, M., ITIÉ, A., WAKEHAM, A., SHAHINIAN, A., HENZEL, W. J., ELIA, A. J., SHILLINGLAW, W., MAK, T. W., CAO, Z. & YEH, W. C. 2000. Deficiency of T2K leads to apoptotic liver degeneration and impaired NF-κB-dependent gene transcription. *The EMBO Journal,* 19**,** 4976-4985.

BOWMAN, T., GARCIA, R., TURKSON, J. & JOVE, R. 2000. STATs in oncogenesis. *Oncogene,* 19**,** 2474.

BROAD INSTITUTE OF MIT AND HARVARD. 2018. *Broad Institute TCGA Genome Analysis Centre* [Online]. Available: http://firebrowse.org/ [Accessed 07, March, 2019.

CALO, V., MIGLIAVACCA, M., BAZAN, V., MACALUSO, M., BUSCEMI, M., GEBBIA, N. & RUSSO, A. 2003. STAT proteins: from normal control of cellular events to tumorigenesis. *J Cell Physiol,* 197**,** 157-68.

CAMICIA, R., WINKLER, H. C. & HASSA, P. O. 2015. Novel drug targets for personalized precision medicine in relapsed/refractory diffuse large B-cell lymphoma: a comprehensive review. *Molecular Cancer,* 14**,** 207.

CARO, P., KISHAN, AMAR U., NORBERG, E., STANLEY, I. A., CHAPUY, B., FICARRO, SCOTT B., POLAK, K., TONDERA, D., GOUNARIDES, J., YIN, H., ZHOU, F., GREEN, MICHAEL R., CHEN, L., MONTI, S., MARTO, JARROD A., SHIPP, MARGARET A. & DANIAL, NIKA N. 2012. Metabolic Signatures Uncover Distinct Targets in Molecular Subsets of Diffuse Large B Cell Lymphoma. *Cancer Cell,* 22**,** 547-560.

CATTORETTI, G., PASQUALUCCI, L., BALLON, G., TAM, W., NANDULA, S. V., SHEN, Q., MO, T., MURTY, V. V. & DALLA-FAVERA, R. 2005. Deregulated BCL6 expression recapitulates the pathogenesis of human diffuse large B cell lymphomas in mice. *Cancer Cell,* 7**,** 445-455.

CERVANTES, F., VANNUCCHI, A. M., KILADJIAN, J. J., AL-ALI, H. K., SIRULNIK, A., STALBOVSKAYA, V., MCQUITTY, M., HUNTER, D. S., LEVY, R. S., PASSAMONTI, F., BARBUI, T., BAROSI, G., HARRISON, C. N., KNOOPS, L. & GISSLINGER, H. 2013. Three-year efficacy, safety, and survival findings from COMFORT-II, a phase 3 study comparing ruxolitinib with best available therapy for myelofibrosis. *Blood,* 122**,** 4047-53.

CHANG, C. C., YE, B. H., CHAGANTI, R. S. & DALLA-FAVERA, R. 1996. BCL-6, a POZ/zinc-finger protein, is a sequence-specific transcriptional repressor. *Proceedings of the National Academy of Sciences,* 93**,** 6947-6952.

CHAPUY, B., CHENG, H., WATAHIKI, A., DUCAR, M. D., TAN, Y., CHEN, L., ROEMER, M. G., OUYANG, J., CHRISTIE, A. L., ZHANG, L., GUSENLEITNER, D., ABO, R. P., FARINHA, P., VON BONIN, F., THORNER, A. R., SUN, H. H., GASCOYNE, R. D., PINKUS, G. S., VAN HUMMELEN, P., WULF, G. G., ASTER, J. C., WEINSTOCK, D. M., MONTI, S., RODIG, S. J., WANG, Y. & SHIPP, M. A. 2016. Diffuse large B-cell lymphoma patient-derived xenograft models capture the molecular and biological heterogeneity of the disease. *Blood,* 127**,** 2203-13.

CHAPUY, B., STEWART, C., DUNFORD, A. J., KIM, J., KAMBUROV, A., REDD, R. A., LAWRENCE, M. S., ROEMER, M. G. M., LI, A. J., ZIEPERT, M., STAIGER, A. M., WALA, J. A., DUCAR, M. D., LESHCHINER, I., RHEINBAY, E., TAYLOR-WEINER, A., COUGHLIN, C. A., HESS, J. M., PEDAMALLU, C. S., LIVITZ, D., ROSEBROCK, D., ROSENBERG, M., TRACY, A. A., HORN, H., VAN HUMMELEN, P., FELDMAN, A. L., LINK, B. K., NOVAK, A. J., CERHAN, J. R., HABERMANN, T. M., SIEBERT, R., ROSENWALD, A., THORNER, A. R., MEYERSON, M. L., GOLUB, T. R., BEROUKHIM, R., WULF, G. G., OTT, G., RODIG, S. J., MONTI, S., NEUBERG, D. S., LOEFFLER,

M., PFREUNDSCHUH, M., TRUMPER, L., GETZ, G. & SHIPP, M. A. 2018. Molecular subtypes of diffuse large B cell lymphoma are associated with distinct pathogenic mechanisms and outcomes. *Nat Med,* 24**,** 679-690.

CHARBONNEAU, B., MAURER, M. J., ANSELL, S. M., SLAGER, S. L., FREDERICKSEN, Z. S., ZIESMER, S. C., MACON, W. R., HABERMANN, T. M., WITZIG, T. E., LINK, B. K., CERHAN, J. R. & NOVAK, A. J. 2012. Pretreatment circulating serum cytokines associated with follicular and diffuse large B-cell lymphoma: A clinic-based case-control study. *Cytokine,* 60**,** 882-889.

CHEN, Z. J. 2005. Ubiquitin signalling in the NF-κB pathway. *Nature Cell Biology,* 7**,** 758.

CHIEN, Y., KIM, S., BUMEISTER, R., LOO, Y.-M., KWON, S. W., JOHNSON, C. L., BALAKIREVA, M. G., ROMEO, Y., KOPELOVICH, L. & GALE, M. 2006. RalB GTPase-mediated activation of the IκB family kinase TBK1 couples innate immune signaling to tumor cell survival. *Cell,* 127**,** 157-170.

CLÉMENT, J.-F., MELOCHE, S. & SERVANT, M. J. 2008. The IKK-related kinases: from innate immunity to oncogenesis. *Cell Research,* 18**,** 889.

COIFFIER, B., LEPAGE, E., BRIÈRE, J., HERBRECHT, R., TILLY, H., BOUABDALLAH, R., MOREL, P., VAN DEN NESTE, E., SALLES, G., GAULARD, P., REYES, F., LEDERLIN, P. & GISSELBRECHT, C. 2002. CHOP Chemotherapy plus Rituximab Compared with CHOP Alone in Elderly Patients with Diffuse Large-B-Cell Lymphoma. *New England Journal of Medicine,* 346**,** 235-242.

COIFFIER, B., THIEBLEMONT, C., VAN DEN NESTE, E., LEPEU, G., PLANTIER, I., CASTAIGNE, S., LEFORT, S., MARIT, G., MACRO, M., SEBBAN, C., BELHADJ, K., BORDESSOULE, D., FERME, C. & TILLY, H. 2010. Long-term outcome of patients in the LNH-98.5 trial, the first randomized study comparing rituximab-CHOP to standard CHOP chemotherapy in DLBCL patients: a study by the Groupe d'Etudes des Lymphomes de l'Adulte. *Blood,* 116**,** 2040-5.

COMPAGNO, M., LIM, W. K., GRUNN, A., NANDULA, S. V., BRAHMACHARY, M., SHEN, Q., BERTONI, F., PONZONI, M., SCANDURRA, M., CALIFANO, A., BHAGAT, G., CHADBURN, A., DALLA-FAVERA, R. & PASQUALUCCI, L. 2009. Mutations of multiple genes cause deregulation of NF-kappaB in diffuse large B-cell lymphoma. *Nature,* 459**,** 717-21.

COOPER, J. M., OU, Y. H., MCMILLAN, E. A., VADEN, R. M., ZAMAN, A., BODEMANN, B. O., MAKKAR, G., POSNER, B. A. & WHITE, M. A. 2017. TBK1 Provides Context-Selective Support of the Activated AKT/mTOR Pathway in Lung Cancer. *Cancer Res,* 77**,** 5077-5094.

CZARNESKI, J., LIN, Y. C., CHONG, S., MCCARTHY, B., FERNANDES, H., PARKER, G., MANSOUR, A., HUPPI, K., MARTI, G. E. & RAVECHE, E. 2004. Studies in NZB IL-10 knockout mice of the requirement of IL-10 for progression of B-cell lymphoma. *Leukemia,* 18**,** 597-606.

DAL PORTO, J. M., GAULD, S. B., MERRELL, K. T., MILLS, D., PUGH-BERNARD, A. E. & CAMBIER, J. 2004. B cell antigen receptor signaling 101. *Molecular Immunology,* 41**,** 599-613.

DAVIES, A. J., CADDY, J., MAISHMAN, T., BARRANS, S., MAMOT, C., CARE, M., POCOCK, C., STANTON, L., HAMID, D., PUGH, K., MCMILLAN, A., FIELDS, P., KRUGER, A., JACK, A. & JOHNSON, P. W. M. 2015. A Prospective Randomised Trial of Targeted Therapy for Diffuse Large B-Cell Lymphoma (DLBCL) Based upon Real-Time Gene Expression Profiling: The Remodl-B Study of the UK NCRI and SAKK Lymphoma Groups (ISRCTN51837425). *Blood,* 126**,** 812-812.

DAVIS, R. E., BROWN, K. D., SIEBENLIST, U. & STAUDT, L. M. 2001. Constitutive nuclear factor kappaB activity is required for survival of activated B cell-like diffuse large B cell lymphoma cells. *J Exp Med,* 194**,** 1861-74.

DAVIS, R. E., NGO, V. N., LENZ, G., TOLAR, P., YOUNG, R. M., ROMESSER, P. B., KOHLHAMMER, H., LAMY, L., ZHAO, H., YANG, Y., XU, W., SHAFFER, A. L., WRIGHT, G., XIAO, W., POWELL, J., JIANG, J. K., THOMAS, C. J., ROSENWALD, A., OTT, G., MULLER-HERMELINK, H. K., GASCOYNE, R. D., CONNORS, J. M., JOHNSON, N. A., RIMSZA, L. M., CAMPO, E., JAFFE, E. S., WILSON, W. H., DELABIE, J., SMELAND, E. B., FISHER, R. I., BRAZIEL, R. M., TUBBS, R. R., COOK, J. R., WEISENBURGER, D. D., CHAN, W. C., PIERCE, S. K. & STAUDT, L. M. 2010. Chronic active B-cell-receptor signalling in diffuse large B-cell lymphoma. *Nature,* 463**,** 88-92.

DE PAEPE, P. & DE WOLF-PEETERS, C. 2006. Diffuse large B-cell lymphoma: a heterogeneous group of non-Hodgkin lymphomas comprising several distinct clinicopathological entities. *Leukemia,* 21**,** 37.

DE VEER MICHAEL, J., HOLKO, M., FREVEL, M., WALKER, E., DER, S., PARANJAPE JAYASHREE, M., SILVERMAN ROBERT, H. & WILLIAMS BRYAN, R. G. 2001. Functional classification of interferon-stimulated genes identified using microarrays. *Journal of Leukocyte Biology,* 69**,** 912-920.

DECKER, T. & KOVARIK, P. 2000. Serine phosphorylation of STATs. *Oncogene,* 19**,** 2628.

DENG, T., LIU, J. C., CHUNG, P. E., UEHLING, D., AMAN, A., JOSEPH, B., KETELA, T., JIANG, Z., SCHACHTER, N. F. & ROTTAPEL, R. 2014a. shRNA kinome screen identifies TBK1 as a therapeutic target for HER2+ breast cancer. *Cancer research,* 74**,** 2119-2130.

DENG, T., LIU, J. C., CHUNG, P. E. D., UEHLING, D., AMAN, A., JOSEPH, B., KETELA, T., JIANG, Z., SCHACHTER, N. F., ROTTAPEL, R., EGAN, S. E., AL-AWAR, R., MOFFAT, J. & ZACKSENHAUS, E. 2014b. shRNA Kinome Screen Identifies TBK1 as a Therapeutic Target for HER2⁺ Breast Cancer. *Cancer Research,* 74**,** 2119-2130.

DER, S. D., ZHOU, A., WILLIAMS, B. R. G. & SILVERMAN, R. H. 1998. Identification of genes differentially regulated by interferon α, β, or γ using oligonucleotide arrays. *Proceedings of the National Academy of Sciences,* 95**,** 15623-15628.

DING, B. B., YU, J. J., YU, R. Y.-L., MENDEZ, L. M., SHAKNOVICH, R., ZHANG, Y., CATTORETTI, G. & YE, B. H. 2008. Constitutively activated STAT3 promotes cell proliferation and survival in the activated B-cell subtype of diffuse large B-cell lymphomas. *Blood,* 111**,** 1515-1523.

DOLCET, X., LLOBET, D., PALLARES, J. & MATIAS-GUIU, X. 2005. NF-kB in development and progression of human cancer. *Virchows Archiv,* 446**,** 475-482.

DUAN, S., CERMAK, L., PAGAN, J. K., ROSSI, M., MARTINENGO, C., DI CELLE, P. F., CHAPUY, B., SHIPP, M., CHIARLE, R. & PAGANO, M. 2011. FBXO11 targets BCL6 for degradation and is inactivated in diffuse large B-cell lymphomas. *Nature,* 481**,** 90.

DUBOIS, N., BERENDSEN, S., HENRY, A., NGUYEN, M., BOURS, V. & ROBE, P. 2018. I-Kappa-B kinase-epsilon activates nuclear factor-kappa B and STAT5B and supports glioblastoma growth but amlexanox shows little therapeutic potential in these tumors. *Cancer Translational Medicine,* 4**,** 1-8.

DUGGAN, D. J., BITTNER, M., CHEN, Y., MELTZER, P. & TRENT, J. M. 1999. Expression profiling using cDNA microarrays. *Nat Genet*.

EDDY, S. F., GUO, S., DEMICCO, E. G., ROMIEU-MOUREZ, R., LANDESMAN-BOLLAG, E., SELDIN, D. C. & SONENSHEIN, G. E. 2005. Inducible IκB Kinase/IκB Kinase ε Expression Is Induced by CK2 and Promotes Aberrant Nuclear Factor-κB Activation in Breast Cancer Cells. *Cancer Research,* 65**,** 11375-11383.

ENNISHI, D., BASHASHATI, A., SABERI, S., MOTTOK, A., MEISSNER, B., BOYLE, M., BEN-NERIAH, S., KRIDEL, R., DOMINGUEZ-SOLA, D., SAVAGE, K. J., SEHN, L. H., CONNORS, J. M., MORIN, R. D., MARRA, M. A., SHAH, S. P., STEIDL, C., SCOTT, D. W. & GASCOYNE, R. D. 2016. Frequent Genetic Alterations of PI3K-AKT Pathway and Their Clinical Significance in Germinal Center B-Cell-like Diffuse Large B-Cell Lymphoma. *Blood,* 128**,** 607-607.

EVERTS, B., AMIEL, E., HUANG, S. C.-C., SMITH, A. M., CHANG, C.-H., LAM, W. Y., REDMANN, V., FREITAS, T. C., BLAGIH, J., VAN DER WINDT, G. J. W., ARTYOMOV, M. N., JONES, R. G., PEARCE, E. L. & PEARCE, E. J. 2014. TLR-driven early glycolytic reprogramming via the kinases TBK1-IKKε supports the anabolic demands of dendritic cell activation. *Nature Immunology,* 15**,** 323.

FEARON, D. T., MANDERS, P. & WAGNER, S. D. 2001. Arrested Differentiation, the Self-Renewing Memory Lymphocyte, and Vaccination. *Science,* 293**,** 248-250.

FELDMAN, R. I., WU, J. M., POLOKOFF, M. A., KOCHANNY, M. J., DINTER, H., ZHU, D., BIROC, S. L., ALICKE, B., BRYANT, J., YUAN, S., BUCKMAN, B. O., LENTZ, D., FERRER, M., WHITLOW, M.,

ADLER, M., FINSTER, S., CHANG, Z. & ARNAIZ, D. O. 2005. Novel Small Molecule Inhibitors of 3-Phosphoinositide-dependent Kinase-1. *Journal of Biological Chemistry,* 280**,** 19867-19874.

FISHER, R. I., GAYNOR, E. R., DAHLBERG, S., OKEN, M. M., GROGAN, T. M., MIZE, E. M., GLICK, J. H., COLTMAN, C. A. & MILLER, T. P. 1993. Comparison of a Standard Regimen (CHOP) with Three Intensive Chemotherapy Regimens for Advanced Non-Hodgkin's Lymphoma. *New England Journal of Medicine,* 328**,** 1002-1006.

FITZGERALD, K. A., MCWHIRTER, S. M., FAIA, K. L., ROWE, D. C., LATZ, E., GOLENBOCK, D. T., COYLE, A. J., LIAO, S.-M. & MANIATIS, T. 2003. IKKε and TBK1 are essential components of the IRF3 signaling pathway. *Nature immunology,* 4**,** 491-496.

FOON, K., SCHROFF, R. & GALE, R. 1982. Surface markers on leukemia and lymphoma cells: recent advances. *Blood,* 60**,** 1-19.

GATTO, D. & BRINK, R. 2010. The germinal center reaction. *J Allergy Clin Immunol,* 126**,** 898-907; quiz 908-9.

GHIA, P., STROLA, G., GRANZIERO, L., GEUNA, M., GUIDA, G., SALLUSTO, F., RUFFING, N., MONTAGNA, L., PICCOLI, P., CHILOSI, M. & CALIGARIS-CAPPIO, F. 2002. Chronic lymphocytic leukemia B cells are endowed with the capacity to attract CD4+, CD40L+ T cells by producing CCL22. *Eur J Immunol,* 32**,** 1403-13.

GRANDVAUX, N., TENOEVER, B. R., SERVANT, M. J. & HISCOTT, J. 2002. The interferon antiviral response: from viral invasion to evasion. *Current Opinion in Infectious Diseases,* 15**,** 259-267.

GUAN, H., ZHANG, H., CAI, J., WU, J., YUAN, J., LI, J., HUANG, Z. & LI, M. 2011. IKBKE is over-expressed in glioma and contributes to resistance of glioma cells to apoptosis via activating NF-kappaB. *J Pathol,* 223**,** 436-45.

GUO, J.-P., SHU, S.-K., HE, L., LEE, Y.-C., KRUK, P. A., GRENMAN, S., NICOSIA, S. V., MOR, G., SCHELL, M. J., COPPOLA, D. & CHENG, J. Q. 2009. Deregulation of IKBKE Is Associated with Tumor Progression, Poor Prognosis, and Cisplatin Resistance in Ovarian Cancer. *The American Journal of Pathology,* 175**,** 324-333.

GUO, J., KIM, D., GAO, J., KURTYKA, C., CHEN, H., YU, C., WU, D., MITTAL, A., BEG, A. A., CHELLAPPAN, S. P., HAURA, E. B. & CHENG, J. Q. 2013. IKBKE is induced by STAT3 and tobacco carcinogen and determines chemosensitivity in non-small cell lung cancer. *Oncogene,* 32**,** 151-159.

GUPTA, M., HAN, J. J., STENSON, M., MAURER, M., WELLIK, L., HU, G., ZIESMER, S., DOGAN, A. & WITZIG, T. E. 2012. Elevated serum IL-10 levels in diffuse large B-cell lymphoma: a mechanism of aberrant JAK2 activation. *Blood,* 119**,** 2844-2853.

HABERMANN, T. M., WELLER, E. A., MORRISON, V. A., GASCOYNE, R. D., CASSILETH, P. A., COHN, J. B., DAKHIL, S. R., WODA, B., FISHER, R. I., PETERSON, B. A. & HORNING, S. J. 2006. Rituximab-CHOP Versus CHOP Alone or With Maintenance Rituximab in Older Patients With Diffuse Large B-Cell Lymphoma. *Journal of Clinical Oncology,* 24**,** 3121-3127.

HANS, C. P., WEISENBURGER, D. D., GREINER, T. C., GASCOYNE, R. D., DELABIE, J., OTT, G., MULLER-HERMELINK, H. K., CAMPO, E., BRAZIEL, R. M., JAFFE, E. S., PAN, Z., FARINHA, P., SMITH, L. M., FALINI, B., BANHAM, A. H., ROSENWALD, A., STAUDT, L. M., CONNORS, J. M., ARMITAGE, J. O. & CHAN, W. C. 2004. Confirmation of the molecular classification of diffuse large B-cell lymphoma by immunohistochemistry using a tissue microarray. *Blood,* 103**,** 275-82.

HARRIS, J., OLIÈRE, S., SHARMA, S., SUN, Q., LIN, R., HISCOTT, J. & GRANDVAUX, N. 2006. Nuclear accumulation of cRel following C-terminal phosphorylation by TBK1/IKKε. *The Journal of Immunology,* 177**,** 2527-2535.

HASAN, M., DOBBS, N., KHAN, S., WHITE, M. A., WAKELAND, E. K., LI, Q.-Z. & YAN, N. 2015. Cutting Edge: Inhibiting TBK1 by Compound II Ameliorates Autoimmune Disease in Mice. *The Journal of Immunology,* 195**,** 4573-4577.

HAYDEN, M. S. & GHOSH, S. 2008. Shared Principles in NF-κB Signaling. *Cell,* 132**,** 344-362.

HEMMI, H., TAKEUCHI, O., SATO, S., YAMAMOTO, M., KAISHO, T., SANJO, H., KAWAI, T., HOSHINO, K., TAKEDA, K. & AKIRA, S. 2004. The Roles of Two IκB Kinase-related Kinases in

Lipopolysaccharide and Double Stranded RNA Signaling and Viral Infection. *The Journal of Experimental Medicine,* 199**,** 1641-1650.

HEXNER, E. O., SERDIKOFF, C., JAN, M., SWIDER, C. R., ROBINSON, C., YANG, S., ANGELES, T., EMERSON, S. G., CARROLL, M., RUGGERI, B. & DOBRZANSKI, P. 2008. Lestaurtinib (CEP701) is a JAK2 inhibitor that suppresses JAK2/STAT5 signaling and the proliferation of primary erythroid cells from patients with myeloproliferative disorders. *Blood,* 111**,** 5663-5671.

HIDALGO, M., AMANT, F., BIANKIN, A. V., BUDINSKÁ, E., BYRNE, A. T., CALDAS, C., CLARKE, R. B., DE JONG, S., JONKERS, J., MÆLANDSMO, G. M., ROMAN-ROMAN, S., SEOANE, J., TRUSOLINO, L. & VILLANUEVA, A. 2014. Patient-Derived Xenograft Models: An Emerging Platform for Translational Cancer Research. *Cancer Discovery,* 4**,** 998-1013.

HIRANO, T., ISHIHARA, K. & HIBI, M. 2000. Roles of STAT3 in mediating the cell growth, differentiation and survival signals relayed through the IL-6 family of cytokine receptors. *Oncogene,* 19**,** 2548-56.

HOBBS, G. A., DER, C. J. & ROSSMAN, K. L. 2016. RAS isoforms and mutations in cancer at a glance. *J Cell Sci,* 129**,** 1287-92.

HONMA, K., TSUZUKI, S., NAKAGAWA, M., TAGAWA, H., NAKAMURA, S., MORISHIMA, Y. & SETO, M. 2009. TNFAIP3/A20 functions as a novel tumor suppressor gene in several subtypes of non-Hodgkin lymphomas. *Blood,* 114**,** 2467-75.

HSIA, H. C., HUTTI, J. E. & BALDWIN, A. S. 2017. Cytosolic DNA Promotes Signal Transducer and Activator of Transcription 3 (STAT3) Phosphorylation by TANK-binding Kinase 1 (TBK1) to Restrain STAT3 Activity. *J Biol Chem,* 292**,** 5405-5417.

HUANG, X., MENG, B., IQBAL, J., DING, B. B., PERRY, A. M., CAO, W., SMITH, L. M., BI, C., JIANG, C., GREINER, T. C., WEISENBURGER, D. D., RIMSZA, L., ROSENWALD, A., OTT, G., DELABIE, J., CAMPO, E., BRAZIEL, R. M., GASCOYNE, R. D., COOK, J. R., TUBBS, R. R., JAFFE, E. S., ARMITAGE, J. O., VOSE, J. M., STAUDT, L. M., MCKEITHAN, T. W., CHAN, W. C., YE, B. H. & FU, K. 2013. Activation of the STAT3 Signaling Pathway Is Associated With Poor Survival in Diffuse Large B-Cell Lymphoma Treated With R-CHOP. *Journal of Clinical Oncology,* 31**,** 4520-4528.

HUSSON, H., FREEDMAN, A. S., CARDOSO, A. A., SCHULTZE, J., MUNOZ, O., STROLA, G., KUTOK, J., CARIDEO, E. G., DE BEAUMONT, R., CALIGARIS-CAPPIO, F. & GHIA, P. 2002. CXCL13 (BCA-1) is produced by follicular lymphoma cells: role in the accumulation of malignant B cells. *Br J Haematol,* 119**,** 492-5.

HUTTI, J. E., SHEN, R. R., ABBOTT, D. W., ZHOU, A. Y., SPROTT, K. M., ASARA, J. M., HAHN, W. C. & CANTLEY, L. C. 2009. Phosphorylation of the Tumor Suppressor CYLD by the Breast Cancer Oncogene IKKε Promotes Cell Transformation. *Molecular Cell,* 34**,** 461-472.

JIANG, J., LIU, Y., TANG, Y., LI, L., ZENG, R., ZENG, S. & ZHONG, M. 2016. ALDH1A1 induces resistance to CHOP in diffuse large B-cell lymphoma through activation of the JAK2/STAT3 pathway. *OncoTargets and therapy,* 9**,** 5349-5360.

KISHORE, N., HUYNH, Q. K., MATHIALAGAN, S., HALL, T., ROUW, S., CREELY, D., LANGE, G., CAROLL, J., REITZ, B., DONNELLY, A., BODDUPALLI, H., COMBS, R. G., KRETZMER, K. & TRIPP, C. S. 2002. IKK-i and TBK-1 are Enzymatically Distinct from the Homologous Enzyme IKK-2: COMPARATIVE ANALYSIS OF RECOMBINANT HUMAN IKK-i, TBK-1, AND IKK-2. *Journal of Biological Chemistry,* 277**,** 13840-13847.

KNUTSON, S. K., KAWANO, S., MINOSHIMA, Y., WARHOLIC, N. M., HUANG, K. C., XIAO, Y., KADOWAKI, T., UESUGI, M., KUZNETSOV, G., KUMAR, N., WIGLE, T. J., KLAUS, C. R., ALLAIN, C. J., RAIMONDI, A., WATERS, N. J., SMITH, J. J., PORTER-SCOTT, M., CHESWORTH, R., MOYER, M. P., COPELAND, R. A., RICHON, V. M., UENAKA, T., POLLOCK, R. M., KUNTZ, K. W., YOKOI, A. & KEILHACK, H. 2014. Selective inhibition of EZH2 by EPZ-6438 leads to potent antitumor activity in EZH2-mutant non-Hodgkin lymphoma. *Mol Cancer Ther,* 13**,** 842-54.

KORHERR, C., GILLE, H., SCHÄFER, R., KOENIG-HOFFMANN, K., DIXELIUS, J., EGLAND, K. A., PASTAN, I. & BRINKMANN, U. 2006. Identification of proangiogenic genes and pathways by high-

throughput functional genomics: TBK1 and the IRF3 pathway. *Proceedings of the National Academy of Sciences of the United States of America,* 103**,** 4240-4245.

KUPPERS, R. 2005. Mechanisms of B-cell lymphoma pathogenesis. *Nat Rev Cancer,* 5**,** 251-62.

LAM, L. T., DAVIS, R. E., PIERCE, J., HEPPERLE, M., XU, Y., HOTTELET, M., NONG, Y., WEN, D., ADAMS, J., DANG, L. & STAUDT, L. M. 2005. Small molecule inhibitors of IkappaB kinase are selectively toxic for subgroups of diffuse large B-cell lymphoma defined by gene expression profiling. *Clin Cancer Res,* 11**,** 28-40.

LAM, L. T., WRIGHT, G., DAVIS, R. E., LENZ, G., FARINHA, P., DANG, L., CHAN, J. W., ROSENWALD, A., GASCOYNE, R. D. & STAUDT, L. M. 2008. Cooperative signaling through the signal transducer and activator of transcription 3 and nuclear factor-κB pathways in subtypes of diffuse large B-cell lymphoma. *Blood,* 111**,** 3701-3713.

LEE, E. G., BOONE, D. L., CHAI, S., LIBBY, S. L., CHIEN, M., LODOLCE, J. P. & MA, A. 2000. Failure to regulate TNF-induced NF-kappaB and cell death responses in A20-deficient mice. *Science,* 289**,** 2350-4.

LENZ, G., DAVIS, R. E., NGO, V. N., LAM, L., GEORGE, T. C., WRIGHT, G. W., DAVE, S. S., ZHAO, H., XU, W., ROSENWALD, A., OTT, G., MULLER-HERMELINK, H. K., GASCOYNE, R. D., CONNORS, J. M., RIMSZA, L. M., CAMPO, E., JAFFE, E. S., DELABIE, J., SMELAND, E. B., FISHER, R. I., CHAN, W. C. & STAUDT, L. M. 2008a. Oncogenic CARD11 mutations in human diffuse large B cell lymphoma. *Science,* 319**,** 1676-9.

LENZ, G., WRIGHT, G., DAVE, S. S., XIAO, W., POWELL, J., ZHAO, H., XU, W., TAN, B., GOLDSCHMIDT, N., IQBAL, J., VOSE, J., BAST, M., FU, K., WEISENBURGER, D. D., GREINER, T. C., ARMITAGE, J. O., KYLE, A., MAY, L., GASCOYNE, R. D., CONNORS, J. M., TROEN, G., HOLTE, H., KVALOY, S., DIERICKX, D., VERHOEF, G., DELABIE, J., SMELAND, E. B., JARES, P., MARTINEZ, A., LOPEZ-GUILLERMO, A., MONTSERRAT, E., CAMPO, E., BRAZIEL, R. M., MILLER, T. P., RIMSZA, L. M., COOK, J. R., POHLMAN, B., SWEETENHAM, J., TUBBS, R. R., FISHER, R. I., HARTMANN, E., ROSENWALD, A., OTT, G., MULLER-HERMELINK, H. K., WRENCH, D., LISTER, T. A., JAFFE, E. S., WILSON, W. H., CHAN, W. C. & STAUDT, L. M. 2008b. Stromal gene signatures in large-B-cell lymphomas. *N Engl J Med,* 359**,** 2313-23.

LEONARD, J. P., KOLIBABA, K., REEVES, J. A., TULPULE, A., FLINN, I. W., KOLEVSKA, T., ROBLES, R., FLOWERS, C., COLLINS, R., DIBELLA, N. J., PAPISH, S. W., VENUGOPAL, P., HORODNER, A., TABATABAI, A., HAJDENBERG, J., MULLIGAN, G., NEUWIRTH, R., SURYANARAYAN, K., ESSELTINE, D.-L. & DE VOS, S. 2015. Randomized Phase 2 Open-Label Study of R-CHOP ± Bortezomib in Patients (Pts) with Untreated Non-Germinal Center B-Cell-like (Non-GCB) Subtype Diffuse Large Cell Lymphoma (DLBCL): Results from the Pyramid Trial (NCT00931918). *Blood,* 126**,** 811-811.

LEVINE, A. J. & OREN, M. 2009. The first 30 years of p53: growing ever more complex. *Nature Reviews Cancer,* 9**,** 749.

LI, B. & DEWEY, C. N. 2011. RSEM: accurate transcript quantification from RNA-Seq data with or without a reference genome. *BMC Bioinformatics,* 12**,** 323.

LI, Q., ANTWERP, D. V., MERCURIO, F., LEE, K.-F. & VERMA, I. M. 1999. Severe Liver Degeneration in Mice Lacking the IκB Kinase 2 Gene. *Science,* 284**,** 321-325.

LIU, S., CAI, X., WU, J., CONG, Q., CHEN, X., LI, T., DU, F., REN, J., WU, Y. T., GRISHIN, N. V. & CHEN, Z. J. 2015. Phosphorylation of innate immune adaptor proteins MAVS, STING, and TRIF induces IRF3 activation. *Science,* 347**,** aaa2630.

LIU, Y., LU, J., ZHANG, Z., ZHU, L., DONG, S., GUO, G., LI, R., NAN, Y., YU, K., ZHONG, Y. & HUANG, Q. 2017. Amlexanox, a selective inhibitor of IKBKE, generates anti-tumoral effects by disrupting the Hippo pathway in human glioblastoma cell lines. *Cell Death &Amp; Disease,* 8**,** e3022.

LOSSOS, I. S., CZERWINSKI, D. K., ALIZADEH, A. A., WECHSER, M. A., TIBSHIRANI, R., BOTSTEIN, D. & LEVY, R. 2004. Prediction of Survival in Diffuse Large-B-Cell Lymphoma Based on the Expression of Six Genes. *New England Journal of Medicine,* 350**,** 1828-1837.

LU, L., ZHU, F., ZHANG, M., LI, Y., DRENNAN, A. C., KIMPARA, S., RUMBALL, I., SELZER, C., CAMERON, H., KELLICUT, A., KELM, A., WANG, F., WALDMANN, T. A. & RUI, L. 2018. Gene regulation and suppression of type I interferon signaling by STAT3 in diffuse large B cell lymphoma. *Proceedings of the National Academy of Sciences,* 115**,** E498-E505.

LUND, F. E. 2008. Cytokine-producing B lymphocytes-key regulators of immunity. *Curr Opin Immunol,* 20**,** 332-8.

MAKRIS, C., GODFREY, V. L., KRÄHN-SENFTLEBEN, G., TAKAHASHI, T., ROBERTS, J. L., SCHWARZ, T., FENG, L., JOHNSON, R. S. & KARIN, M. 2000. Female Mice Heterozygous for IKKγ/NEMO Deficiencies Develop a Dermatopathy Similar to the Human X-Linked Disorder Incontinentia Pigmenti. *Molecular Cell,* 5**,** 969-979.

MARCHLIK, E., THAKKER, P., CARLSON, T., JIANG, Z., RYAN, M., MARUSIC, S., GOUTAGNY, N., KUANG, W., ASKEW, G. R., ROBERTS, V., BENOIT, S., ZHOU, T., LING, V., PFEIFER, R., STEDMAN, N., FITZGERALD, K. A., LIN, L.-L. & HALL, J. P. 2010. Mice lacking Tbk1 activity exhibit immune cell infiltrates in multiple tissues and increased susceptibility to LPS-induced lethality. *Journal of Leukocyte Biology,* 88**,** 1171-1180.

MITSUTOSHI, Y. & TAKASHI, F. 2009. RNA recognition and signal transduction by RIG-I-like receptors. *Immunological Reviews,* 227**,** 54-65.

MONTI, S., SAVAGE, K. J., KUTOK, J. L., FEUERHAKE, F., KURTIN, P., MIHM, M., WU, B., PASQUALUCCI, L., NEUBERG, D., AGUIAR, R. C. T., CIN, P. D., LADD, C., PINKUS, G. S., SALLES, G., HARRIS, N. L., DALLA-FAVERA, R., HABERMANN, T. M., ASTER, J. C., GOLUB, T. R. & SHIPP, M. A. 2005. Molecular profiling of diffuse large B-cell lymphoma identifies robust subtypes including one characterized by host inflammatory response. *Blood,* 105**,** 1851-1861.

MONTOTO, S. & FITZGIBBON, J. 2011. Transformation of Indolent B-Cell Lymphomas. *Journal of Clinical Oncology,* 29**,** 1827-1834.

MOOTHA, V. K., LINDGREN, C. M., ERIKSSON, K.-F., SUBRAMANIAN, A., SIHAG, S., LEHAR, J., PUIGSERVER, P., CARLSSON, E., RIDDERSTRÅLE, M., LAURILA, E., HOUSTIS, N., DALY, M. J., PATTERSON, N., MESIROV, J. P., GOLUB, T. R., TAMAYO, P., SPIEGELMAN, B., LANDER, E. S., HIRSCHHORN, J. N., ALTSHULER, D. & GROOP, L. C. 2003. PGC-1α-responsive genes involved in oxidative phosphorylation are coordinately downregulated in human diabetes. *Nature Genetics,* 34**,** 267.

MORI, S., REMPEL, R. E., CHANG, J. T., YAO, G., LAGOO, A. S., POTTI, A., BILD, A. & NEVINS, J. R. 2008. Utilization of Pathway Signatures to Reveal Distinct Types of B Lymphoma in the Eμ-myc Model and Human Diffuse Large B-Cell Lymphoma. *Cancer Research,* 68**,** 8525-8534.

MORIN, R. D., JOHNSON, N. A., SEVERSON, T. M., MUNGALL, A. J., AN, J., GOYA, R., PAUL, J. E., BOYLE, M., WOOLCOCK, B. W., KUCHENBAUER, F., YAP, D., HUMPHRIES, R. K., GRIFFITH, O. L., SHAH, S., ZHU, H., KIMBARA, M., SHASHKIN, P., CHARLOT, J. F., TCHERPAKOV, M., CORBETT, R., TAM, A., VARHOL, R., SMAILUS, D., MOKSA, M., ZHAO, Y., DELANEY, A., QIAN, H., BIROL, I., SCHEIN, J., MOORE, R., HOLT, R., HORSMAN, D. E., CONNORS, J. M., JONES, S., APARICIO, S., HIRST, M., GASCOYNE, R. D. & MARRA, M. A. 2010. Somatic mutations altering EZH2 (Tyr641) in follicular and diffuse large B-cell lymphomas of germinal-center origin. *Nat Genet,* 42**,** 181-5.

MURRAY, MEGAN Y., AUGER, MARTIN J. & BOWLES, KRISTIAN M. 2014. Overcoming bortezomib resistance in multiple myeloma. *Biochemical Society Transactions,* 42**,** 804-808.

NEVES, P., LAMPROPOULOU, V., CALDERON-GOMEZ, E., ROCH, T., STERVBO, U., SHEN, P., KÜHL, A. A., LODDENKEMPER, C., HAURY, M., NEDOSPASOV, S. A., KAUFMANN, S. H. E., STEINHOFF, U., CALADO, D. P. & FILLATREAU, S. 2010. Signaling via the MyD88 Adaptor Protein in B Cells Suppresses Protective Immunity during Salmonella typhimurium Infection. *Immunity,* 33**,** 777-790.

NG, S. L., FRIEDMAN, B. A., SCHMID, S., GERTZ, J., MYERS, R. M., TENOEVER, B. R. & MANIATIS, T. 2011. IkappaB kinase epsilon (IKK(epsilon)) regulates the balance between type I and type II interferon responses. *Proc Natl Acad Sci U S A,* 108**,** 21170-5.

NGO, V. N., DAVIS, R. E., LAMY, L., YU, X., ZHAO, H., LENZ, G., LAM, L. T., DAVE, S., YANG, L., POWELL, J. & STAUDT, L. M. 2006. A loss-of-function RNA interference screen for molecular targets in cancer. *Nature,* 441**,** 106-10.

NGO, V. N., YOUNG, R. M., SCHMITZ, R., JHAVAR, S., XIAO, W., LIM, K.-H., KOHLHAMMER, H., XU, W., YANG, Y., ZHAO, H., SHAFFER, A. L., ROMESSER, P., WRIGHT, G., POWELL, J., ROSENWALD, A., MULLER-HERMELINK, H. K., OTT, G., GASCOYNE, R. D., CONNORS, J. M., RIMSZA, L. M., CAMPO, E., JAFFE, E. S., DELABIE, J., SMELAND, E. B., FISHER, R. I., BRAZIEL, R. M., TUBBS, R. R., COOK, J. R., WEISENBURGER, D. D., CHAN, W. C. & STAUDT, L. M. 2010. Oncogenically active MYD88 mutations in human lymphoma. *Nature,* 470**,** 115.

NOIA, J. M. D. & NEUBERGER, M. S. 2007. Molecular Mechanisms of Antibody Somatic Hypermutation. *Annual Review of Biochemistry,* 76**,** 1-22.

O'GARRA, A., STAPLETON, G., DHAR, V., PEARCE, M., SCHUMACHER, J., RUGO, H., BARBIS, D., STALL, A., CUPP, J., MOORE, K. & ET AL. 1990. Production of cytokines by mouse B cells: B lymphomas and normal B cells produce interleukin 10. *Int Immunol,* 2**,** 821-32.

OFFIT, K., COCO, F. L., LOUIE, D. C., PARSA, N. Z., LEUNG, D., PORTLOCK, C., YE, B. H., LISTA, F., FILIPPA, D. A., ROSENBAUM, A., LADANYI, M., JHANWAR, S., DALLA-FAVERA, R. & CHAGANTI, R. S. K. 1994. Rearrangement of the bcl-6 Gene as a Prognostic Marker in Diffuse Large-Cell Lymphoma. *New England Journal of Medicine,* 331**,** 74-80.

OGANESYAN, G., SAHA, S. K., PIETRAS, E. M., GUO, B., MIYAHIRA, A. K., ZARNEGAR, B. & CHENG, G. 2008. IRF3-dependent Type I Interferon Response in B Cells Regulates CpG-mediated Antibody Production. *Journal of Biological Chemistry,* 283**,** 802-808.

OLIVER, F. J., DE LA RUBIA, G., ROLLI, V., RUIZ-RUIZ, M. C., DE MURCIA, G. & MURCIA, J. M. 1998. Importance of poly(ADP-ribose) polymerase and its cleavage in apoptosis. Lesson from an uncleavable mutant. *J Biol Chem,* 273**,** 33533-9.

ORAL, E. A., REILLY, S. M., GOMEZ, A. V., MERAL, R., BUTZ, L., AJLUNI, N., CHENEVERT, T. L., KORYTNAYA, E., NEIDERT, A. H., HENCH, R., RUS, D., HOROWITZ, J. F., POIRIER, B., ZHAO, P., LEHMANN, K., JAIN, M., YU, R., LIDDLE, C., AHMADIAN, M., DOWNES, M., EVANS, R. M. & SALTIEL, A. R. 2017. Inhibition of IKKε and TBK1 Improves Glucose Control in a Subset of Patients with Type 2 Diabetes. *Cell Metabolism,* 26**,** 157-170.e7.

OTT, G., ZIEPERT, M., KLAPPER, W., HORN, H., SZCZEPANOWSKI, M., BERND, H. W., THORNS, C., FELLER, A. C., LENZE, D., HUMMEL, M., STEIN, H., MULLER-HERMELINK, H. K., FRANK, M., HANSMANN, M. L., BARTH, T. F., MOLLER, P., COGLIATTI, S., PFREUNDSCHUH, M., SCHMITZ, N., TRUMPER, L., LOEFFLER, M. & ROSENWALD, A. 2010. Immunoblastic morphology but not the immunohistochemical GCB/nonGCB classifier predicts outcome in diffuse large B-cell lymphoma in the RICOVER-60 trial of the DSHNHL. *Blood,* 116**,** 4916-25.

OU, Y.-H., TORRES, M., RAM, R., FORMSTECHER, E., ROLAND, C., CHENG, T., BREKKEN, R., WURZ, R., TASKER, A. & POLVERINO, T. 2011. TBK1 directly engages Akt/PKB survival signaling to support oncogenic transformation. *Molecular cell,* 41**,** 458-470.

PASQUALUCCI, L. & DALLA-FAVERA, R. 2015. The genetic landscape of diffuse large B-cell lymphoma. *Semin Hematol,* 52**,** 67-76.

PASQUALUCCI, L., DOMINGUEZ-SOLA, D., CHIARENZA, A., FABBRI, G., GRUNN, A., TRIFONOV, V., KASPER, L. H., LERACH, S., TANG, H., MA, J., ROSSI, D., CHADBURN, A., MURTY, V. V., MULLIGHAN, C. G., GAIDANO, G., RABADAN, R., BRINDLE, P. K. & DALLA-FAVERA, R. 2011a. Inactivating mutations of acetyltransferase genes in B-cell lymphoma. *Nature,* 471**,** 189.

PASQUALUCCI, L., TRIFONOV, V., FABBRI, G., MA, J., ROSSI, D., CHIARENZA, A., WELLS, V. A., GRUNN, A., MESSINA, M., ELLIOT, O., CHAN, J., BHAGAT, G., CHADBURN, A., GAIDANO, G., MULLIGHAN, C. G., RABADAN, R. & DALLA-FAVERA, R. 2011b. Analysis of the coding genome of diffuse large B-cell lymphoma. *Nature Genetics,* 43**,** 830.

PÉANT, B., GILBERT, S., LE PAGE, C., POISSON, A., L'ECUYER, E., BOUDHRAA, Z., BIENZ, M. N., DELVOYE, N., SAAD, F. & MES-MASSON, A.-M. 2017. IκB-Kinase-epsilon (IKKε) over-expression promotes the growth of prostate cancer through the C/EBP-β dependent activation of IL-6 gene expression. *Oncotarget,* 8**,** 14487-14501.

PEDERSEN, L. M., JÜRGENSEN, G. W. & JOHNSEN, H. E. 2005. Serum levels of inflammatory cytokines at diagnosis correlate to the bcl-6 and CD10 defined germinal centre (GC) phenotype and bcl-2 expression in patients with diffuse large B-cell lymphoma. *British Journal of Haematology,* 128**,** 813-819.

PERRY, A. K., CHOW, E. K., GOODNOUGH, J. B., YEH, W.-C. & CHENG, G. 2004. Differential Requirement for TANK-binding Kinase-1 in Type I Interferon Responses to Toll-like Receptor Activation and Viral Infection. *The Journal of Experimental Medicine,* 199**,** 1651-1658.

PETERS, R. T., LIAO, S.-M. & MANIATIS, T. 2000. IKKε Is Part of a Novel PMA-Inducible IκB Kinase Complex. *Molecular Cell,* 5**,** 513-522.

PFAFFL, M. W. 2001. A new mathematical model for relative quantification in real-time RT–PCR. *Nucleic Acids Research,* 29**,** e45-e45.

PFEIFER, M., GRAU, M., LENZE, D., WENZEL, S.-S., WOLF, A., WOLLERT-WULF, B., DIETZE, K., NOGAI, H., STOREK, B., MADLE, H., DÖRKEN, B., JANZ, M., DIRNHOFER, S., LENZ, P., HUMMEL, M., TZANKOV, A. & LENZ, G. 2013. PTEN loss defines a PI3K/AKT pathway-dependent germinal center subtype of diffuse large B-cell lymphoma. *Proceedings of the National Academy of Sciences,* 110**,** 12420-12425.

PFREUNDSCHUH, M., SCHUBERT, J., ZIEPERT, M., SCHMITS, R., MOHREN, M., LENGFELDER, E., REISER, M., NICKENIG, C., CLEMENS, M., PETER, N., BOKEMEYER, C., EIMERMACHER, H., HO, A., HOFFMANN, M., MERTELSMANN, R., TRÜMPER, L., BALLEISEN, L., LIERSCH, R., METZNER, B., HARTMANN, F., GLASS, B., POESCHEL, V., SCHMITZ, N., RUEBE, C., FELLER, A. C. & LOEFFLER, M. 2008. Six versus eight cycles of bi-weekly CHOP-14 with or without rituximab in elderly patients with aggressive CD20+ B-cell lymphomas: a randomised controlled trial (RICOVER-60). *The Lancet Oncology,* 9**,** 105-116.

PHAM, A. & TENOEVER, B. 2010. The IKK Kinases: Operators of Antiviral Signaling. *Viruses,* 2**,** 55.

PHAN, R. T. & DALLA-FAVERA, R. 2004. The BCL6 proto-oncogene suppresses p53 expression in germinal-centre B cells. *Nature,* 432**,** 635.

PHELAN, J. D., YOUNG, R. M., WEBSTER, D. E., ROULLAND, S., WRIGHT, G. W., KASBEKAR, M., SHAFFER, A. L., CERIBELLI, M., WANG, J. Q., SCHMITZ, R., NAKAGAWA, M., BACHY, E., HUANG, D. W., JI, Y., CHEN, L., YANG, Y., ZHAO, H., YU, X., XU, W., PALISOC, M. M., VALADEZ, R. R., DAVIES-HILL, T., WILSON, W. H., CHAN, W. C., JAFFE, E. S., GASCOYNE, R. D., CAMPO, E., ROSENWALD, A., OTT, G., DELABIE, J., RIMSZA, L. M., RODRIGUEZ, F. J., ESTEPHAN, F., HOLDHOFF, M., KRUHLAK, M. J., HEWITT, S. M., THOMAS, C. J., PITTALUGA, S., OELLERICH, T. & STAUDT, L. M. 2018. A multiprotein supercomplex controlling oncogenic signalling in lymphoma. *Nature,* 560**,** 387-391.

PLATANIAS, L. C. 2005. Mechanisms of type-I- and type-II-interferon-mediated signalling. *Nature Reviews Immunology,* 5**,** 375.

POMERANTZ, J. L. & BALTIMORE, D. 1999. NF-kappaB activation by a signaling complex containing TRAF2, TANK and TBK1, a novel IKK-related kinase. *EMBO J,* 18**,** 6694-704.

RAWLINGS, D. J., SOMMER, K. & MORENO-GARCIA, M. E. 2006. The CARMA1 signalosome links the signalling machinery of adaptive and innate immunity in lymphocytes. *Nat Rev Immunol,* 6**,** 799-812.

RE, D., KUPPERS, R. & DIEHL, V. 2005. Molecular pathogenesis of Hodgkin's lymphoma. *J Clin Oncol,* 23**,** 6379-86.

REDDY, A., ZHANG, J., DAVIS, N. S., MOFFITT, A. B., LOVE, C. L., WALDROP, A., LEPPA, S., PASANEN, A., MERIRANTA, L., KARJALAINEN-LINDSBERG, M.-L., NØRGAARD, P., PEDERSEN, M., GANG, A. O., HØGDALL, E., HEAVICAN, T. B., LONE, W., IQBAL, J., QIN, Q., LI, G., KIM, S. Y., HEALY, J., RICHARDS, K. L., FEDORIW, Y., BERNAL-MIZRACHI, L., KOFF, J. L., STATON, A. D., FLOWERS, C.

R., PALTIEL, O., GOLDSCHMIDT, N., CALAMINICI, M., CLEAR, A., GRIBBEN, J., NGUYEN, E., CZADER, M. B., ONDREJKA, S. L., COLLIE, A., HSI, E. D., TSE, E., AU-YEUNG, R. K. H., KWONG, Y.-L., SRIVASTAVA, G., CHOI, W. W. L., EVENS, A. M., PILICHOWSKA, M., SENGAR, M., REDDY, N., LI, S., CHADBURN, A., GORDON, L. I., JAFFE, E. S., LEVY, S., REMPEL, R., TZENG, T., HAPP, L. E., DAVE, T., RAJAGOPALAN, D., DATTA, J., DUNSON, D. B. & DAVE, S. S. 2017. Genetic and Functional Drivers of Diffuse Large B Cell Lymphoma. *Cell,* 171**,** 481-494.e15.

REILLY, S. M., CHIANG, S.-H., DECKER, S. J., CHANG, L., UHM, M., LARSEN, M. J., RUBIN, J. R., MOWERS, J., WHITE, N. M. & HOCHBERG, I. 2013. An inhibitor of the protein kinases TBK1 and IKK-ε improves obesity-related metabolic dysfunctions in mice. *Nature medicine,* 19**,** 313-321.

RELJIC, R., WAGNER, S. D., PEAKMAN, L. J. & FEARON, D. T. 2000. Suppression of Signal Transducer and Activator of Transcription 3–Dependent B Lymphocyte Terminal Differentiation by Bcl-6. *The Journal of Experimental Medicine,* 192**,** 1841-1848.

RICCARDI, C. & NICOLETTI, I. 2006. Analysis of apoptosis by propidium iodide staining and flow cytometry. *Nature Protocols,* 1**,** 1458.

RICKERT, R. C. 2013. New insights into pre-BCR and BCR signalling with relevance to B cell malignancies. *Nature Reviews Immunology,* 13**,** 578.

RILEY, J. K., TAKEDA, K., AKIRA, S. & SCHREIBER, R. D. 1999. Interleukin-10 receptor signaling through the JAK-STAT pathway. Requirement for two distinct receptor-derived signals for anti-inflammatory action. *J Biol Chem,* 274**,** 16513-21.

RIMSZA, L. M., LEBLANC, M. L., UNGER, J. M., MILLER, T. P., GROGAN, T. M., PERSKY, D. O., MARTEL, R. R., SABALOS, C. M., SELIGMANN, B., BRAZIEL, R. M., CAMPO, E., ROSENWALD, A., CONNORS, J. M., SEHN, L. H., JOHNSON, N. & GASCOYNE, R. D. 2008. Gene expression predicts overall survival in paraffin-embedded tissues of diffuse large B-cell lymphoma treated with R-CHOP. *Blood,* 112**,** 3425-3433.

ROSENWALD , A., WRIGHT , G., CHAN , W. C., CONNORS , J. M., CAMPO , E., FISHER , R. I., GASCOYNE , R. D., MULLER-HERMELINK , H. K., SMELAND , E. B., GILTNANE , J. M., HURT , E. M., ZHAO , H., AVERETT , L., YANG , L., WILSON , W. H., JAFFE , E. S., SIMON , R., KLAUSNER , R. D., POWELL , J., DUFFEY , P. L., LONGO , D. L., GREINER , T. C., WEISENBURGER , D. D., SANGER , W. G., DAVE , B. J., LYNCH , J. C., VOSE , J., ARMITAGE , J. O., MONTSERRAT , E., LÓPEZ-GUILLERMO , A., GROGAN , T. M., MILLER , T. P., LEBLANC , M., OTT , G., KVALOY , S., DELABIE , J., HOLTE , H., KRAJCI , P., STOKKE , T. & STAUDT , L. M. 2002. The Use of Molecular Profiling to Predict Survival after Chemotherapy for Diffuse Large-B-Cell Lymphoma. *New England Journal of Medicine,* 346**,** 1937-1947.

RUAN, J., MARTIN, P., FURMAN, R. R., LEE, S. M., CHEUNG, K., VOSE, J. M., LACASCE, A., MORRISON, J., ELSTROM, R., ELY, S., CHADBURN, A., CESARMAN, E., COLEMAN, M. & LEONARD, J. P. 2011. Bortezomib Plus CHOP-Rituximab for Previously Untreated Diffuse Large B-Cell Lymphoma and Mantle Cell Lymphoma. *Journal of Clinical Oncology,* 29**,** 690-697.

RUI, L., DRENNAN, A. C., CERIBELLI, M., ZHU, F., WRIGHT, G. W., HUANG, D. W., XIAO, W., LI, Y., GRINDLE, K. M., LU, L., HODSON, D. J., SHAFFER, A. L., ZHAO, H., XU, W., YANG, Y. & STAUDT, L. M. 2016. Epigenetic gene regulation by Janus kinase 1 in diffuse large B-cell lymphoma. *Proceedings of the National Academy of Sciences,* 113**,** E7260-E7267.

SANDER, J. D. & JOUNG, J. K. 2014. CRISPR-Cas systems for editing, regulating and targeting genomes. *Nature Biotechnology,* 32**,** 347.

SANKAR, S., CHAN, H., ROMANOW, W. J., LI, J. & BATES, R. J. 2006. IKK-i signals through IRF3 and NFκB to mediate the production of inflammatory cytokines. *Cellular Signalling,* 18**,** 982-993.

SCHINDLER, C., LEVY, D. E. & DECKER, T. 2007. JAK-STAT signaling: from interferons to cytokines. *J Biol Chem,* 282**,** 20059-63.

SCHMITZ, R., WRIGHT, G. W., HUANG, D. W., JOHNSON, C. A., PHELAN, J. D., WANG, J. Q., ROULLAND, S., KASBEKAR, M., YOUNG, R. M., SHAFFER, A. L., HODSON, D. J., XIAO, W., YU, X., YANG, Y., ZHAO, H., XU, W., LIU, X., ZHOU, B., DU, W., CHAN, W. C., JAFFE, E. S.,

GASCOYNE, R. D., CONNORS, J. M., CAMPO, E., LOPEZ-GUILLERMO, A., ROSENWALD, A., OTT, G., DELABIE, J., RIMSZA, L. M., TAY KUANG WEI, K., ZELENETZ, A. D., LEONARD, J. P., BARTLETT, N. L., TRAN, B., SHETTY, J., ZHAO, Y., SOPPET, D. R., PITTALUGA, S., WILSON, W. H. & STAUDT, L. M. 2018. Genetics and Pathogenesis of Diffuse Large B-Cell Lymphoma. *New England Journal of Medicine,* 378**,** 1396-1407.

SCUTO, A., KUJAWSKI, M., KOWOLIK, C., KRYMSKAYA, L., WANG, L., WEISS, L. M., DIGIUSTO, D., YU, H., FORMAN, S. & JOVE, R. 2011. STAT3 inhibition is a therapeutic strategy for ABC-like diffuse large B-cell lymphoma. *Cancer Res,* 71**,** 3182-8.

SEHN, L. H., DONALDSON, J., CHHANABHAI, M., FITZGERALD, C., GILL, K., KLASA, R., MACPHERSON, N., O'REILLY, S., SPINELLI, J. J., SUTHERLAND, J., WILSON, K. S., GASCOYNE, R. D. & CONNORS, J. M. 2005. Introduction of combined CHOP plus rituximab therapy dramatically improved outcome of diffuse large B-cell lymphoma in British Columbia. *J Clin Oncol,* 23.

SEHN, L. H. & GASCOYNE, R. D. 2015. Diffuse large B-cell lymphoma: optimizing outcome in the context of clinical and biologic heterogeneity. *Blood,* 125**,** 22-32.

SHAFFER, A. L., ROSENWALD, A. & STAUDT, L. M. 2002. Lymphoid Malignancies: the dark side of B-cell differentiation. *Nature Reviews Immunology,* 2**,** 920.

SHARMA, S., GRANDVAUX, N., ZHOU, G.-P., LIN, R. & HISCOTT, J. 2003. Triggering the interferon antiviral response through an IKK-related pathway. *Science,* 300**,** 1148-1151.

SHEN, R. R. & HAHN, W. C. 2011. Emerging roles for the non-canonical IKKs in cancer. *Oncogene,* 30**,** 631-41.

SHIMADA, T., KAWAI, T., TAKEDA, K., MATSUMOTO, M., INOUE, J., TATSUMI, Y., KANAMARU, A. & AKIRA, S. 1999. IKK-i, a novel lipopolysaccharide-inducible kinase that is related to IkappaB kinases. *Int Immunol,* 11**,** 1357-62.

SHIPP, M. A., ROSS, K. N., TAMAYO, P., WENG, A. P., KUTOK, J. L., AGUIAR, R. C. T., GAASENBEEK, M., ANGELO, M., REICH, M., PINKUS, G. S., RAY, T. S., KOVAL, M. A., LAST, K. W., NORTON, A., LISTER, T. A., MESIROV, J., NEUBERG, D. S., LANDER, E. S., ASTER, J. C. & GOLUB, T. R. 2002. Diffuse large B-cell lymphoma outcome prediction by gene-expression profiling and supervised machine learning. *Nature Medicine,* 8**,** 68.

SHUAI, K. & LIU, B. 2003. Regulation of JAK–STAT signalling in the immune system. *Nature Reviews Immunology,* 3**,** 900.

SMITH, A., CROUCH, S., LAX, S., LI, J., PAINTER, D., HOWELL, D., PATMORE, R., JACK, A. & ROMAN, E. 2015. Lymphoma incidence, survival and prevalence 2004-2014: sub-type analyses from the UK's Haematological Malignancy Research Network. *Br J Cancer,* 112**,** 1575-84.

SONG, B., ZHENG, K., MA, H., LIU, A., JING, W., SHAO, C., LI, G. & JIN, G. 2015. MiR-429 Determines Poor Outcome and Inhibits Pancreatic Ductal Adenocarcinoma Growth by Targeting TBK1. *Cellular Physiology and Biochemistry,* 35**,** 1846-1856.

STAUDT, L. M. 2010. Oncogenic activation of NF-kappaB. *Cold Spring Harb Perspect Biol,* 2**,** a000109.

SUBRAMANIAN, A., TAMAYO, P., MOOTHA, V. K., MUKHERJEE, S., EBERT, B. L., GILLETTE, M. A., PAULOVICH, A., POMEROY, S. L., GOLUB, T. R., LANDER, E. S. & MESIROV, J. P. 2005. Gene set enrichment analysis: A knowledge-based approach for interpreting genome-wide expression profiles. *Proceedings of the National Academy of Sciences,* 102**,** 15545-15550.

SUN, L., WU, J., DU, F., CHEN, X. & CHEN, Z. J. 2013. Cyclic GMP-AMP Synthase Is a Cytosolic DNA Sensor That Activates the Type I Interferon Pathway. *Science,* 339**,** 786-791.

SUN, S.-C. 2010. Non-canonical NF-κB signaling pathway. *Cell Research,* 21**,** 71.

SURVEXPRESS. 2015. *SurvExpress, biomarker validation for cancer gene expression* [Online]. Available: http://bioinformatica.mty.itesm.mx:8080/Biomatec/SurvivaX.jsp [Accessed 08, March, 2019.

SWENSON, W. T., WOOLDRIDGE, J. E., LYNCH, C. F., FORMAN-HOFFMAN, V. L., CHRISCHILLES, E. & LINK, B. K. 2005. Improved Survival of Follicular Lymphoma Patients in the United States. *Journal of Clinical Oncology,* 23**,** 5019-5026.

SWERDLOW, S. H., CAMPO, E., PILERI, S. A., HARRIS, N. L., STEIN, H., SIEBERT, R., ADVANI, R., GHIELMINI, M., SALLES, G. A., ZELENETZ, A. D. & JAFFE, E. S. 2016. The 2016 revision of the World Health Organization classification of lymphoid neoplasms. *Blood,* 127**,** 2375-2390.

TAKAHASHI, K., SIVINA, M., HOELLENRIEGEL, J., OKI, Y., HAGEMEISTER, F. B., FAYAD, L., ROMAGUERA, J. E., FOWLER, N., FANALE, M. A., KWAK, L. W., SAMANIEGO, F., NEELAPU, S., XIAO, L., HUANG, X., KANTARJIAN, H., KEATING, M. J., WIERDA, W., FU, K., CHAN, W. C., VOSE, J. M., O'BRIEN, S., DAVIS, R. E. & BURGER, J. A. 2015. CCL3 and CCL4 are biomarkers for B cell receptor pathway activation and prognostic serum markers in diffuse large B cell lymphoma. *British Journal of Haematology,* 171**,** 726-735.

TAMAI, H., YAMAGUCHI, H., MIYAKE, K., TAKATORI, M., KITANO, T., YAMANAKA, S., YUI, S., FUKUNAGA, K., NAKAYAMA, K. & INOKUCHI, K. 2017. Amlexanox Downregulates S100A6 to Sensitize KMT2A/AFF1-Positive Acute Lymphoblastic Leukemia to TNFalpha Treatment. *Cancer Res,* 77**,** 4426-4433.

TENOEVER, B. R., NG, S.-L., CHUA, M. A., MCWHIRTER, S. M., GARCÍA-SASTRE, A. & MANIATIS, T. 2007. Multiple Functions of the IKK-Related Kinase IKKε in Interferon-Mediated Antiviral Immunity. *Science,* 315**,** 1274-1278.

TOJIMA, Y., FUJIMOTO, A., DELHASE, M., CHEN, Y., HATAKEYAMA, S., NAKAYAMA, K.-I., KANEKO, Y., NIMURA, Y., MOTOYAMA, N., IKEDA, K., KARIN, M. & NAKANISHI, M. 2000. NAK is an I[kappa]B kinase-activating kinase. *Nature,* 404**,** 778-782.

TUNYAPLIN, C., SHAFFER, A. L., ANGELIN-DUCLOS, C. D., YU, X., STAUDT, L. M. & CALAME, K. L. 2004. Direct Repression of prdm1 by Bcl-6 Inhibits Plasmacytic Differentiation. *The Journal of Immunology,* 173**,** 1158-1165.

TUSHER, V. G., TIBSHIRANI, R. & CHU, G. 2001. Significance analysis of microarrays applied to the ionizing radiation response. *Proceedings of the National Academy of Sciences,* 98**,** 5116-5121.

VAZQUEZ, C. & HORNER, S. M. 2015. MAVS Coordination of Antiviral Innate Immunity. *J Virol,* 89**,** 6974-7.

VERMES, I., HAANEN, C., STEFFENS-NAKKEN, H. & REUTELLINGSPERGER, C. 1995. A novel assay for apoptosis Flow cytometric detection of phosphatidylserine expression on early apoptotic cells using fluorescein labelled Annexin V. *Journal of Immunological Methods,* 184**,** 39-51.

VOORZANGER, N., TOUITOU, R., GARCIA, E., DELECLUSE, H.-J., ROUSSET, F., JOAB, I., FAVROT, M. C. & BLAY, J.-Y. 1996. Interleukin (IL)-10 and IL-6 Are Produced in vivo by Non-Hodgkin's Lymphoma Cells and Act as Cooperative Growth Factors. *Cancer Research,* 56**,** 5499-5505.

WANG, X., LI, Z., NAGANUMA, A. & YE, B. H. 2002. Negative autoregulation of BCL-6 is bypassed by genetic alterations in diffuse large B cell lymphomas. *Proceedings of the National Academy of Sciences,* 99**,** 15018-15023.

WILLIAMS, R., TIMMIS, J. & QWARNSTROM, E. 2014. Computational Models of the NF-KB Signalling Pathway. *Computation,* 2**,** 131.

WILSON, W. H., YOUNG, R. M., SCHMITZ, R., YANG, Y., PITTALUGA, S., WRIGHT, G., LIH, C.-J., WILLIAMS, P. M., SHAFFER, A. L., GERECITANO, J., DE VOS, S., GOY, A., KENKRE, V. P., BARR, P. M., BLUM, K. A., SHUSTOV, A., ADVANI, R., FOWLER, N. H., VOSE, J. M., ELSTROM, R. L., HABERMANN, T. M., BARRIENTOS, J. C., MCGREIVY, J., FARDIS, M., CHANG, B. Y., CLOW, F., MUNNEKE, B., MOUSSA, D., BEAUPRE, D. M. & STAUDT, L. M. 2015. Targeting B cell receptor signaling with ibrutinib in diffuse large B cell lymphoma. *Nature Medicine,* 21**,** 922.

WRIGHT, G., TAN, B., ROSENWALD, A., HURT, E. H., WIESTNER, A. & STAUDT, L. M. 2003. A gene expression-based method to diagnose clinically distinct subgroups of diffuse large B cell lymphoma. *Proceedings of the National Academy of Sciences,* 100**,** 9991-9996.

WU, Z. L., SONG, Y. Q., SHI, Y. F. & ZHU, J. 2011. High nuclear expression of STAT3 is associated with unfavorable prognosis in diffuse large B-cell lymphoma. *J Hematol Oncol,* 4**,** 31.

XU-MONETTE, Z. Y., WU, L., VISCO, C., TAI, Y. C., TZANKOV, A., LIU, W.-M., MONTES-MORENO, S., DYBKÆR, K., CHIU, A., ORAZI, A., ZU, Y., BHAGAT, G., RICHARDS, K. L., HSI, E. D., ZHAO, X. F.,

CHOI, W. W. L., ZHAO, X., VAN KRIEKEN, J. H., HUANG, Q., HUH, J., AI, W., PONZONI, M., FERRERI, A. J. M., ZHOU, F., KAHL, B. S., WINTER, J. N., XU, W., LI, J., GO, R. S., LI, Y., PIRIS, M. A., MØLLER, M. B., MIRANDA, R. N., ABRUZZO, L. V., MEDEIROS, L. J. & YOUNG, K. H. 2012. Mutational profile and prognostic significance of TP53 in diffuse large B-cell lymphoma patients treated with R-CHOP: report from an International DLBCL Rituximab-CHOP Consortium Program Study. *Blood,* 120**,** 3986-3996.

XU, Z.-Z., XIA, Z.-G., WANG, A.-H., WANG, W.-F., LIU, Z.-Y., CHEN, L.-Y. & LI, J.-M. 2013. Activation of the PI3K/AKT/mTOR pathway in diffuse large B cell lymphoma: clinical significance and inhibitory effect of rituximab. *Annals of Hematology,* 92**,** 1351-1358.

YANG, W., QU, Y., TAN, B., JIA, Y., WANG, N., HU, P. & WANG, J. 2018. Prognostic significance of preoperative IKBKE expression in esophageal squamous cell carcinoma. *OncoTargets and therapy,* 11**,** 1305-1314.

YANG, Y., SHAFFER, ARTHUR L., EMRE, N. C. T., CERIBELLI, M., ZHANG, M., WRIGHT, G., XIAO, W., POWELL, J., PLATIG, J., KOHLHAMMER, H., YOUNG, RYAN M., ZHAO, H., YANG, Y., XU, W., BUGGY, JOSEPH J., BALASUBRAMANIAN, S., MATHEWS, LESLEY A., SHINN, P., GUHA, R., FERRER, M., THOMAS, C., WALDMANN, THOMAS A. & STAUDT, LOUIS M. 2012. Exploiting Synthetic Lethality for the Therapy of ABC Diffuse Large B Cell Lymphoma. *Cancer Cell,* 21**,** 723-737.

YE, B. H. 2000. BCL-6 in the pathogenesis of non-Hodgkin's lymphoma. *Cancer Invest,* 18**,** 356-65.

YE, B. H., RAO, P. H., CHAGANTI, R. S. & DALLA-FAVERA, R. 1993. Cloning of bcl-6, the locus involved in chromosome translocations affecting band 3q27 in B-cell lymphoma. *Cancer research,* 53**,** 2732-2735.

YOUNG, R. M. & STAUDT, L. M. 2013. Targeting pathological B cell receptor signalling in lymphoid malignancies. *Nat Rev Drug Discov,* 12**,** 229-43.

YU, H., PARDOLL, D. & JOVE, R. 2009. STATs in cancer inflammation and immunity: a leading role for STAT3. *Nature Reviews Cancer,* 9**,** 798.

YU, T., YI, Y.-S., YANG, Y., OH, J., JEONG, D. & CHO, J. Y. 2012. The Pivotal Role of TBK1 in Inflammatory Responses Mediated by Macrophages. *Mediators of Inflammation,* 2012**,** 8.

ZHANG, H., CHEN, L., CAI, S.-H. & CHENG, H. 2016. Identification of TBK1 and IKKε, the non-canonical IκB kinases, as crucial pro-survival factors in HTLV-1-transformed T lymphocytes. *Leukemia Research,* 46**,** 37-44.

ZHANG, S. Q., KOVALENKO, A., CANTARELLA, G. & WALLACH, D. 2000. Recruitment of the IKK signalosome to the p55 TNF receptor: RIP and A20 bind to NEMO (IKKgamma) upon receptor stimulation. *Immunity,* 12**,** 301-11.

ZHANG, Z., BRYAN, J. L., DELASSUS, E., CHANG, L. W., LIAO, W. & SANDELL, L. J. 2010. CCAAT/enhancer-binding protein beta and NF-kappaB mediate high level expression of chemokine genes CCL3 and CCL4 by human chondrocytes in response to IL-1beta. *J Biol Chem,* 285**,** 33092-103.

ZHOU, L. F., ZENG, W., SUN, L. C., WANG, Y., JIANG, F., LI, X., ZHENG, Y. & WU, G. M. 2018. IKKepsilon aggravates inflammatory response via phosphorylation of ERK in rheumatoid arthritis. *Eur Rev Med Pharmacol Sci,* 22**,** 2126-2133.

ZHU, Z., AREF, A. R., COHOON, T. J., BARBIE, T. U., IMAMURA, Y., YANG, S., MOODY, S. E., SHEN, R. R., SCHINZEL, A. C., THAI, T. C., REIBEL, J. B., TAMAYO, P., GODFREY, J. T., QIAN, Z. R., PAGE, A. N., MACIAG, K., CHAN, E. M., SILKWORTH, W., LABOWSKY, M. T., ROZHANSKY, L., MESIROV, J. P., GILLANDERS, W. E., OGINO, S., HACOHEN, N., GAUDET, S., ECK, M. J., ENGELMAN, J. A., CORCORAN, R. B., WONG, K.-K., HAHN, W. C. & BARBIE, D. A. 2014. Inhibition of KRAS - Driven Tumorigenicity by Interruption of an Autocrine Cytokine Circuit. *Cancer Discovery,* 4**,** 452-465.

ZUBAIR, H., AZIM, S., SRIVASTAVA, S. K., AHMAD, A., BHARDWAJ, A., KHAN, M. A., PATEL, G. K., ARORA, S., CARTER, J. E., SINGH, S. & SINGH, A. P. 2016. Glucose Metabolism Reprogrammed

by Overexpression of IKKε Promotes Pancreatic Tumor Growth. *Cancer Research,* 76**,** 7254-7264.

ZUCCHETTO, A., BENEDETTI, D., TRIPODO, C., BOMBEN, R., DAL BO, M., MARCONI, D., BOSSI, F., LORENZON, D., DEGAN, M., ROSSI, F. M., ROSSI, D., BULIAN, P., FRANCO, V., DEL POETA, G., DEAGLIO, S., GAIDANO, G., TEDESCO, F., MALAVASI, F. & GATTEI, V. 2009. CD38/CD31, the CCL3 and CCL4 Chemokines, and CD49d/Vascular Cell Adhesion Molecule-1 Are Interchained by Sequential Events Sustaining Chronic Lymphocytic Leukemia Cell Survival. *Cancer Research,* 69**,** 4001-4009.